EBERHARD KARLS
UNIVERSITÄT
TÜBINGEN

Zentrum für Angewandte Geowissenschaften (ZAG)

TÜBINGER GEOWISSENSCHAFTLICHE ARBEITEN (TGA)

Reihe C: Hydro-, Ingenieur- und Umweltgeologie

Schriftleitung: P. Grathwohl, G. Teutsch

Md. Mokhlesur Rahman

Sorption and Transport Behaviour of Hydrophobic Organic Compounds in Soils and Sediments of Bangladesh and their Impact on Groundwater Pollution - Laboratory Investigations and Model Simulations

TGA, C63, 2002

Sorption and Transport Behaviour of Hydrophobic Organic Compounds in Soils and Sediments of Bangladesh and their Impact on Groundwater Pollution – Laboratory Investigations and Model Simulations

Md. Mokhlesur Rahman

Lehrstuhl für Angewandte Geologie
Institut für Geologie und Paläontologie
Universität Tübingen
Sigwartstraße 10
72076 Tübingen
Germany

Herausgeber:	Institut und Museum für Geologie und Paläontologie der Universität Tübingen Sigwartstraße 10, D-72076 Tübingen
Schriftleitung der Reihe C:	Lehrstuhl für Angewandte Geologie Prof. Dr. Peter Grathwohl & Prof. Dr. Georg Teutsch
Redaktion:	Dipl.-Geol. Björn Sack-Kühner

ISSN 0935-4948

To my beloved parents
And to the memory of my grandparents

Tübinger. Geowiss. Arbeiten	Reihe C	Nr. 63	73 p., 45 Figs. 24 Tabs.	Tübingen, June, 2002

Sorption and Transport Behaviour of Hydrophobic Organic Compounds in Soils and Sediments of Bangladesh and their Impact on Groundwater Pollution – Laboratory Investigations and Model Simulations

Md. Mokhlesur Rahman[1]

Abstract: Groundwater can be contaminated by a variety of compounds, both of natural origin and man-made. Anthropogenic contamination has occurred for centuries, but industrialization, agricultural activities, urbanization and increased populations have greatly aggravated the problems in most of the countries of the world. This thesis focuses on the elucidation of the processes (e.g., sorption and related transport processes) controlling the fate and transport of hydrophobic organic compounds (HOCs) (contaminants and pesticide) in the subsurface environment. For a variety of organic compounds (phenanthrene, 1,2-DCB, TCE and carbofuran) batch and column experiments were carried out with different natural geosorbents (deltaic, floodplain and residuum soils, aquifer sediments and peat) to simulate the effect in Bangladesh top soils and sediments and the ultimate impact on groundwater.

Sorption of HOCs by natural sorbents is often dominated by partitioning processes. However, adsorption (pore-filling) mechanisms may also be important for heterogeneous reactions where the overall sorption may well be treated as the combination of the above mentioned processes resulting in combined sorption isotherms. This dissertation explores both types of processes using experimental data.

Overall, the results reported here so far indicate that sorption in these samples for the chemicals investigated is dominated by the partitioning processes. A nonlinear type sorption isotherm is described by the combination of the partitioning and pore-filling mechanisms. Both, the partitioning and the pore-filling models indicate to plot sorptive uptake vs. solubility (S) normalized aqueous concentrations, which yields "collapsing" sorption isotherms for similar compounds. The solubility normalized Freundlich model predicts an inverse linear relationship between the sorption coefficient measured at a given relative concentration vs. S, which is demonstrated for three partitioning dominated samples from Bangladesh (deltaic soil, aquifer sediment, peat) and 4 compounds investigated.

While neither the partitioning nor the pore-filling models are novel, the combination of both is considered as a new approach to explain the often observed nonlinear Freundlich-type sorption isotherms of hydrophobic compounds in soils and sediments: the pore-filling mechanism dominates at low aqueous concentrations whereas partitioning dominates close to S. S-normalized sorption isotherms facilitate the prediction of sorption of a variety of pollutants based on measured data of one probe compound. The normalization procedure presented here has to be considered as a first step, which certainly can be improved by including in addition to S other normalization parameters such as molar volume, polarizability, etc. Thus a wide variety of compounds with one representative sorption isotherm can be covered in a soil or sediment sample.

An effect of preferential solute transport coupled with diffusion into the surrounding matrix region has been examined in a surface soil (silty loam) by conducting macropore flow column experiments. To model the breakthrough curves an analytical solution was developed which accounts for advection in the macropore region, diffusion into the matrix region and linear sorption in both regions. The model fitted very well with the experimental data implying that the model covers all relevant processes acting in the macropore-matrix system. From the experimental results and the model assumptions it was concluded that sorption equilibrium was not achieved during matrix diffusion at the time scale of the macropore flow experiment.

In column experiments with continuous injection, both deltaic soil (silty loam) and aquifer sediment (sandy silt) showed nonequilibrium transport behaviour especially with phenanthrene while almost equilibrium conditions were achieved with 1,2-DCB, TCE and carbofuran. The combination of batch and column experimental results together with materials (solids) and environmental properties and a use of the analytical models of Ogata and Banks (1961) and Rosen (1954) for equilibrium and nonequilibrium sorption, respectively, can provide tools for cost-effective soil and groundwater risk assessment.

[1]Dissertation at the faculty of Geosciences, University of Tübingen, Germany

Author's present address: Institute for Water Chemistry, Dresden University of Technology, 01062, Germany

Sorption und Transport Verhalten von hydrophoben organischen Verbindungen im Boden und in Sedimenten von Bangladesh und ihre Auswirkung auf die Verunreinigung des Grundwassers - Laboruntersuchungen und Modellsimulationen

Kurzfassung: Grundwasser kann durch eine Vielzahl von Verbindungen, natürlichen wie synthetischen Ursprungs verunreinigt werden. Anthropogene Verunreinigung tritt seit Jahrhunderten auf, aber Industrialisierung, landwirtschaftliche Nutzung, Versiegelung und Bevölkerungszunahme haben die Probleme in den meisten Ländern der Welt verschlimmert. Diese Dissertation konzentriert sich auf die Aufklärung der Prozesse (wie z. B. Sorption und damit zusammenhängende Transportprozesse),die den Rückhalt und den Transport der hydrophoben organischen Verbindungen (HOCs) (Schadstoffe und Pestizide) unter der Erdoberfläche steuern. Für eine Vielzahl der organischen Verbindungen (Phenanthren, 1-2DCB, TCE und Karbofuran) wurden Batch- und Säulenversuche mit unterschiedlichen natürlichen Geosorbenten (Delta-, Überschwemmungs- und Restböden, Aquifersedimente und Torf) durchgeführt, um den Effekt in Bangladeshs Oberböden und Sedimenten sowie die entscheidenden Auswirkungen auf das Grundwasser zu simulieren.

Die Sorption von HOCs durch natürliche Sorbenten wird häufig durch Partitionsierungsprozesse beherrscht. Jedoch können Adsorptionsmechanismen (Porenfüllung) auch für heterogene Reaktionen von Bedeutung sein, bei denen die gesamte Sorption als Kombination der oben erwähnten Prozesse betrachtet werden kann, die in kombinierten Sorptionsisothermen resultiert. Diese Dissertation erforscht beide Arten von Reaktionsprozessen mit Hilfe experimenteller Daten.

Die Ergebnisse dieser Arbeit zeigen, dass die Sorption in den untersuchten Proben für die verwendeten Chemikalien von Partitionierungsprozessen beherrscht wird. Eine nichtlineare Typ-Sorptionsisotherme wird durch die Kombination der Partitionierungs- und Porenfüllungsmechanismen beschrieben. Beide, das Partitionierungs- und das Porenfüllungsmodell zeigen, dass sich beim Auftragen der sorptiven Ladung gegen die bzgl. der Wasserlöslichkeit (S) normalisierte Konzentration für ähnliche Chemikalien zusammenfallende Sorptionsisothermen ergeben. Wie für drei partitionierungsdominierte Proben aus Bangladesh (Deltaboden, Aquifersediment, Torf) gezeigt wird, sagt das bzgl. der Löslichkeit normalisierte Freundlich-Modell ein umgekehrt lineares Verhältnis zwischen dem Sorptionskoeffizienten, der bei einer gegebenen relativen Konzentraion (bzgl.S) gemessen wird, und vier untersuchten Verbindungen voraus.

Während weder die Partitionierungs- noch die Porenfüllungsmodelle neuartig sind, ist die Kombination von beiden als neuer Ansatz anzusehen, um die häufig beobachteten nichtlinearen Freundlich-Sorptionsisothermen hydrophober Verbindungen in Böden und Sedimenten zu erklären: Der Porenfüllungsmechanismus herrscht bei niedrigen wässrigen Konzentrationen vor, während die Partitionierung nahe der Löslichkeit S dominiert. Löslichkeitsnormalisierte Sorptionsisothermen erleichtern die Vorhersage der Sorption einer Vielzahl von Schadstoffen auf der Basis von Daten, die für eine einzige repräsentative Verbindung gemessen wurden. Die hier dargestellte Normalisierung ist als erster Schritt zu betrachten, der durch die Einbeziehung weiterer Normalisierungparameter wie molare Volumen, Polarisierbarkeit usw. zweifellos verbessert werden kann. Auf diese Weise kann eine breite Vielzahl von Verbindungen mit einer einzigen repräsentativen Sorptionsisotherme für eine Boden- und Sedimentprobe abgedeckt werden.

Die Ausbildung von präferentiellen Fließwegen und die damit verbundene Diffusion in die umgebende Matrix wurde anhand eines Oberbodens in Säulenexperimenten untersucht. Um die Durchbruchskurve zu modellieren, wurde eine analytische Lösung entwickelt, die die Advektion in der Makropore, die Diffusion in der Matrix und die lineare Sorption in beiden Regionen berücksichtigt. Die Modellergebnisse stimmen sehr gut mit den experimentell ermittelten Daten überein. Dies zeigt, dass das Modell alle relevanten Prozesse beinhaltet, die im Makroporen-Matrix-System relevant sind,. Aus den experimentell ermittelten Daten und den abgeschätzten Eingabeparametern für das Modell ist ersichtlich, dass während der Matrixdiffusion kein Sorptionsgleichgewicht im Makroporen-Strömungsexperiment erzielt wurde.

Die Elutionskurven der Säulenversuche mit kontinuierlicher Zugabe zeigten für den Deltaboden (schluffiger Lehm) und die Aquifersedimente (sandiger Schluff) überwiegend Ungleichgewichtsbedingungen, v. a. für Phenanthren; während für die Substanzen 1,2-DCB, TCE und Karbofuran nahezu Gleichgewichtsbedingungen erzielt wurden. Die Kombination aus den Ergebnissen von Batch- und Säulenversuchen und die Anwendung von analytischen Modellen von Ogata und Banks (1961) sowie von Rosen (1954) für Gleichgewichts- und Ungleichgewichtssorption erweisen sich als kosteneffektive Hilfsmittel zur Grundwassergefährdungsabschätzung.

Acknowledgements

When all is said and done, it remains to thank all those who have contributed in many different ways to the coming of the final stage of the dissertation. It is a pleasure to express my deep gratitude to the following:

It is with sincere gratitude that I acknowledge the continuous support of my supervisor Prof. Dr. Peter Grathwohl that I have been fortunate enough to receive throughout this research. Thanks for his timely, decisive, and knowledgeable suggestions and criticisms. I am especially indebted to my co-supervisor PD Dr. Rudolf Liedl for his help regarding the modelling of preferential flow transport and fruitful discussions in many aspects. Thanks also to Prof. Dr. K.-D. Balke who paved the way for me to come to Germany and especially for his support and kindness.

I would also like to acknowledge and extend my thanks to Dr. Christoph Schüth for his ideas about column experimental set-up and for many helpful discussions and suggestions during the course of the research. I would never forget the patience of Dr. Sybille Kleineidam who helped me to assess the sorption kinetic experimental data in the very beginning of this research and to prepare a poster as well as a paper for GW 2000 conference held in Copenhagen, Denmark. I am very much grateful to Bernice Nisch, Renate Riehle, Anne Hartmann-Renz, Renate Seelig and Annegret Walz for their technical assistance in the hydrogeochemistry laboratory of Applied Geology Group and for keeping a free and pleasant working atmosphere there.

Financial support for this research was provided by Wilhelm Schüler Stiftung, University of Tübingen which proved to be essential for the completion of this work. Additional financial support was provided by the Center for Applied Geoscience, Chair of Applied Geology, University of Tübingen. I am also grateful to Mr. H. Merkle for his help in organizing some financial support during my overstay after the completion of advanced studies course here in Tübingen.

I am very grateful to Uwe Schmidt for his deepening sense of brotherhood. It was his consistent encouragement, advice and help which kept me on track during my whole study in Germany.

My best gratitude go to my former M.Sc. supervisor Prof. Dr. M. Qumrul Hassan for his numerous valuable suggestions which helped me to build my confidence towards the completion of the research. Thanks to Dr. Kazi Matin Ahmed, S.Z.K.M. Shamsad, Aziz Hasan, Mohammad Hossain Tipu, Dr. Kamrul Hasan for their support and kindness. It would have been impossible for me to do the field work in Bangladesh without the kind support of Md. Saiful Islam, Sirajul Islam Khan and Abdul Baki Khan Majlish.

I also appreciate the support of my colleagues in Hilzinger Bau, unfortunately too numerous to mention, in particular Iris Madlener, Andreas Yida-de Mattos, Åsa Olsson, Dr. Sayonara Brederode Ferreira Reckhorn, Andreas Lamprou, Tilman Gocht, Rainer Henzler, Uli Maier and Matthias Piepenbrink who have answered questions, given advice and, often unwittingly, provided invaluable tips to accelerate my work. I really enjoyed the discussion with Andreas Lamprou with whom once I planned to do mediation on the top of a nearby hill but finally did not succeed.

Special thanks to Zohra Bouhouche, Akhtaruzzaman Akhtar, Anwar Zahid, Khaled Mahmud (Shams), Arifur Rahman, Shamim Winkler (Siraj), Samsul Arefin Tarafdar, Muhit Razzak, Matthias Flegr and Ludwig Biermanns for their companionship during various social and leisure activities. Special thanks to Bettina Exner for her love, support and patience during hard times and for sharing the good times with me.

Last but not least, I would like to express special thanks to my parents, uncles, sisters and brothers, cousins Engr. Monir and Advocate Madina, Hira Khala, Mazid Khalu, Babul bhai, who all supported and encouraged me in pursuing my career in Germany. Without them a little could have been achieved. They make my life filled with happiness.

Table of contents

Abbreviations and notations

The abbreviation shown in brackets represent the dimensionality of the variables used: M = mass; L = length; L^3 = volume; T = time; K = temperature in Kelvin

BC	Boundary condition
DhaRs A	Residuum soil collected from A horizon from Dhaka region
DIN	Deutsche industrie norm
EPA	Environment protection agency
ERFC	Complementary error function
GC	Gas chromatography
GRACOS	Groundwater risk assessment at contaminated site
HL	Half life
HPLC	High performance liquid chromatography
HSACM	High surface area carbonaceous material
IC	Initial condition
IUPAC	International union of pure and applied chemistry
Kh Aqfr	Aquifer sediment collected from Khulna region
Kh PeatPeat collected from Khulna region	
KhDs A	Deltaic soil collected from A horizon from Khulna region
KhDs B	Deltaic soil collected from B horizon from Khulna region
KhDs C	Deltaic soil collected from C horizon from Khulna region
KhDs ABC	Deltaic soil collected from A, B and C horizon from Khulna region and mixed together for sorption experiments
MW	Molecular weight
MWSE	Mean weighted square error
NMR	Nuclear magnetic resonance
NOM	Natural organic matter
OC	Organic carbon
PESTAN	Pesticide analytical model
PF	Preferential flow
PV	Pore volume
Raj Aqfr	Aquifer sediment collected from Rajshahi region
RajFs A	Floodplain soil collected from A horizon from Rajshahi region
SatDs A	Deltaic soil collected from A horizon from Satkhira region
SIM	System interface module
SOC	Soil/sediment organic carbon
VP	Vapour pressure [mm Hg]

ε_{sw}	Adsorption potential [J mol^{-1}]
σ	Standard deviation [-]
ρ_o	Density of organic compound [M L^{-3}]
ρ_s	Solid density [M L^{-3}]
γ_{om}	Activity coefficient of a compound in an organic matter phase [-]
ρ_{om}	Density of organic matter [M L^{-3}]
β	Affinity or similarity coefficient [-]; ratio of mass of solutes dissolved in the aqueous phase to the mass in the solids [-]
γ_w	Activity coefficient in aqueous phase [-]
ρ_b	Bulk density [ML^{-3}]
τ_f	Tortuosity factor [-]
ε	Intraparticle porosity [-]
$\Delta G°$	Gibbs´ free energy [kJ mol^{-1}]
$\Delta H°$	Changes in enthalpy [kJ mol^{-1}]

$\Delta S°$	Changes in entropy [kJ mol^{-1} K^{-1}]
ΔS_f	Entropy of fusion [kJ mol^{-1} K^{-1}]
α_l	Mechanical longitudinal dispersivity [L]
λ	First order decay coefficient [T^{-1}]
δ	Dirac function [-]
ρ_m	Bulk density in the macropore region [M L^{-3}]
ρ_a	Apparent particle density [M L^{-3}]
λ_s	Solid phase decay constant [T^{-1}]
ρ_{im}	Bulk density in the matrix region [M L^{-3}]
μ_{rs}	First moment of reactive solute [T]
μ_{ct}	First moment of conservative tracer [T]
$1/n$	Freundlich exponent [-]
A	Area [L^2]
a	Sphere radius or particle radius [L]
b	Empirical constant [-]
$\overline{C_{im}}$	Average concentration in immobile region [M L^{-3}]
C/C_0	Normalized concentration [-]
C_0	Initial concentration [M L^{-3}]
C_G	Contaminant concentration in gas phase [M L^{-3}]
C_{im}	Concentration in the immobile/matrix region [M L^{-3}]
C_m	Concentration in the macropore/mobile region [M L^{-3}]
C_{om}	Solute concentration in the organic matter [M M^{-1}]
C_{ref}	Concentration in reference vials [M L^{-3}]
C_s	Sorbed phase concentration [M M^{-1}]
C_s'	Adsorbed concentration [M M^{-1}]
C_w	Concentration of solute in aqueous phase [M L^{-3}]
C_{w+m}	Concentration of extracted phenanthrene from solid plus phenanthrene solution remained in soil [M L^{-3}]
D_a	Apparent diffusion coefficient [L^2 T^{-1}]
D_a/a^2	Diffusion rate constant [T^{-1}]
D_{aq}	Aqueous diffusion coefficient [L^2 T^{-1}]
D_e	Effective diffusion coefficient [L^2 T^{-1}]
D_H	Hydrodynamic dispersion coefficient [L^2 T^{-1}]
D_p	Pore diffusion coefficient [L^2 T^{-1}]
E	Characteristic free energy of adsorption other than a reference compound [J mol^{-1}]
E_o	Characteristic free energy of adsorption for a reference vapour/compound [J mol^{-1}]
F	Mass flux [M L^{-2} T^{-1}]
f_{oc}	Mass fraction of organic carbon [-]
f_{om}	Mass fraction of organic matter [-]
H	Henry constant [-]
K	Proportionality constant either as equilibrium constant [-] or hydraulic conductivity [L T^{-1}]
K_d	Distribution coefficient between soil and water [L^3 M^{-1}]
$K_{d,0.5}$	Distribution coefficient determined from $R_{o.5}$ in a column system [L^3 M^{-1}]
$K_{d,app}$	Apparent distribution coefficient [L^3 M^{-1}]
$K_{d,eq}$	Distribution coefficient in equilibrium [L^3 M^{-1}]
$K_{d,im}$	Distribution coefficient in the matrix region [L^3 M^{-1}]
$K_{d,m}$	Distribution coefficient in the macropore region [L^3 M^{-1}]
K_{fr}	Freundlich coefficient [L^3 M^{-1}]
K^*_{Fr}	Unit-equivalent Freundlich coefficient [-]
K_{oc}	Distribution coefficient between dissolved phase and soil organic carbon [L^3 M^{-1}]
K_{om}	Distribution coefficient between dissolved phase and soil organic matter [L^3 M^{-1}]

K^*_{om}	Unit equivalent organic matter and aqueous solubility based partition coefficient [-]
K_{ow}	Octanol water partition coefficient [-]
K_p	Partition coefficient [L^3 M^{-1}]
K_{sg}	Distribution coefficient between soil and gas phase [L^3 M^{-1}]
K_{sys}	System loss [L^3]
l	Straight line macroscopic distance [L]
l_e	Microscopic or effective distance [L]
m_d	Mass of solid [M]
M_{eq}	Mass of solutes at equilibrium [M]
m_{im}	Mass of solute in the matrix per unit volume [M L^{-3}]
M_t	Mass of solutes at time t [M]
n	Volumetric water content or porosity of saturated media [-]
n_e	Effective porosity [-]
n_{im}	Immobile/matrix region porosity [-]
n_m	Macropore/mobile region porosity [-]
P/P_0	Normalized vapour pressure [-]
Q	Flow rate [L^3 T^{-1}]
q	Specific discharge (Darcy's velocity) [L T^{-1}]
R	Ideal gas constant [J mol^{-1} K^{-1}]
r	Radial distance [L]
$R_{0.5}$	Retardation factor determined from the $t_{0.5}$ ratio of the conservative tracer and reactive solutes [-]
R_f	Retardation factor [-]
R_{im}	Retardation factor in the matrix region [-]
R_m	Retardation factor in the macropore region [-]
S	Water solubility [M L^{-3} or mol L^{-3}]
S_{scl}	Subcooled liquid solubility [M L^{-3}]
T	Temperature [K]
t	Time [T]
t_0	Pulse duration [T]
$t_{0.5}$	Time required for the effluent concentration to reach $C/C_0 = 0.5$[T]
t_r	Time lapse between application and recharge [T]
v_a	Average linear velocity [L T^{-1}]
V_G	Volume of gas phase [L^3]
v_m	Mobile region velocity [L T^{-1}]
$V_{methanol}$	Volume of methanol [L^3]
V_{mw}	Molar volume of aqueous phase [L^3 mol^{-1}]
V_o	Maximum sorption capacity [L^3 M^{-1}]
V_{om}	Molar volume of organic matter [L^3 mol^{-1}]
V_{ref}	Volume of water in reference vial [L^3]
V_s	Adsorbed gas volume [L^3 M^{-1}]
V_w	Volume of water [L^3]
$V_{w,soil}$	Volume of water retained in soil [L^3]
x	Distance/Spatial co-ordinate perpendicular to flow direction [L]
X_G	Mass of contaminant in the gas phase [M]
X_S	Mass of contaminant in solid phase [M]
X_W	Mass of contaminant in liquid phase [M]
z	Spatial co-ordinate along flow direction [L]

1. MOTIVATIONS AND GOALS

1.1 Problem approach

Contamination of soil, sediments and groundwater by anthropogenic organic chemicals has become a matter of increasing public and regulatory concern because of their toxicity and long-term source of contamination. The most severe contamination problems are due to point sources (local spills), which frequently involve organic solvents (e.g., chlorinated hydrocarbons, aromatic hydrocarbons etc.), gasoline, lubricants in general as well as coal tars (from manufactured gas plants and cookeries), wood preservatives (e.g., creosote which may contain pentachlorophenol), transformer fluids (polychlorinated biphenyls) and plasticizers (phthalates). Non point sources, which cause usually much lower contaminant concentrations than point sources, result from the application of pesticides (e.g. lindane, DDT etc.) in agriculture or the atmospheric deposition of a wide variety of anthropogenic chemicals. Occurrence of shallow groundwater in industrialized and irrigated regions can thus be especially vulnerable to this contamination problem. Moreover, since groundwater is the major source of drinking water and remediations of contaminated sites are not feasible for most of the countries in the world, "scenario-based" integrated risk assessment models/guidelines are needed which will allow to predict the risk of groundwater pollution, to categorize the sites for further use and remedial actions and to support decision making in a scientifically rational and cost effective way.

Fate, transport and finally the groundwater risk assessment of hydrophobic organic compounds (HOCs) strongly depend on the physico-chemical properties of the compounds (e.g. water solubility and vapour pressure) and the sorption capacity of the soil and sediment solids (e.g. Schwarzenbach and Westall, 1981). Increased sorption leads to a reduced bioavailability and higher persistence of compounds in the environment. Pollutants may thus become a long term source of groundwater contamination. Fig. 1.1 shows pollution pathways, that include the physical movement of the contaminants and the chemical and biological processes that occur en route.

Research during the last 2 decades showed that organic matter is the key sorbent at least for the non-ionic hydrophobic compounds and that adsorption to clay minerals is of minor importance with the exception of specific interactions, e.g. of nitrogen containing compounds and clay mineral surfaces (Haderlein et al., 1996) and intermolecular polar bonds between functional groups of organic matter and pollutants (Graber and Borisover, 1998). The fact, that organic matter (and organic carbon) normalized sorption coefficients correlate well with other compound properties such as the octanol/water partitioning coefficient (K_{ow}), leads to the conclusion that sorptive uptake of hydrophobic compounds in organic matter can also be described by a partitioning mechanism with essentially linear sorption isotherms (Chiou et al., 1979; 1983; 1989; Karickhoff et al., 1979; Kenaga and Goring, 1980). Recently, however, more and more studies were published which proved that sorption is nonlinear especially if concentrations range over many orders of magnitude and that sorption capacities are much higher than expected from a partitioning process (e.g.: Grathwohl, 1990; Allen-King et al., 1996; Borisover and Graber, 1997; Chiou and Kile, 1998; Kleineidam et al., 1999; Karapanagioti et al., 2000; Bucheli and Gustaffson, 2001; Wefer-Roehl et al., 2001). This is generally explained by adsorption mechanisms in specific regions of the organic matter (glassy or hard carbon; e.g.: Weber et al., 1992; LeBeouf and Weber, 1997; 1999; Xing and Pignatello, 1997) or more specifically by a pore-filling process (Xia and Ball, 1999; Kleineidam et al., 2002; Allen-King et al., 2002) analogous to adsorption in micro- and mesoporous activated carbon or (hydrophobic) zeolites (Manes, 1998; Kleineidam et al., 2002).

Prediction of the fate of hydrophobic organic compounds (HOCs) often relies on the constants derived from sorption isotherm models. The Freundlich model is the most commonly used model to describe the retention of HOCs by heterogeneous sorbents showing a linear/nonlinear type of sorption isotherm. But because of inconsistent units of constants

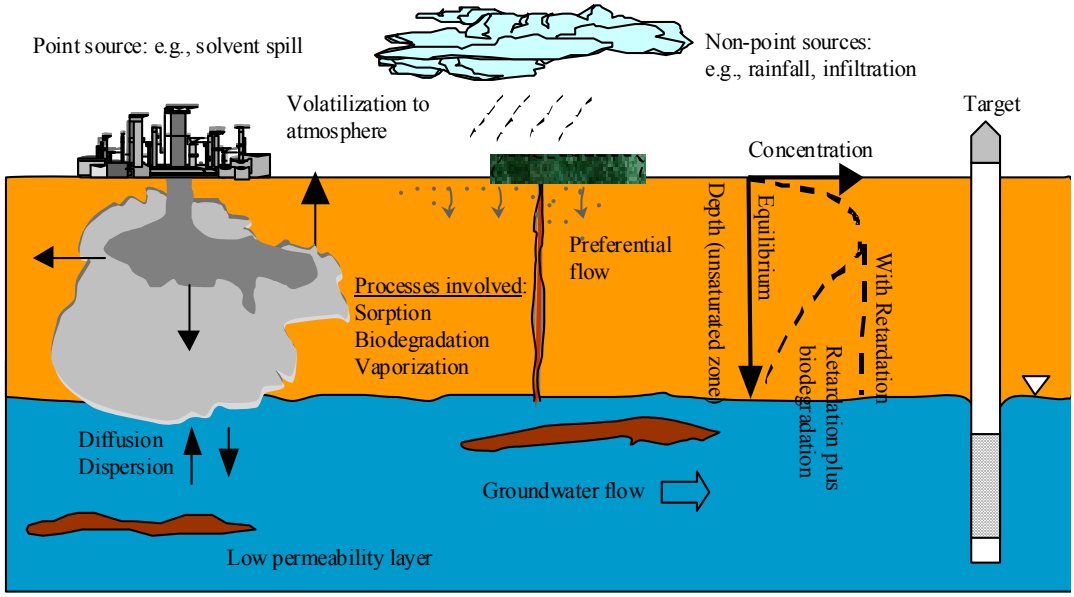

Fig. 1.1 Pollution pathways showing the physical movement of contaminants and the processes affecting the fate of contaminants in the subsurface environment. Persistent organic chemicals (e.g., phenanthrene) can reach groundwater with seepage water. If the contaminants are persistent and volatile (e.g., TCE) they can travel relatively quickly over large distances by vapour phase diffusion (vertical and lateral) and are finally transported across the capillary fringe by diffusion and dispersion into the groundwater. Biodegradable compounds may reach the groundwater in very low concentrations. If there is a facilitated transport (e.g., preferential flow), some contaminants will travel too quickly to be significantly affected by sorption and biodegradation.

calculated from Freundlich models, it is difficult to compare the sorption of organic compounds by different geosorbents. Normalization of equilibrium aqueous concentrations to the water solubility of compounds leads to unit equivalent Freundlich coefficients that remove the ambiguities regarding the concentration dependent nature of the Freundlich coefficients. These methods have been used both in soils and sediments (Carmo, 2000) and in activated carbon filtration (Manes, 1998; Crittenden et al., 1999; Paulsen and Cannon, 1999; Wood, 2001). Nonlinear Freundlich type sorption isotherms are well described by the combination of partitioning and pore-filling (Xia and Ball, 1999), suggesting the solubility normalized concentration as well.

Assessment of the groundwater contamination risk by HOCs also focuses our interest on transport processes that take place in both, the unsaturated and the saturated zone. Especially the low conductivity regions like clay and silt layers and lenses, low permeable bed rock formations, mineral layers at landfills or slurry walls used as containments at contaminated sites, are of major importance as they primarily control the overall fate of a contaminant applied at the surface. In this low conductivity region, advection is negligible and diffusion becomes the dominant mass transfer mechanism. Moreover, the presence of preferential flow paths serves to greatly increase the risk of groundwater contamination through soil fractures, shrink-swell cracks, worm holes etc., that exist under field conditions. On the other hand, attenuation of the contaminants can take place both in the unsaturated and in the saturated zone. The unsaturated zone and especially the capillary fringe can be a region of very active aerobic biodegradation, that would result in low contaminant concentrations at the groundwater table. In the aquifer, attenuation of the contaminants may take place through dilution, volatilization, buffering, neutralization and ion exchange. Diffusion and dispersion again will bring contaminants into contact with material that may retard their propagation progress; thus attenuation may vary with time and travel distance.

Bangladesh is a highly populated and agriculture based country where a rapid increase in the use of pesticides and chemical fertilisers is necessary

for the growth of rice to feed its boosting population. Very little is known about the effect of highly toxic pesticides and fertilisers that are run-off to nearby water body and finally enter the groundwater. Industrial pollution in Bangladesh is still limited to small pocket areas. But as almost all the industries do not use any treatments for effluents, pollution in these areas is highly concentrated. Most of the industries are indiscriminately discharging industrial wastewaters that can easily reach the groundwater by bank filtration from rivers or from soil to groundwater through seepage water. Apart from agricultural and industrial based soil or groundwater contamination problems, urbanization and population pressure are also adding problems as they represent the combined results of industrial, commercial and domestic activities. Especially urban pollution is present in all common forms as wastewater and polluted surface water, air emissions from vehicles and urban point sources and solid wastes. Recently, the natural contamination of groundwater by arsenic has become a crucial water quality problem throughout Bangladesh which is described by Smith et al. (2000) as the largest poisoning of a population in history with millions of people exposed.

1.1 Objectives of the study

The main objective of the dissertation is to assess the risk of groundwater pollution by environmental organic compounds by using uncontaminated soils and sediments collected from Bangladesh. In order to predict the risk, the necessary parameters were obtained by:

a) characterizing the samples in terms of grain size distribution, organic carbon content and particle density,

b) carrying out batch sorption experiment using pulverised samples for the determination of the sorption behaviour of the solids and for the chemicals tested and identifying the parameters to be used in a solute transport model,

c) investigating the impact of preferential flow (PF) coupled with matrix diffusion on solute transport in the unsaturated zone and

d) performing column experiments to obtain the transport parameters that are needed to predict the percolation/leaching rate of contaminants from the top soil and their transport in the subsoil to the groundwater table.

The results to be obtained from batch and column experiments together with hydrological (e.g. groundwater recharge rate) and chemical properties and a simple analytical model of contaminant transport under equilibrium (e.g., Ogata and Banks, 1961) and nonequilibrium conditions (e.g., Rosen, 1954) can be used for the risk assessment. The risk assessment procedure in this way will take the form of a scenario approach as it may be intended to be applied to different situations in terms of classes/combination of pollutants and site-specific conditions, such as hydrologic conditions, permeability and distance between contamination and groundwater table. Such a scenario approach will allow to determine *a priori* whether under given site conditions (subsurface permeability, distance to groundwater table, type of material) and contaminant properties (volatile/non-volatile/water soluble/hydrophobic etc.) a minor, medium or high risk of groundwater pollution exists.

The research presented in this dissertation has been organized into six major chapters including this overview and references.

Chapter 2 (**THEORETICAL BACKGROUND**) describes the theoretical basis for the prediction of sorption of HOCs in soils and sediments. Partitioning and pore-filling processes are described individually and are combined for the description of sorption in heterogeneous sorbents. As both partitioning and pore-filling processes suggest solubility normalized concentrations, the most frequently used Freundlich model is also normalized by water solubility of compounds, which leads to unit equivalent Freundlich sorption isotherms. The advantage of this normalization approach is that a generalized sorption isotherm can be obtained, which is based on the water solubility of compounds. The theoretical basis of some analytical solutions of 1D solute transport models is reviewed in this chapter as well. Furthermore, this chapter provides an analytical solution for modelling preferential flow

(macropore) transport coupled with matrix diffusion which, together with an experimental set-up, allows for the determination of the pore diffusion coefficient of conservative tracers and the retardation of the pore diffusion for reactive solutes.

In chapter 3 (**MATERIALS AND METHODS**) methodological aspects of sample collection and preparations, characterization of samples and batch and column measurement of sorption and transport parameters are discussed and evaluated. Modelling of sorption kinetics experiments is done using the intraparticle pore diffusion model for a finite bath (Crank, 1975). The diffusion coefficient D_a is used as a fitting parameter in the model.

Chapter 4 (**RESULTS AND DISCUSSIONS**) fully describes the sorption behaviour of four HOCs onto soils and sediments of Bangladesh. Data are interpreted using the combined partitioning and pore-filling approach and the solubility normalized unit-equivalent Freundlich model. Some important findings include that the solubility normalized Freundlich model predicts an inverse linear relationship between the sorption coefficient measured at a given relative concentration vs. *S*, that will allow to predict the sorption of compounds similar to those investigated in the study. This simple normalization (by water solubility/subcooled liquid solubility of the compound) procedure leads to similar sorption isotherms for various compounds in a specific sorbent, as to be expected from partitioning and the pore filling mechanism as well, indicating that a given sorbent has the same capacity to sorb solutes at a given relative concentration. Column experiment results with continuous injection reflect that except for phenanthrene almost equilibrium was achieved between chemicals and solids investigated. In the macropore experiment with a finite pulse injection, sorption equilibrium in the matrix was not obtained during the time scale of the experiment and this presumably also affects contaminant transport in the field, i.e., faster migration than expected from batch equilibrium sorption isotherms.

In chapter 5 (**APPLICATION OF RESULTS: Groundwater Risk Assessment**) simulations for the assessment of groundwater risk are done using analytical models of solute transport having different initial and boundary conditions. Simulations are done using batch and column derived data together with hydrological and contaminant properties and the analytical models discussed. Three scenarios are considered for such simulations being distinguished by the boundary conditions: continuous input of contaminants (e.g. effluents from an industry) in the subsurface, Dirac pulse input (e.g., application of pesticides in the field) and finite pulse input with the impact of preferential flow.

2. THEORETICAL BACKGROUND

2.1 Distribution and migration of organic chemicals in a three phase system (solid, air and liquid) in the unsaturated zone

The subsurface zone lying above the groundwater table, the unsaturated zone, is a three phase system consisting of a solid, liquid and gas phase. Mineral matrix, soil and organic matter cover the solid phase, water is the liquid phase and the gas phase contains the air-filled pore space (soil air) (Fig. 2.1).

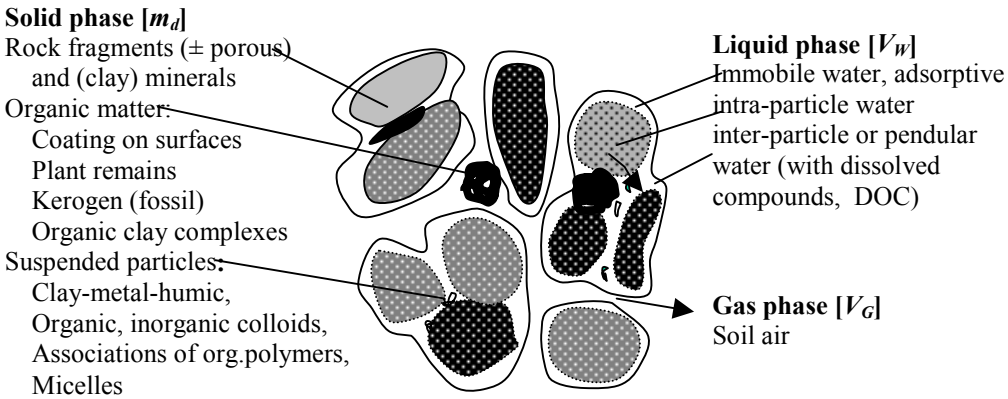

Fig. 2.1: The unsaturated zone (Grathwohl, 1998)

The fate of chemicals in the subsurface environment depends on their physico-chemical properties such as vapour pressure and water solubility or octanol water partition coefficient which is especially important for hydrophobic organic chemicals. After being introduced into the environment organic chemicals are distributed in the three different phases: 1) as a solute dissolved in water; 2) as a gas in the vapour phase and 3) as a sorbed compound in the solid phase. Some parts may move to the atmosphere due to vapour phase diffusion. Fig. 2.2 schematically shows vadose zone contaminant pathways.

Volatile contaminants will be distributed in all the three phases and their distribution in each phase can be determined only by measuring the gas phase concentration. By applying Henry's law and mass balance consideration the distribution in aqueous and solid phases can be ascertained. Non-volatile contaminants will not be transferred to the gas phase significantly and thus their distribution can be determined only by knowing the aqueous phase concentration and mass balance consideration. Fig. 2.3 shows a scheme of determining the concentration and their distribution in the three phase system.

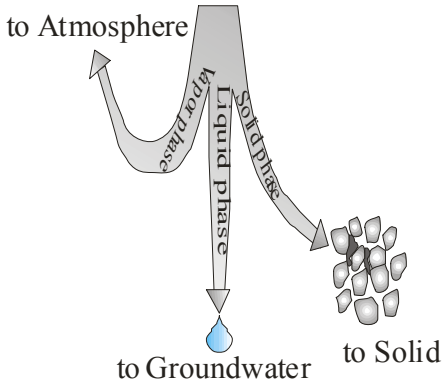

Fig. 2.2: Schematic diagram illustrating the contaminant pathways in the environment

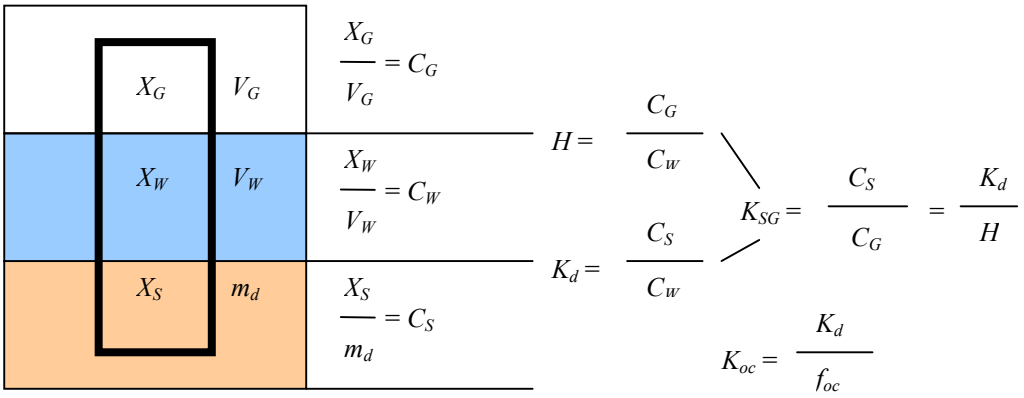

Fig. 2.3 Distribution of contaminants in the soil/water/air – 3 phase system

The terms X_G, X_W and X_S denote the mass of contaminants in the gas (V_G), water (V_W) and soil phases (m_d) [M], respectively; C_G, C_W and C_S denote the contaminant concentration in gas [M L^{-3}], water [M L^{-3}] and soil [M M^{-1}] phases, respectively; K_d, K_{sg}, K_{oc}, f_{oc} and H denote the distribution coefficient between soil and water [L^3 M^{-1}], soil and gas phase [L^3 M^{-1}], the organic carbon normalized distribution coefficient [L^3 M^{-1}] mass fraction of organic carbon [-] and Henry's constant, respectively.

Once introduced into the subsurface environment, spreading of contaminants depends upon the hydrodynamic dispersion and diffusion in the vapour and aqueous phase. In the unsaturated zone, seepage water and soil air may represent a mobile phase as shown in Fig. 2.4. The immobile phase consists of soil solids including stagnant water (adsorbed and pendular water as well as capillary water). At larger scale, low permeability layers such as clay or silt layers, which allow only very limited advection of groundwater, may be considered as immobile phase. In fractured geologic material, matrix diffusion controls the mass transfer into the immobile phase (Grathwohl, 1998).

During the transport process in the vadose zone, contaminants participate in the phase transfer process (dissolution into soil moisture and sorption to soil components). The transfer to the soil water may lead to leaching of contaminants through the unsaturated zone, potentially leading to transport over the capillary fringe and finally into the groundwater. The contaminants also degrade aerobically in the vadose zone and anaerobically if the oxygen content in the soil gas is depleted in regions close to or within the source zone.

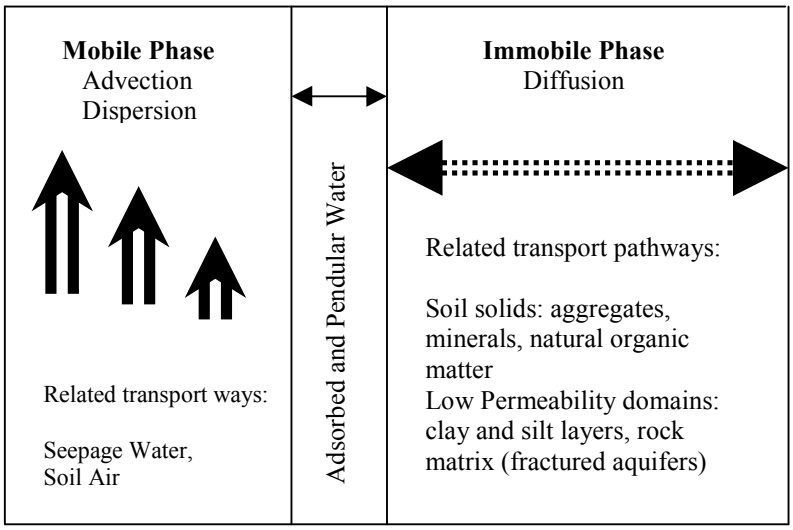

Fig. 2.4: Transport mechanism at the grain scale: mobile and immobile phases (Grathwohl, 1998)

Diffusion is the most dominant transport mechanism in the water unsaturated zone and in low permeability zones such as clay or silt

layers, porous aggregates or particles (grain scale) as well as interface mass transfer between soil air or groundwater. Fig. 2.5 shows the diffusive mass transport within the solid phase (intraparticle and intrasorbent diffusion) and the mass transfer from the solid to the mobile phase.

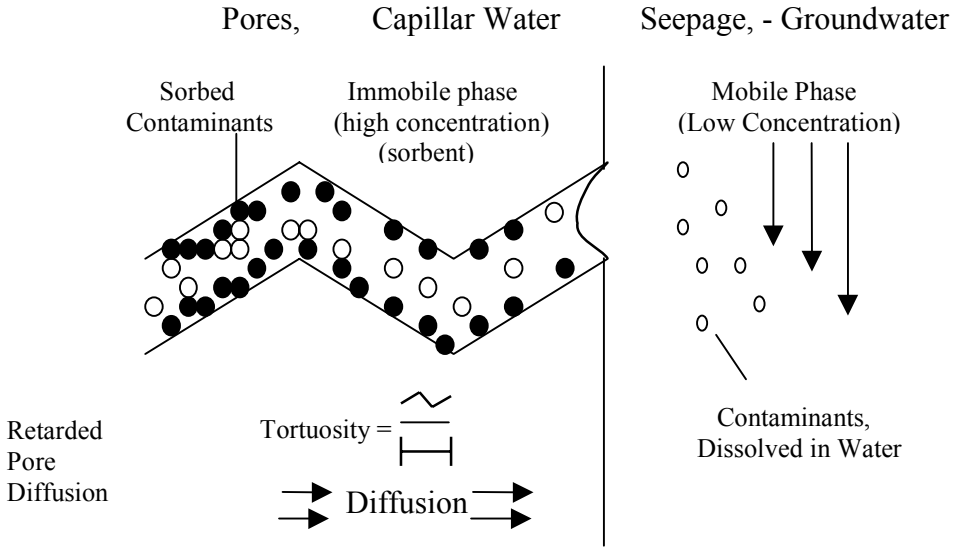

Fig. 2.5: Diffusion in porous particles (Grathwohl, 1998)

Slow diffusion related sorption/desorption affects or even controls the mass transfer between mobile and immobile phases and that results in nonequilibrium transport and hence e.g., long-term sources of contamination for groundwater. Fig. 2.6 shows a conceptual scheme of diffusive mass transfer between mobile and immobile phase for sorptive uptake and release of solutes in natural porous media.

2.2 Sorption phenomena

The general term *sorption* is used to indicate the process in which solutes (ions, molecules or compounds) are distributed between the liquid and the soil/sediment particles or more precisely soil/sediment organic carbon. In soils and sediments two sorption phenomena may be distinguished: adsorption and absorption. Due to the heterogeneous nature of soils and sediments both processes may occur simultaneously.

The sorption processes can be enthalpy and entropy driven, depending on the properties of the solid sorbent and chemical solute (Hamaker and Thomson, 1972). Enthalpy-related forces include van der Walls interactions, electrostatic interactions, hydrogen bonding, ligand exchange, direct and induced dipole-dipole interactions and chemisorption while hydrophobic bonding or partitioning is considered the primary entropy driven force (Bailey, 1972; Hamaker and Thompson, 1972; Koskinen and Harper, 1990 and von Oepen et al., 1991).

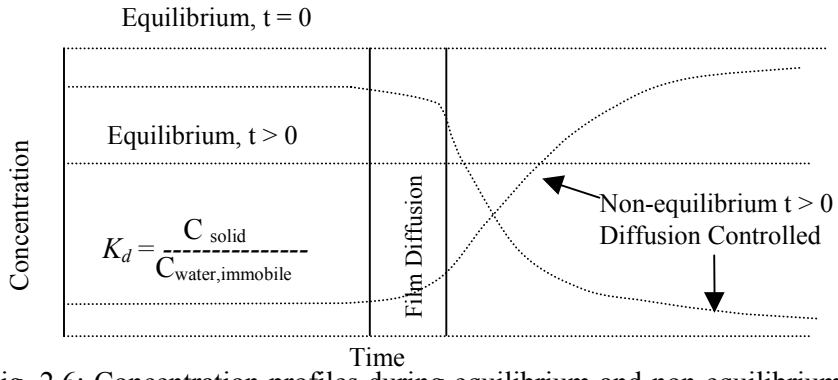

Fig. 2.6: Concentration profiles during equilibrium and non-equilibrium transport of contaminants in the subsurface environment

Sorption processes play a major role in determining the environmental fate and impact of mainly organic chemicals. Sorption affects a variety of specific fate processes, including volatilisation (Chiou and Shoup, 1985), bioavailability (Alexander, 1999; Ditoro et al., 1991), biodegradability (Scow and Johnson, 1997; Miller et al., 1987; Mihelcic and Luthy, 1991; Shelton and Parkin, 1991; Smith, 1991; Webb et al., 1991; Falatko and Novak, 1992; Scow and Alexander, 1992; Weissenfels et al., 1992), photolysis (Tao et al., 1999; Miller et al., 1989) and hydrolysis (Deeley et al., 1991).

Sorption of hydrophobic organic chemicals by natural solids or aquatic sediments can be predominated by partitioning of the dissolved solutes between water and naturally occurring organic matter (NOM) (Chiou et al., 1979; Chiou et al., 1983; Karickhoff et al., 1979). Nonetheless, many studies have found that sorption isotherms for such systems can show substantial deviations from a linear partition model and extremely high sorption capacities. Two basic concepts have been developed to explain such sorption phenomena. While one concept favours the analogy of NOM as a polymer (e.g., Weber et al., 2001) others see the explanation in the heterogeneity of the NOM and the presence of high surface area carbonaceous material (HSACM) with high sorption capacities (e.g., Xia and Ball, 1999; Chiou et al., 2000; Kleineidam et al., 1999).

A comprehensive review on the different varieties of organic matter occurring in soils and sediments (humins, coals, charcoals, soot etc.) and a model to simulate HOCs sorption in heterogeneous solids is provided by Allen-King et al. (2002).

2.2.1 Partitioning

Sorption of organic compounds to natural organic matter (NOM) can be described analogous to Raoult's law, which allows to define directly an inverse empirical relationship between the partition coefficient (K_{om} [L^3 M^{-1}]) and the water solubility S [M L^{-3}] (e.g. Schwarzenbach et al., 1993):

$$K_{om} = \frac{M}{V_{om}\,\rho_{om}\,\gamma_{om}\,S} \qquad (2.1)$$

where γ_{om} is the activity coefficient of a compound in the organic phase - in this case the NOM - and M is the molecular weight of the compound [M mol^{-1}]. γ_{om} equals 1 if partitioning occurs into an ideal organic solvent. V_{om} and ρ_{om} denote the molar volume [L^3 mol^{-1}] and density of OM [M L^{-3}]. If γ_{om} is independent on concentration, then K_{om} represents the slope of a linear sorption isotherm:

$$C_s = K_{om}\,C_w = \frac{M}{V_{om}\,\rho_{om}\,\gamma_{om}}\,\frac{C_w}{S} = K^*_{om}\,\frac{C_w}{S} \qquad (2.2)$$

In the above equation, V_{om} and ρ_{om} are constants for a given organic phase and therefore the sorbed concentration C_s [M M^{-1}] in the organic phase is the same for all compounds with similar values of γ_{om} and similar molecular weights if calculated based on the normalized aqueous concentration (C_w/S). With that a generalized partitioning isotherm can be defined which is based on the water solubility of solutes. K^*_{om} (= K_{om} S) is then a unit-equivalent partitioning coefficient [e.g. in mg kg^{-1}], which can be considered as a constant for similar compounds in a given partitioning medium. Although γ_{om} in some cases may depend slightly on the concentration, the resulting sorption isotherms are essentially linear as long as the concentration of the compound does not change the organic matter/phase significantly (e.g. ρ_{om}, V_{om}, structure etc.).

2.2.2 Adsorption – pore filling

Adsorption of organic compounds in activated carbon and other porous materials (e.g. charcoal, bituminous coal, anthracite etc.; Kleineidam et al., 2002) is very well described by a pore-filling mechanism, where the maximum sorption capacity is given by the micropore (and mesopore) volume of the adsorbent. It is generally described by the Dubinin-Polanyi (DP) equations originally derived for vapour phase adsorption (Dubinin, 1960; 1975). The DP-equations are based on Polanyi's potential theory which defines the adsorption potential [J mol^{-1}] as $\varepsilon = R\,T\,\ln P_o/P$. Manes and coworkers (Manes, 1998) extended the DP-equations to aqueous systems and defined the adsorption potential based on the solubility of the

compound: $\varepsilon_{sw} = RT \ln (S/C_w)$. The Polanyi-Manes model describes adsorption as:

$$C_s = V_o \rho_o \exp\left[-\left(\frac{R\,T \ln \frac{S}{C_w}}{E}\right)^b\right] \qquad (2.3)$$

where V_o and ρ_o denote the maximum adsorption capacity [L^3 M^{-1}] and the density of the adsorbed organic compound [M L^{-3}] (to calculate the adsorbed concentration C_s [M M^{-1}]). R and T denote the ideal gas constant [J mol^{-1} K^{-1}] and the temperature [K]. E [J mol^{-1}] is the characteristic free energy of adsorption and b is an empirical exponent. In adsorption studies with activated carbon often the free energy of a reference compound (e.g. benzene) E_o in a specific adsorbent and an empirical coefficient β are used to estimate E: $E = E_o \beta$ (Choma et al., 1993; Wood, 2001) According to Crittenden et al. (1999) and Wood (2001), β [-] is an 'affinity' or 'similarity' coefficient, which for example can be estimated from the ratios of molar volumes, molar polarizabilities or parachors between a sorbate and the reference compound. In extension to the original work (Dubinin, 1975), Condon (2000a/b) showed by quantum-mechanical simulations, that the DP-equations hold over a wide concentration range (> 5 orders of magnitude) and that they also apply for open surfaces. If the standard deviation σ of log-normal distributed adsorption energies equals 0.25 the Dubinin-Radushkevich equation ($b = 2$) is obtained. $\sigma = 0.5$ results in $b = 1$ and eq. (2.3) corresponds to the Freundlich model (if furthermore $R\ T$ equals E the linear "Henry" sorption isotherm is obtained).

The advantage of this approach is that as in eq. (2.2) a generalized adsorption isotherm can be derived, which for compounds with similar E in eq. (2.3) (or βE_o) predicts the same loading onto a given porous adsorbent (e.g. activated carbon, charcoal) at a given relative concentration of the solute (C_w/S). Solubility normalized sorption isotherms are commonly used in activated carbon filtration (Crittenden et al., 1999; Manes, 1998; Paulsen and Cannon, 1999; Wood, 2001).

2.2.3 Heterogeneous sorbents – partitioning and pore-filling combined

Due to the heterogeneous nature of NOM, sorption may be treated as a combination of processes resulting in combined sorption isotherms. Xia and Ball (1999) were first to introduce the combination of partitioning (linear isotherm) and pore-filling (non-linear isotherm) to fit experimental data on sorption of organic compounds in soils. Combining eqs. (2.2) and 2.3) results in:

$$C_s = V_o\ \rho_o \exp\left[-\left(\frac{R\,T\left(-\ln \frac{C_w}{S}\right)}{E}\right)^b\right] + f_{om}\, K^*_{om}\, \frac{C_w}{S} \qquad (2.4)$$

where f_{om} denotes the fraction of the partitioning medium [M M^{-1}] in the sample. In this model, V_o and E are the only fitting parameters in the above equation. K_{om} (= K^*_{om}/S) can be predicted from empirical relationships e.g. following Schwarzenbach et al. (1993) or K_{oc} - K_{ow} relationships (Tab. 2.1) and the fraction of organic carbon in the sample (f_{oc}) (e.g. Karickhoff et al., 1979; Chiou et al., 1983). K_{oc} is the f_{oc}-normalised sorption coefficient in soils and sediments or organic matter. Assuming that in average $f_{oc} = 0.58\ f_{om}$ yields $K_{oc} = 1.724\ K_{om}$ (Lyman et al., 1982).

Tab. 2.1: Representative example of regression models used to estimate log K_{oc} from log K_{ow}

Regression equation	Chemical class	References
Class specific		
$\log K_{oc} = 1.00 \log K_{ow} - 0.21$	PAHs, $\log K_{ow} > 2$	Karickhoff et al., 1979
$\log K_{oc} = 0.99 \log K_{ow} - 0.35$	PAHs, $\log K_{ow} < 2$	Karickhoff et al., 1981
$\log K_{oc} = 0.36 \log K_{ow} + 1.15$	$\log K_{ow}$ from 1to 2.4	Sontheimer et al.,1983
$\log K_{oc} = 0.81 \log K_{ow} + 0.07$	$\log K_{ow}$ from 2.4 to 7.4	Sontheimer et al.,1983
$\log K_{oc} = 0.94 \log K_{ow} - 0.54$	Chlori. hydroc., PAHs	Chiou et al.,1983
$\log K_{oc} = 1.03 \log K_{ow} - 0.18$	Chlori. hydroc., pesticides	Rao and Davidson,1980
$\log K_{oc} = 0.402 \log K_{ow} + 1.017$	Pesticides	Kanazawa, 1989
$\log K_{oc} = 0.433 \log K_{ow} + 0.92$	Carbamates	Gerstl,1990
General		
$\log K_{oc} = 0.81 \log K_{ow} + 0.10$	Hydrophobics	Sabljic et al.,1995
$\log K_{oc} = 0.52 \log K_{ow} + 1.02$	Nonhydrophobics	Sabljic et al.,1995
$\log K_{oc} = 0.903 \log K_{ow} + 0.094$	Wide variety	Baker et al.,1997

Fig. 2.7 shows an example for a combined pore-filling - partitioning sorption isotherm. Pore-filling contributes most to the overall sorption at relatively low concentrations (and partitioning dominates at high concentration) and therefore maybe considered as the main reason for the often observed nonlinearity of sorption isotherms. The combination of pore-filling and partitioning in a wide variety of geosorbents can be fitted very well by the Freundlich model (Allen-King et al., 2002; Kleineidam et al., 2002).

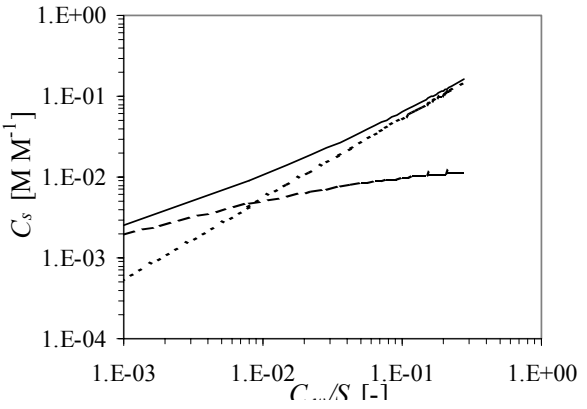

Fig. 2.7 Example of a combined pore-filling - partitioning sorption isotherm. Solid line: partitioning + adsorption (pore-filling); dotted line: only partitioning; dash line: only adsorption (pore-filling). K_p (partition coefficient) = 3.7 , C_s (adsorbed concentration) = 0.01

2.2.4 Normalization of sorption (Freundlich) isotherms

Since both, the partitioning and the pore-filling theory suggest solubility normalized concentrations it may be concluded that other sorption models such as the most frequently used Freundlich equation (Freundlich, 1909) should be normalized by the compounds solubility. This is already applied e.g. in activated carbon adsorption (Manes, 1998) and was recently suggested for soils by others (e.g. Carmo et al., 2000; Allen-King et al., 2002; Kleineidam et al., 2002). It has the big advantage, that a unit equivalent-Freundlich coefficient can be used:

$$C_s = K_{Fr} C_w^{1/n} = K_{Fr}^* \left(\frac{C_w}{S} \right)^{1/n} \qquad (2.5)$$

where K_{Fr} and K^*_{Fr} denote the Freundlich sorption coefficient and the unit-equivalent Freundlich coefficient, respectively ($K^*_{Fr} = K_{Fr} S^{1/n}$). *1/n* is the empirical Freundlich exponent. K^*_{Fr} has the advantage that ambiguities

concerning the concentration dependent nature of the K_{Fr} are avoided. Again for similar compounds K^*_{Fr} should be more or less constant for a given adsorbent. If this is the case, then from eq. (2.5) an inverse linear relationship between a distribution coefficient (K_d) obtained at a given relative concentration (C_w/S) and S is expected (Allen-King et al., 2002):

$$K_d = \frac{C_s}{C_w} = K_{Fr}\, C_w^{1/n-1} = \frac{K^*_{Fr}}{S}\left(\frac{C_w}{S}\right)^{1/n-1} \tag{2.6}$$

Since the Freundlich model fits linear and non-linear sorption data regardless of the sorbent (and the sorption mechanism), this inverse linear relationship between K_d and S is expected to hold in general in many soil and sediment samples.

2.2.5 Sorption kinetics

In the sorption model and in the K_{oc} approach, it is postulated that sorption is a rapid process and equilibrium is reached fast between the sorbed phase and the aqueous phase. In the recent past, it has been observed from several studies that sorption may not reach equilibrium within the time period characteristics for column or even batch experiments. Ball and Roberts (1991) and Grathwohl and Reinhard (1993) observed an increasing sorption of PCE and TCE in batch experiments over several months. In column experiments, asymmetrical breakthrough and extended tailing as well as increasing sorption with decreasing flow velocities were attributed to nonequilibrium conditions (Nkedi-Kizza et al., 1989; Brusseau, 1992; Kookana et al., 1993).

Generally two procedures govern the rate limited or nonequilibrium sorption: transport of the substance to the sorption site and the sorption process itself (Brusseau et al., 1991a, b). Transport related nonequilibrium typically results from the existence of a heterogeneous flow domain. Sorption related nonequilibrium caused by the rate limited interaction between the sorbate and sorbent may be the result of chemical nonequilibrium (chemisorption) or diffusive mass transfer limitations, i.e., diffusion of solutes within the pores of microporous particles (intraparticle diffusion) or molecular diffusion into macromolecular organic matter (intrasorbent diffusion) (Ball and Roberts, 1991, Grathwohl and Reinhard, 1993; Brusseau et al., 1991a, b). According to Weber and Huang (1996) and Leboeuf and Weber (1997), condensed regions in the soil organic matter with properties similar to microporous aggregates may also be responsible for slow sorption/desorption kinetics. However, since every kind of sorption site is reached via intraparticle pores, it is in most cases not possible to distinguish between the different processes.

Under steady state conditions, the diffusive contaminant mass flux in the porous medium depends on the concentration gradient and is expressed by Fick's 1st law:

$$F = -D_e \frac{\partial C}{\partial x} \tag{2.7}$$

where F, D_e and C refer to the mass flux [M L^{-2} T^{-1}], effective diffusion coefficient [L^2 T^{-1}] and the solute concentration [M L^{-3}] in the pore water. The diffusion coefficient D_e can be determined from the molecular diffusion coefficient of the solute in the water and accounts for the porosity and the tortuosity:

$$D_e = \frac{D_{aq}\varepsilon}{\tau_f} \tag{2.8}$$

where D_{aq}, ε and τ_f denote the aqueous diffusion coefficient [L^2 T^{-1}], intraparticle porosity [-] and the tortuosity factor of the intraparticle pores [-]. In case of transient boundary conditions, the term D_a [L^2 T^{-1}] (apparent diffusion coefficient) is used which incorporates the physical effects of diffusive restriction due to tortuosity, intraparticle porosity as well as retardation of solutes due to sorption. For a linear sorption isotherm (constant K_d), D_a can be defined as:

$$D_a = \frac{D_{aq}\varepsilon}{(\varepsilon + K_d \rho_b)\tau_f} = \frac{D_e}{\alpha} \tag{2.9}$$

where the term (ε + K_d ρ_b) is known as the capacity factor (α) of the porous medium [-].

For non-linear sorption isotherms, K_d and thus D_a become concentration dependent quantities. As a first linear approximation for a Freundlich type non-linear sorption isotherm, D_a can be estimated for a certain concentration range by combining eqs. (2.6: $K_d = K_{fr}\, C_w^{\,1/n-1}$) and (2.9) as:

$$D_a = \frac{D_e}{\varepsilon + K_{fr} C_w^{\frac{1}{n}-1} \rho_b} \quad (2.10)$$

The tortuosity factor τ_f included in eqs. (2.8) and (2.9) is used to evaluate the effect of diffusion paths at the intragrain scale compared to straight distances. This factor cannot be measured independently and therefore is often used as a fitting parameter. The tortuosity factor can be estimated on the basis of intraparticle porosity analogous to the electrical conductivity in porous media (Archie, 1942), e.g., $\tau_f = \varepsilon^m$ where m is an empirical exponent that in sedimentary rock is usually close to 2.

The long term sorptive uptake in batch experiments can be modelled using Fick's 2nd law in spherical co-ordinates:

$$\frac{\partial C}{\partial t} = D_a \left[\frac{\partial^2 C}{\partial r^2} + \frac{2}{r} \frac{\partial C}{\partial r} \right] \quad (2.11)$$

where C, t and r denote concentration [M L^{-3}], time [T] and radial distance [L] from the centre of the sphere, respectively.

For a constant D_a (e.g. linear sorption isotherm) and a variety of initial and boundary conditions analytical solutions of eq. (2.11) are available which allow the calculation of the solute mass in the sphere after a time t as well as sorption and desorption rates (bath of limited volume).

2.2.6 Temperature dependence of sorption equilibrium

The short-term sorption of organic chemicals in soil/sediment is often described by either a linear distribution coefficient, $K_{d,}$ which describes the concentration ratio between sediment and water or a partition coefficient K_{oc} when the sorption is expressed per unit mass of organic carbon. The variation of K_d or K_{oc} with temperature gives information about the thermodynamic quantities of equilibrium partitioning: Gibbs´ free energy ($\Delta G°$), enthalpy ($\Delta H°$) and entropy ($\Delta S°$). These thermodynamical quantities give insight in the sorption processes involved. A net sorption occurs when the free energy of the sorptive exchange is negative (Hassett and Banwart, 1989). $\Delta G°$ is related to $\Delta H°$ and $\Delta S°$ through:

$$\Delta G° = \Delta H° - T\Delta S° \quad (2.12)$$

where $\Delta G°$, $\Delta H°$, T and $\Delta S°$ denote changes in Gibbs´ free energy [kJ mol^{-1}], changes in enthalpy [kJ mol^{-1}], temperature [K] and changes in entropy [kJ mol^{-1} K^{-1}], respectively.

At equilibrium, the equilibrium constant K is related to the standard free energy change by:

$$\Delta G° = -RT \ln K \quad (2.13)$$

where R represents the universal gas constant [8.3144×10^{-3} kJ K^{-1} mol^{-1}].

Taking the derivatives of both sides, yields,

$$\frac{d(\ln K)}{dT} = \frac{\Delta G°}{RT^2} \approx \frac{\Delta H°}{RT^2} \quad (2.14)$$

Assuming that for small changes in temperature $\Delta S^0 \approx 0$, we can approximate $\Delta G° \approx \Delta H°$, the standard enthalpy (Schnoor, 1996). Integrating the equation yields:

$$\int_{K_1}^{K_2} d(\ln K) = \int_{T_1}^{T_2} \frac{\Delta H°}{RT^2} dT \quad (2.15)$$

The result is the van't Hoff equation, after rearranging:

$$\ln \frac{K_1}{K_2} = \frac{\Delta H°}{R} \left(\frac{1}{T_2} - \frac{1}{T_1} \right) \quad (2.16)$$

which becomes,

$$\Delta H° = R \frac{\ln \frac{K_1}{K_2}}{\frac{1}{T_2} - \frac{1}{T_1}} \quad (2.17)$$

where K_1, K_2, $\Delta H°$, T_1 and T_2 denote the equilibrium constant or distribution coefficient at the new temperature [- or L^3 M^{-1}], the equilibrium constant at the reference temperature (e.g. 20° C), the standard enthalpy (kJ mol^{-1}) at 20° C, the new temperature [K] and the reference temperature [K].

The understanding of the influence of temperature variations on sorption equilibrium and kinetics is also important for transferring values obtained at room temperature (e.g., 20 -

25 °C) to environmental temperature. In other words, if the sorption enthalpy is known then K or K_d can be calculated following eq. (2.17) for a temperature of interest. For temperature changes more that ± 30 °C, errors will increase and a more rigorous analysis including entropy effects on $\Delta G°$ ($\ln K = - \Delta G^0 / RT$) is required.

The influence of temperature on the sorption process could also be used to reveal thermodynamic information of the process involved, e.g., the type of sorptive interaction and the properties of organic matter. Hamaker and Thompson (1972) state that the effect of temperature on the sorption equilibrium is a direct indication of the strength of sorption. For weaker bonds, less influence of temperature is expected because of the lower equilibrium sorption enthalpy. For most compounds, equilibrium sorption decreases with increasing temperature. According to Chiou et al., (1979) increased sorption at higher temperatures can be expected for compounds for which solubility decreases at higher temperature. This was observed by Chiou et al., (1979) for 1,1,1-trichloroethane.

The increase in K_d with a decrease in temperature can be predicted assuming that the aqueous phase activity coefficient is the driving force for PAHs like phenanthrene as (Piatt et al., 1996):

$$\frac{K_{d,4}}{K_{d,20}} \approx \left(\frac{X_{s,20}}{X_{s,4}} \right) \exp\left[-\left(\frac{\Delta S_f}{R} \right) T_m \left(\frac{1}{T_4} - \frac{1}{T_{20}} \right) \right] \tag{2.18}$$

where X_s, T, T_m, ΔS_f denote the mole fraction solubility at temperatures 4 °C and 20 °C, for example [-], experimental temperature [K], the melting point of phenanthrene [K] and entropy of fusion [J mol^{-1} K^{-1}], respectively. For planar rigid molecules like phenanthrene ΔS_f is nearly constant at 50 - 62 J mol^{-1} K^{-1} (Karickhoff, 1984). The increase in K_d with decrease in temperature is mainly related to water solubility of phenanthrene at reduced temperature. Solubility of PAHs decreases by 2-3 times with a decrease in temperature of 20 °C (S of phenanthrene at 20 °C = 6.1 mmol/m³) to 4 °C (S of phenanthrene at 4 °C = 2.09 mmol/m³).

2.3 Solute transport

Two basic elements affecting the transport and fate of contaminants in the subsurface are properties of subsurface materials and physico-chemical and biological properties of contaminants. The natural processes affecting the subsurface fate and transport are hydrodynamic, abiotic (non-biological) and biotic processes.

Hydrodynamic processes affect contaminant transport by impacting the flow of groundwater (in terms of quantity of flow and flow paths followed) in the subsurface. Examples of hydrodynamic processes are advection and dispersion. Abiotic processes affect contaminant transport by causing interactions between the contaminant and the stationary subsurface material (e.g., sorption) or by affecting the form of the contaminant (e.g., hydrolysis, redox reactions). Biotic processes can affect contaminant transport by metabolising or mineralising the contaminant (e.g., organic contaminants) or possibly by utilising the contaminant in the metabolic process (e.g., nutrients, nitrate under denitrifying conditions). Examples of biotic processes are aerobic, anoxic and anaerobic biodegradation. All the processes may take place simultaneously and lead to similar results (spreading of contaminants plume and decrease of concentration). It is sometimes difficult to assign the relevant process from the observed transport behaviour. However, in order to develop an understanding of the basic mechanics of each of the processes some sort of categorized approach is necessary. Abiotic processes (e.g., sorption) were already discussed in chapter 2.2. Here hydrodynamic processes will be discussed rather elaborately as this processes also affect the transport of dissolved constituents in the subsurface.

2.3.1 Hydrodynamic processes

The combined hydrodynamic effects can be subdivided into two basic processes: advection and hydrodynamic dispersion.

2.3.1.1 Advection

The basic equation governing 1D fluid flow through a saturated medium is known as Darcy's law and can be written as:

$$q = -K\frac{\partial h}{\partial x} \tag{2.19}$$

where q, K and $\partial h/\partial x$ denote the specific discharge (Darcy's velocity) of the fluid [L T^{-1}], hydraulic conductivity [L T^{-1}] and hydraulic gradient [-], respectively.

Advection is the portion of solute movement that is solely attributed to the transport by the bulk motion of flowing groundwater. The actual velocity or average linear velocity (v_a) in advective transport can readily be obtained by dividing Darcy's velocity by the fractional effective porosity under saturated conditions:

$$v_a = -\frac{K}{n_e}\frac{\partial h}{\partial x} \tag{2.20}$$

where v_a, and n_e denote the average linear velocity [L T^{-1}] and the effective porosity [-], respectively. The negative sign in Darcy's equation means water flows from areas of high head to low head. To achieve a positive value for v_a a negative hydraulic gradient is required.

2.3.1.2 Hydrodynamic dispersion

Hydrodynamic dispersion occurs as a consequence of two different processes – mechanical dispersion and diffusive dispersion. Both of them lead to a spreading of a solute during transport. The hydrodynamic dispersion coefficient of a solute during transport can be expressed mathematically as:

$$D_H = \alpha_l v_a + nD_{aq}/\tau_f \tag{2.21}$$

where the first term on the right hand side of eq. (2.21) corresponds to mechanical dispersion and the second term represents the diffusive dispersion. D_H, α_l, D_{aq}, n and τ_f denote the hydrodynamic dispersion coefficient [L^2 T^{-1}], mechanical longitudinal dispersivity [L], aqueous diffusion coefficient [L^2 T^{-1}] porosity and tortuosity factor [-], respectively. This tortuosity factor now refers to the inter-particle pore space in contrast to τ_f in eq. (2.8).

The mechanical dispersion coefficient is a function of the magnitude of v_a and accounts for the spreading of the solute during transport due to the variations in the seepage velocity (Freeze and Cherry, 1979). Dispersivity is closely related to the scale under consideration. At larger scale α_l reflects aquifer heterogeneities, at the pore scale diffusion and differential pore velocities. Upscaling generally leads to increasing values of D_H as more and more inhomogeneties are encountered by the transported particles. Pore scale diffusivity measured in the laboratory is on the order of centimeters whereas macro dispersivity measured in the field is on the order of meters or more. Neuman (1990) made a study of the relationship between the apparent longitudinal mechanical dispersivity (α_l, m) and flow length (x, m). He found that for flow paths less than 3500 m long these could be related by the equation:

$$\alpha_l = 0.0175x^{1.46} \tag{2.22}$$

The tortuosity factor, τ_f [-], is purely geometric and accounts for the increased distance of transport and can be expressed as:

$$\tau_f = \left(\frac{l_e}{l}\right)^2 \tag{2.23}$$

where l is the straight line, macroscopic distance between two points defining the flow path [L] and l_e is the actual, microscopic or effective distance of flow through the soil between the two same points. Since $l_e > l$ for porous media, τ_f becomes more than 1. In some cases, the tortuosity factor has been defined as the reciprocal of eq. (2.23) and, therefore, will have a value less than unity (Porter et al., 1960; Olsen and Kemper, 1968; Bear, 1972). Values of τ_f using the reciprocal eq. of (2.23) are reported to be in the range from 0.01 to 0.84 for saturated soils and from 0.025 to 0.57 for unsaturated soils (Shackelford and Daniel, 1991a, b). The determination of dispersion and diffusion coefficients is generally accomplished via

laboratory testing (e.g., column method) or through calculations using the inverse technique.

Although diffusive fluxes are generally small and advective transport, if present, accounts for the bulk shape of solute movement, diffusion plays an important role in the mass transfer from low permeability zones in the top soils, across the interface between the water-saturated and unsaturated zone - the capillary zone. If there is only a concentration gradient, v_a and therefore mechanical dispersion (first term on the right – hand side of eq. (2.21)) are zero. The one-dimensional diffusive transport in saturated soil can be expressed following Fick's first law:

$$F = -D\frac{\partial C}{\partial x} \qquad (2.24)$$

where D refers to the diffusion coefficient [L^2 T^{-1}] which provides a measure for the rate at which the molecules spread.

2.4 Modelling of solute transport

Within the last several years a number of mathematical models of groundwater, particularly solute (contaminant) transport models have been developed with a view: to gain a better understanding of the fate and transport of chemicals by quantifying their movement, reactions etc.; to determine chemical exposure concentrations to aquatic organisms and /or human in the past, present or future and to predict the future condition under various loading scenarios (e.g., groundwater risk assessment).

In this section some analytical solutions of 1D solute transport models will be discussed which will later be used for fitting the column data. Based on fitting of experimental data these analytical models can be used for the risk assessment in groundwater. Moreover, an analytical solution is developed to model the breakthrough curves for the quantification of the effect of matrix diffusion of contaminants in a fine grained soil (low permeability regions) coupled with the effect of preferential flow paths (macropores).

2.4.1 Equilibrium model - continuous input

The vertical transport of a solute dissolved in water through the soil can be described by the partial differential transport equation:

$$\frac{\partial C}{\partial t} = D_H \frac{\partial^2 C}{\partial x^2} - v_a \frac{\partial C}{\partial x} - \frac{\rho_b}{n}\frac{\partial S^*}{\partial t} - \lambda C \qquad (2.25)$$

The first, second, third and fourth term on the right hand side of eq. (2.25) correspond to dispersion, advection, sorption and reaction, respectively. C, t, x, n, S^*, λ denote the liquid phase concentration [M L^{-3}], time [T], distance along flow path [L], volumetric water content or porosity of the saturated media [L^3 L^{-3}], solid phase concentration [M M^{-1}] and first order decay coefficient in the liquid phase [T^{-1}].

Eq. (2.25) allows for analytical solutions for simple initial (IC) and boundary conditions (BCs). For a continuous input of contaminant at t = 0, the following initial and boundary conditions apply:

IC : $C(x,0) = 0$ for $x > 0$

BC : $C(0,t) = C_0$ $t \geq 0$

BC : $C(\infty,t) = 0$, $t \geq 0$

For the above IC and BCs, Ogata and Banks (1961) obtained the following solution to the advection - dispersion eq. of (2.25) for a non-sorbed and non-reactive substance in saturated homogeneous porous media (semi-infinite case with $S^* = 0$ and $\lambda = 0$):

$$\frac{C}{C_0} = 0.5\left[\operatorname{erfc}\left(\frac{x - v_a t}{2\sqrt{D_H t}}\right) + \exp\left(\frac{v_a x}{D_H}\right)\operatorname{erfc}\left(\frac{x + v_a t}{2\sqrt{D_H t}}\right)\right] \qquad (2.26)$$

where erfc represents the complementary error function. When the dispersivity of the porous medium is large or when x or t is large, the second term on the right hand side of the eq. (2.26) is negligible. In situations where the above boundary conditions are applicable and where the groundwater velocity is so small that mechanical dispersion is negligible relative to molecular diffusion, eq. (2.26) reduces to a one

dimensional solution (Crank, 1975) of Fick's 2nd law:

$$\frac{C}{C_0} = \text{erfc}\left(\frac{x}{2\sqrt{D_e t}}\right) \tag{2.27}$$

where D_e refers to the effective diffusion coefficient [$L^2\ T^{-1}$].

In case of retarded chemicals (linear isotherm) involving first-order reaction kinetics eq. (2.26) can be written as (considering only dissolved phase decay),:

$$\frac{C}{C_0} = 0.5\left[\text{erfc}\left(\frac{x - v_a/R_f\ t}{2\sqrt{D_H/R_f\ t}}\right) + \exp\left(\frac{v_a x/R_f}{D_H/R_f}\right)\text{erfc}\left(\frac{x + v_a/R_f\ t}{2\sqrt{D_H/R_f\ t}}\right)\right]\exp(-\lambda / R_f t) \tag{2.28}$$

where R_f is the retardation factor that can be obtained from regression correlation or determined experimentally.

In case of a linear sorption coefficient (K_d), the retardation factor R_f can be determined as:

$$R_f = 1 + \frac{K_d \rho_b}{n} \tag{2.29}$$

where ρ_b [ML^{-3}] is bulk density and n [-] is the porosity. Generally for different soilds or aquifer materials ρ_b and n do not vary to the extent that K_d varies; therefore R_f depends most strongly on K_d. In case of non-linear sorption isotherm the above expression takes the form:

$$R_f = 1 + \frac{K_{fr} C_w^{\,1/n-1} \rho_b}{n} \tag{2.30}$$

The impact of the above mentioned processes on the fate of a solute can be visualised by computing the breakthrough curves and concentration profiles illustrated in Fig. 2.8.

The first breakthrough curve (1) in Fig. 2.8 is slightly s-shaped due to dispersion, but the mean travel time is equal to the mean residence time of water molecules in the porous media (PV = 1). The second curve is more s-shaped because more time has elapsed for dispersion and the retardation factor is 5. Curve 2 has $\lambda = 0$, i.e. no degradation reactions. The third curve illustrates breakthrough for a contaminant that disperses, sorbs and undergoes a first order decay reaction as in eq. (2.25). The steady state concentration is less than the initial contaminant concentration C_0 because of degradation.

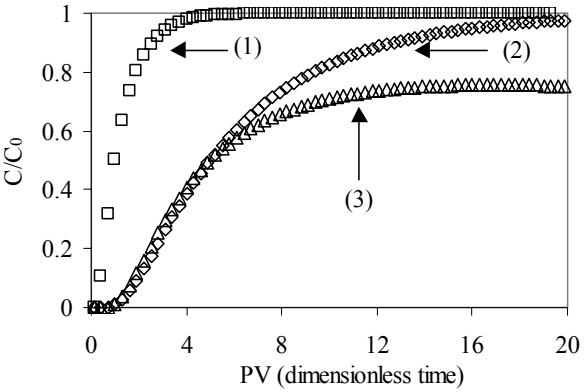

Fig. 2.8: Normalised concentration versus time breakthrough curves showing the effect of dispersion, sorption and first order kinetic reactions on contaminant fate and transport in porous media. Symbols used: squares: advection plus dispersion; diamonds: advection, dispersion plus sorption; triangles: advection, dispersion, sorption plus biodegradation. R_f = 5, HL = 0.5 year, α_l = 2 cm

2.4.2 Equilibrium model – Dirac pulse input

If the source of contamination is not continuous or a step function but rather a pulse input (e.g. pesticide application in the field) where mass is injected into a unit area, the partial differential eq. of (2.25) has to be solved for the following initial and boundary conditions:

IC: $C\,(x,0) = M/A\,\delta\,(x)$

BC: $C\,(+\infty,t) = 0$

BC: $C\,(-\infty,t) = 0$

Where δ and M/A denote the Dirac function and the injected mass per cross sectional area.

The solution for an infinite case and for non-sorbing but reactive/degrading chemicals is given as follows (Sun, 1996):

$$C(x,t) = \frac{M}{An\sqrt{4\pi D_H t}} \exp\left[-\frac{(x - v_a t)^2}{4 D_H t} - \lambda t \right] \tag{2.31}$$

where M, A and x denote the mass applied [M], area [L²] and length [L], respectively.

In case of retarded chemicals the above equation can be rearranged as:

$$C(x,t) = \frac{M / R_f}{An\sqrt{4\pi \frac{D_H}{R_f} t}} \exp\left[-\frac{\left(x - \frac{v_a}{R_f} t \right)^2}{4 \frac{D_H}{R_f} t} - \frac{\lambda}{R_f} t \right] \tag{2.32}$$

where R_f stands for the retardation factor defined before.

2.4.3 Nonequilibrium model

It is evident that the transport of solute in soil/groundwater frequently occurs under nonequilibrium conditions. The processes responsible for nonequilibrium are the rate limited mass transfer which can happen during both the sorption (chemical nonequilibrium) and transport processes (physical nonequilibrium) in porous media consisting of a mobile and an immobile region. The reasons for such nonequilibrium were discussed in section 2.2.5.

Various models have been developed to describe nonequilibrium solute transport in porous media. The most common approaches include two site models, which refer to the chemical nonequilibrium or two region models, which account for physical nonequilibrium (Coats and Smith, 1964; Selim et al., 1976; van Genuchten and Wierenga, 1976)

In one-dimensional form, a two region model can be expressed as a partial differential equation by considering mobile and immobile phase mass balance:

$$(n_m + \rho_b K_d)\frac{\partial C_m}{\partial t} + [n_{im} + \rho_b K_d]\frac{\partial \overline{C_{im}}}{\partial t} + v_m n_m \frac{\partial C_m}{\partial x} - n_m D_H \frac{\partial^2 C_m}{\partial x^2} = 0 \tag{2.33}$$

where C_m, $\overline{C_{im}}$, n_m, n_{im}, ρ_b and v_m denote the mobile region concentration [M L^{-3}], average concentration in immobile region [M L^{-3}], mobile region porosity [-], immobile region porosity [-], bulk density [M L^{-3}] and mobile region velocity [L T^{-1}], respectively. The term $\partial\overline{C_{im}} / \partial t$ represents the diffusion limited uptake by or release from the immobile zone.

The spherical intraparticle diffusion model can be coupled to the two region model. Considering a linear sorption isotherm, this spherical diffusion model can be written as:

$$\frac{\partial C_{im}}{\partial t} = \frac{D_a}{r^2}\frac{\partial}{\partial r}\left[r^2 \frac{\partial C_{im}}{\partial r} \right] \tag{2.34}$$

where C_{im} and r denote the concentration of solute in the pore space of the immobile region [M L^{-3}] and radial distance [L], respectively and D_a is given by eq. (2.9). The average immobile concentration for use in eq. (2.33) is found by integrating the concentration distribution with respect to the radial co-ordinate:

$$\overline{C_{im}} = \frac{3}{4\pi a^3}\int_0^a 4\pi r^2 (n_{im} + \rho_b K_d) C_{im} dr \tag{2.35}$$

where a refers to the sphere radius [L]. The initial and boundary conditions for the mobile and immobile regions are:

Mobile region:

IC: $C_m\ (x>0,\ t=0) = 0$ (initially uncontaminated model domain)

BC: $C_m\ (x=0,\ t) = C_0$ (continuous injection)

Immobile region:

IC: $C_{im}(x,r,t=0) = 0$ (initially uncontaminated model domain)

BC: $C_{im}(x,r=a,t) = C_m(x,t)$ (interaction between mobile and immobile phase)

BC: $\partial C/\partial r\ (x,r=0,t) = 0$ (no mass flux at the centre of the spheres)

Using the above initial and boundary conditions, the following approximate solution to eq. (2.33) was adapted from an asymptotic solution also given by Rosen (1954):

$$\frac{C}{C_0}(x,t) = 0.5\,\mathrm{erfc}\left\{\left[1+\frac{n}{(1-n)\rho_a K_d}\left(1-\frac{v_a t}{x}\right)\right]\frac{1}{2\sqrt{\dfrac{a^2 n v_a}{15 D_a \rho_a K_d (1-n)x}}}\right\} \qquad (2.36)$$

where ρ_a denotes the apparent particle density [M L^{-3}] which includes particle porosity.

The approximate solution is valid if the following condition holds:

$$\frac{3D_a\rho_a(1-n)K_d x}{n v_a a^2} \geq 40 \qquad (2.37)$$

2.4.4 Pesticide analytical model (PESTAN)

The PESTAN (pesticide analytical) model is a computer code developed by Enfield et al., (1982) for US EPA for estimating the vertical transport of organic solutes through soil to groundwater. The vertical transport is simulated as a slug of contaminated water that migrates into a homogeneous soil.

A granular pollutant is dissolved as a slug with a concentration equal to the pollutant solubility. The total available mass is defined as the mass existing at the time of recharge (Fig. 2.9). When the time of recharge is the same as the time of application all the pollutants enter the soil. When the time of recharge occurs after the time of application pollutant mass will be lost due to decay, hence the dissolved mass entering the soil will be less than the original mass of the pollutant (Fig. 2.10).

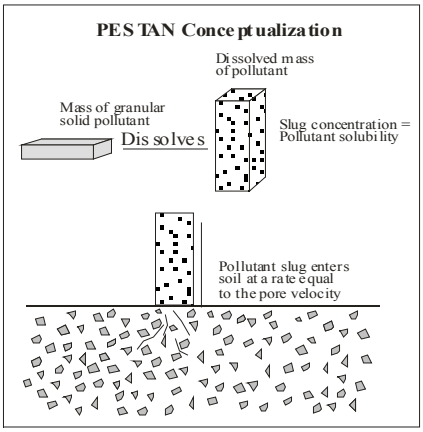

Fig. 2.9: PESTAN conceptualisation of pollutant migration through the soil system

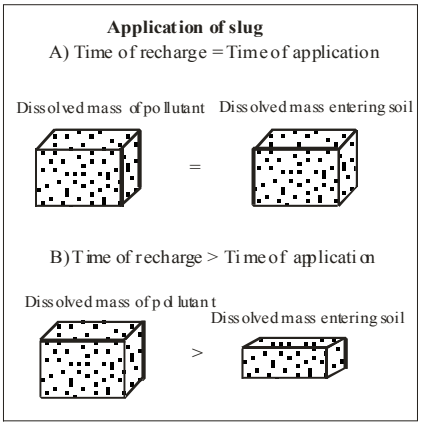

Fig. 2.10: PESTAN conceptualisation of pollutant application

Mathematical Formulation:

The mathematical model is developed based on the advective-dispersive-reactive transport eq. (2.25). The solution of this partial differential equation is obtained with the following initial and boundary conditions (Enfield et al., 1982):

$$(ICs)\qquad C(x,t=0) = \begin{cases} 0, & -\infty < x < -x_0 \\ C_0, & -x_0 \leq x < 0 \\ 0, & 0 \leq x < \infty \end{cases}$$

$$(BC)\qquad C(x,t) = 0,\ |x| \to \infty$$

The solution is given as follows:

$$C(x,t)=\frac{C_0}{2}\exp(-\lambda t)\left\{\operatorname{erf}\left[\frac{x+x_0-\frac{v_a t}{R_f}}{2\sqrt{\frac{D_H}{R_f}t}}\right]-\operatorname{erf}\left[\frac{x-\frac{v_a}{R_f}t}{2\sqrt{\frac{D_H}{R_f}t}}\right]\right\} \tag{2.38}$$

where x_0 denotes the slug thickness which can be calculated as:

$$x_0=\frac{M/A\exp(-\lambda_s t_r)}{S(n_e+K_d\rho_b)} \tag{2.39}$$

where M/A, λ_s, t_r and S denote the total mass applied per unit area [M L^{-2}], the solid phase decay constant [T^{-1}], the time lapse between application as well as groundwater recharge [T] and solubility of chemicals [M L^{-3}], respectively.

2.5 Modelling preferential flow (macropore) transport coupled with matrix diffusion

Suppose that a column consists of a medium grained quartz sand creating a central cylindrical macropore region and the aquitard material created the surrounding part of the central macropore region, that is the matrix region (Fig. 2.11). Assume that:

- Mass transport along the macropore region is much faster than transport within the matrix region.
- Advection and hydrodynamic dispersion are the transport mechanisms in the macropore region.
- Mass flux from the macro pore region to the matrix region will be perpendicular to the axis of the macropore region.
- Linear sorption occurs in both the macropore and matrix region.
- Molecular diffusion will be the main transport mechanism within the matrix region.

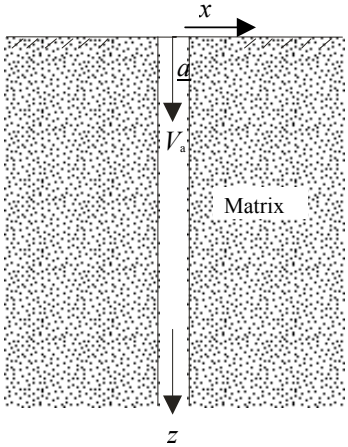

Fig. 2.11: Macropore-Matrix system

These assumptions actually allow us to reduce the two dimensional equation to two one-dimensional equations that are much more amenable to solution by analytical techniques.

The transport processes in the system of Fig. 2.11 can be described by two coupled one dimensional equations, one for the macropore region and one for the matrix region with the coupling being provided by the continuity of concentration at the interface. The differential equation (mass balance) describing the distribution of solute species along the macropore and interface is:

$$\frac{\partial}{\partial t}\left(n_m C_m+\rho_m K_{d,m} C_m+m_{im}\right)+n_m v_a\frac{\partial C_m}{\partial z}-$$
$$n_m D_H\frac{\partial^2 C_m}{\partial z^2}=0$$

where the first term on the left-hand side of eq. (2.40) corresponds to the temporal changes of total mass in the system and the second and third term refer to the advection and dispersion processes, respectively. n_m, C_m, ρ_m $K_{d,m}$, m_{im}, v_a, z, t and D_H denote the porosity in the macropore region [-], the solute concentration in the macropore (mobile) region [M L^{-3}], the bulk density in the macropore region [M L^{-3}], the distribution coefficient in the macropore region [L^3 M^{-1}], the total mass of solute in the matrix per unit volume [M L^{-3}], the average linear velocity in the macropore region [L T^{-1}], the spatial co-ordinate along flow direction [L], the time [T] and the hydrodynamic dispersion coefficient [L^2T^{-1}], respectively. The subscript m stands for the mobile or macropore region and im for the immobile or matrix region.

In case of certain instances of further simplification, for example, when the advective flux of solute in the macropore is dominant, it is reasonable to neglect longitudinal dispersion

along the macropore region. This is of interest from a practical point of view because dispersivity is a difficult parameter to determine quantitatively. The mathematical consequence of neglecting dispersion is also of interest because eq. (2.40) is reduced to an equation of first order, thus simplifying the analytical solution (Rasmuson and Neretnieks, 1981). Ignoring the dispersion term the above equation becomes:

$$\frac{\partial}{\partial t}\left(n_m C_m + \rho_m K_{d,m} C_m + m_{im}\right) + n_m v_a \frac{\partial C_m}{\partial z} = 0 \tag{2.41}$$

The mass of solute per unit volume in the matrix (immobile region) is given by:

$$m_{im} = \frac{2}{a}\int_a^{\infty}\left(n_{im} C_{im} + \rho_{im} K_{d,im} C_{im}\right)dx \tag{2.42}$$

where $n_{im,}$ $C_{im,}$ $\rho_{im,}$ $K_{d,im,}$ a and x denote the porosity in the matrix region [-], the solute concentration (mass of dissolved chemical/volume of mobile water) in the fluid phase of the matrix region [M L^{-3}], the bulk density of the matrix region [M L^{-3}], the distribution coefficient in the matrix region [L^3 M^{-1}], the radius of the macropore region [L], and the spatial co-ordinate perpendicular to the flow direction [L], respectively. In eq. (2.42) a Cartesian co-ordinate x is used instead of a radial co-ordinate as it is reasonable to assume that the solute does not migrate into the matrix far enough such that the cylindrical shape of the system would become relevant (see section 4.4.2.1 with regard to quantitative considerations). $2/a$ denotes the surface-to-volume ratio of the macro pore region [L^{-1}].

By combining eqs. (2.41) and (2.42), the advective mass transport in the macropore region and exchange of mass in the matrix region can be expressed as:

$$\frac{\partial}{\partial t}\left[n_m R_m C_m + n_{im} R_{im}\frac{2}{a}\int_a^{+\infty} C_{im}dx\right] + n_m v_a \frac{\partial C_m}{\partial z} = 0 \tag{2.43}$$

with

$$R_{im} = 1 + \frac{K_{d,im}\rho_{im}}{n_{im}} \tag{2.44}$$

and

$$R_m = 1 + \frac{K_{d,m}\rho_m}{n_m} \tag{2.45}$$

R_{im} [-] and R_m [-] are the retardation factors of the matrix and the macropore region, respectively.

Dividing eq. (2.43) by $n_m R_m$ yields,

$$\frac{\partial C_m}{\partial t} + \frac{v_a}{R_m}\frac{\partial C_m}{\partial z} = -\frac{2}{a}\frac{n_{im} R_{im}}{n_m R_m}\int_a^{+\infty}\frac{\partial C_{im}}{\partial t}dx \tag{2.46}$$

This equation is to be solved by considering the following initial and boundary conditions:

(IC) $C_m\,(z, 0) = 0$ no contaminant present at $t = 0$

(BC) $C_m\,(0,t) = C_0$ for $0<t<t_0$ (finite pulse)

(BC) $C_m\,(0,t) = 0$ for $t>t_0$

The differential equation describing the diffusive transport of the solute in the direction perpendicular to the macropore is (Fick's 2nd law):

$$\frac{\partial}{\partial t}\left(n_{im} R_{im} C_{im}\right) = n_{im} D_p \frac{\partial^2 C_{im}}{\partial x^2} \tag{2.47}$$

where D_p denotes the pore diffusion coefficient in the [L^2 T^{-1}].

Dividing eq. (2.47) by $n_{im} R_{im}$ yields,

$$\frac{\partial C_{im}}{\partial t} = \frac{D_p}{R_{im}}\frac{\partial^2 C_{im}}{\partial x^2} = D_a \frac{\partial^2 C_{im}}{\partial x^2} \tag{2.48}$$

where D_a denotes the apparent diffusion coefficient [L^2T^{-1}].

The initial and boundary conditions for the matrix region are:

(IC) $C_{im}(z,x,0) = 0$ no contaminant present initially

(BC) $C_{im}(z, +\infty, t) = 0$ semi-infinite matrix region is studied

(BC) $C_{im}(z,a,t) = C_m(z,t)$ continuous concentration at the matrix-macropore interface

By replacing the integrand in eq. (2.46) by the right–hand side of eq. (2.48) the transport equation for the macropore region can be re-written as:

$$\frac{\partial C_m}{\partial t} + \frac{v_a}{R_m}\frac{\partial C_m}{\partial z} = \frac{2}{a}\frac{n_{im}R_{im}}{n_m R_m} D_a \frac{\partial C_{im}}{\partial x}(z,a,t) \tag{2.49}$$

Solutions of eqs. (2.48) and (2.49) for a finite pulse of duration t_0 can be obtained for three cases as described in the following:

The system of differential eqs. (2.48) and (2.49) is mathematically equivalent to the problem studied by Grisak and Pickens (1981). However, a finite pulse of duration t_0 is considered here, while Grisak and Pickens (1981) studied a continuous injection of solute ($t_0 \rightarrow +\infty$). Therefore, their solution can be adapted only for time intervals $0 < t \leq z\,R_m / v_a + t_0$, i.e. until the termination of the pulse is noticed at position "z" in the column. Identifying coefficients occurring in eqs. (2.48) and (2.49) with parameters used by Grisak and Pickens (1981) it is found that:

$$C_m(z,t) = 0 \tag{2.50}$$

and

$$C_{im}(z,x,t) = 0 \tag{2.51}$$

for the time interval $0 < t \leq z\,R_m / v_a$. During this period the pulse has not arrived at "z". If $zR_m / v_a < t \leq zR_m / v_a + t_0$ concentrations in the macropore and the matrix region are given by:

$$C_m(z,t) = C_0 \operatorname{erfc}\frac{\frac{2}{a}\frac{n_{im}R_{im}}{n_m R_m}\sqrt{D_a}\frac{zR_m}{v_a}}{\sqrt{4\left(t - \frac{zR_m}{v_a}\right)}} \tag{2.52}$$

and

$$C_{im}(z,x,t) = C_0 \operatorname{erfc}\frac{\frac{x-a}{\sqrt{D_a}} + \frac{2}{a}\frac{n_{im}R_{im}}{n_m R_m}\sqrt{D_a}\frac{zR_m}{v_a}}{\sqrt{4\left(t - \frac{zR_m}{v_a}\right)}} \tag{2.53}$$

respectively.

For later times $t > z\,R_m / v_a + t_0$ it is helpful to conceptualize the pulse as the superposition of two continuous solute injections with concentrations C_0 and $-C_0$, respectively. The influence of the injection with 'negative concentration' can then be directly obtained from eqs. (2.52) and (2.53) by replacing C_0 by $-C_0$ and t by $t - t_0$ as the beginning of the 'negative injection' is shifted by t_0 as compared to the beginning of the pulse. For $t > z\,R_m / v_a + t_0$ both impacts are active and can be added due to the linearity of the problem, thus yielding:

$$C_m(z,t) = C_0\left[\operatorname{erfc}\frac{\frac{2}{a}\frac{n_{im}R_{im}}{n_m R_m}\sqrt{D_a}\frac{zR_m}{v_a}}{\sqrt{4\left(t - \frac{zR_m}{v_a}\right)}} - \operatorname{erfc}\frac{\frac{2}{a}\frac{n_{im}R_{im}}{n_m R_m}\sqrt{D_a}\frac{zR_m}{v_a}}{\sqrt{4\left(t - \frac{zR_m}{v_a} - t_0\right)}}\right] \tag{2.54}$$

in the macropore region and

$$C_{im}(z,x,t) = C_0\left[\operatorname{erfc}\frac{\frac{x-a}{\sqrt{D_a}} + \frac{2}{a}\frac{n_{im}R_{im}}{n_m R_m}\sqrt{D_a}\frac{zR_m}{v_a}}{\sqrt{4\left(t - \frac{zR_m}{v_a}\right)}} - \operatorname{erfc}\frac{\frac{x-a}{\sqrt{D_a}} + \frac{2}{a}\frac{n_{im}R_{im}}{n_m R_m}\sqrt{D_a}\frac{zR_m}{v_a}}{\sqrt{4\left(t - \frac{zR_m}{v_a} - t_0\right)}}\right] \tag{2.55}$$

in the matrix region.

It has been verified that the expressions given by eqs. (2.50) – (2.55) are solutions of the partial differential eqs. (2.48) and (2.49) subject to the initial and boundary conditions given above (Rahman et al., 2002; paper submitted to Water Resources Research).

3. MATERIALS AND METHODS

3.1 Materials

Natural geologic solids of different origin were collected from Bangladesh in order to determine their sorption capacity and transport properties with some selected environmental organic chemicals.

3.1.1 Site description – geology and hydrogeology in brief

Across the tropic of cancer, Bangladesh lies in the northeastern part of South Asia and extends between 20°34´ and 26°38´ north latitudes and 88°01´ and 92°41´ east longitudes. The country is surrounded by India on the west, the north and northwest and Myanmar on the southeast and the Bay of Bengal on the south. Physically Bangladesh can be divided into two broad distinct regions namely the high land area (hilly region and terrace area) and low land area (deltaic and floodplain area). The elevation in the hilly region varies from 100 - 1000 m and the average elevation of the terrace area, which mostly occupies higher ground than the floodplain, is likely to be more than 15 m above sea level (range 15 – 60 m). High land area occupies about 25 % of Bangladesh and the rest is covered by the deltaic and flood plain area. Fig. 3.1 shows a sketch of the map of Bangladesh with sampling locations.

Recent deltaic and alluvial sediments cover most of low land of Bangladesh. The sedimentary sequence varies in thickness from a few tens of meters in the north to a few hundreds of meters in the south (Alam et al., 1990; Khan, 1991). The sediments are brought in by the Ganges-Brahmaputra-Meghna river system and are composed of sand, silt and clay sized particles with a distinct fining upward sequence.

Recent sands are generally medium to dark grey in colour and composed dominantly of quartz, feldspar and mica. Unweathered black biotite mica and amphiboles impart a characteristic colour to the sediments. Older, Pleistocene sands beneath the terrace areas are usually brown or pale grey in colour and contain less mica and amphiboles. Biotite, when present, is visibly weathered. The brown colour is associated with the formation of secondary clays and ferric hydroxides. The permeability of sands beneath the flood plains is typically double the permeability of sands of the same medium grain size beneath Pleistocene terraces. This difference is attributed to the effect of weathering products (clay and iron minerals) plugging the pores of the sands (Ahmed et al., 1998).

With respect to geologic build-up, the overall hydrogeological situation of Bangladesh is rather complex. A fairly broad correlation between lithology and depth has been established for the sediments of Bangladesh. From the hydrogeological point of view, sediments of

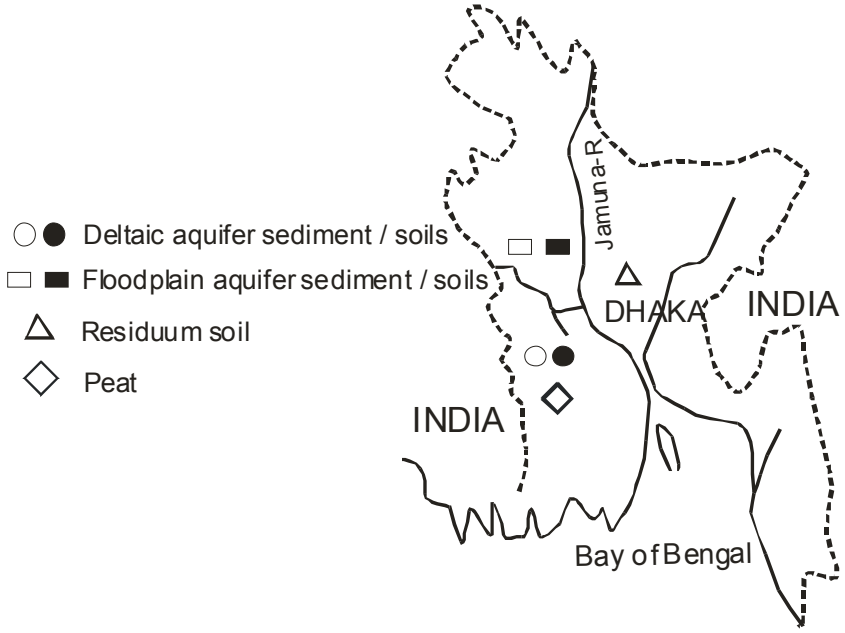

Fig. 3.1: Map of Bangladesh showing the sampling location

Bangladesh can be divided in three units: an upper surface layer of mainly clay and silt, which in parts of the southern region (Khulna, Barisal and Faridpur) contains peat layers; an intermediate layer of mainly fine sand and clay referred to as the composite aquifer and a deeper layer, known as the deep aquifer, containing mainly fine to coarse sand.

In general in the southwest and south central area the upper clay layer (in other words the distance to the groundwater table) is comparatively thick and this is particularly true in southern Barisal district where the thickness may be up to 150 m (Halcrow, 1993).

Groundwater generally occurs within a depth of 10 m in most areas. The aquifer is unconfined to semi-confined with locally confined conditions in places. The recharge comes from rainfall and annual flooding in low-lying areas. Water quality is generally good with sporadic occurrence of saline water (Hoque et al., 1997). Arsenic poses a significant health hazard in many areas of Bangladesh.

3.1.2 Sample collection and preparation

Soils, aquifer sediments and peat samples were collected from three typical physiographic locations of Bangladesh (deltaic, floodplain and terrace area) (Fig. 3.1). Soil samples were collected on horizon basis from existing excavated pits that were specially made for the construction of ponds or manufacture of bricks. The horizon was identified based on the visual observation of colour and texture (Fig. 3.2). The aquifer sample was either augured to the surface from a depth range of 2 - 5 m with a 20 cm hollow stem auger or by using the sludger method (a cheap and simple indigenous method of well construction in Bangladesh) from a depth of range of about 5 - 25 m. After collection, the samples were spread on aluminum sheets, air dried, homogenised and stored in polyethylene bags at room temperature until shipment to Germany.

For batch sorption experiments, the samples were pulverised for 30-40 minutes in a planet ball mill (Fritsch, Laborette). All mill components in contact with the samples (balls and cups) were of zirconium oxide in order to prevent contamination of samples with carbon e.g., from steel which might affect the f_{oc} measurements.

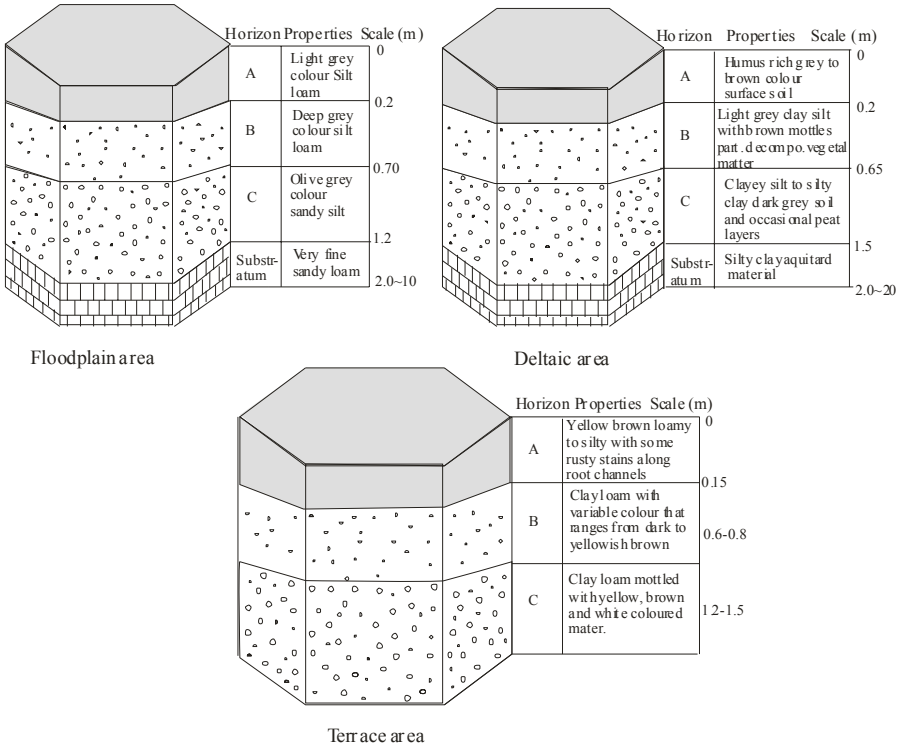

Fig. 3.2: Typical soil pedons in three-dimensional form (information in ID) from floodplain, deltaic and terrace areas of Bangladesh

3.1.3 Determination of grain size, particle density and organic carbon content

The particle or grain size distribution of the sample was determined by a combined sieving (wet and dry) and sedimentation method. This was done using a standard method (DIN 18123) in the soil mechanics laboratory of the Institute for Geology, University of Tuebingen, Germany. Grain size distribution data were plotted on semi-logarithmic paper in Excel to construct cumulative soil/sediment curves and to determine the percentage of sand, silt and clay fractions. Percentages of sand, silt and clay were plotted in a triangular diagram (USDA, 1992) to classify the soil/sediments.

The solid density was measured using capillary pycnometry (DIN 18124). For this, approximately 15 g oven dried (at 105 °C) and pulverised samples were transferred to pycnometer flasks (volumetric flasks with ground glass stoppers and a capillary overflow) and weighed. Deionised and degassed water was added to the flasks which were then stored under vacuum until no further degassing was observed. This was repeated until the flasks were completely filled with water. The solid density is obtained from the known volume of each flask, the sample weight and the volume of water added as determined from the weight with a temperature correction.

Prior to the measurement of organic carbon, the carbonate content was determined by titration using hydrochloric acid (1N) and back titration of residual HCL with caustic soda (1N). Phenolphthalein was used as the indicator. The organic carbon (OC) content was measured (after pre-treatment of the samples with HCl in order to remove inorganic carbon) by dry combustion method using a CHN analyser (Vario EL, thermal conductivity detector, temperature 960 °C). The OC content of some samples was also measured using wet oxidation method and the results are compared with the dry combustion method (Tab. 4.1). But for better accuracy, OC content data measured by the dry combustion method were used for the evaluation of sorption and column experimental results.

3.2 Selection of solutes

Fate and distribution of chemicals within the soil-air-water 3-phase system strongly depends on their physical and chemical properties. For example, chemicals which are low viscous and more dense relative to the water can move faster than water and can easily sink down to the groundwater table. Chemicals which have extensive propensity to cause groundwater contamination and are frequently used in Bangladesh were chosen for the study. Theses include pesticide related compounds e.g., carbofuran and 1,2- dichlorobenzene (1,2-DCD), chlorinated solvents (e.g., trichloroethene, TCE) and PAHs (e.g., phenanthrene).

Carbofuran is a Restricted Use Pesticide (RUP) because it is highly toxic by inhalation and ingestion and moderately toxic by dermal adsorption to humans. It is also highly toxic to birds and to many fishes. TCE is an extensively used organic chemical in the industry for degreasing purposes and it may easily reach the groundwater table and cause extensive groundwater contamination because of its higher density, low viscosity and high dissolved phase mobility. Phenanthrene is the most frequent organic contaminant for soil and groundwater and in many cases it is used as a representative chemical for characterising the solute – sorbent interaction. The physico-chemical properties used for determining the distribution behaviour, the sources in groundwater and potential health effects of the selected chemicals are summerized in Tab. 3.1. The ratio of solubility to drinking water limit gives the hint how a minimum quantity of such chemicals can cause an extended groundwater contamination problem.

3.3 Laboratory experiments – conception and objectives

To study the fate and transport of organic chemicals two experimental techniques are commonly applied in the laboratory: 1) batch experiments and 2) column experiments. Batch experiments are generally designed to study equilibrium sorption of solids and apply to sorbent suspensions where all the solids are exposed to be available for the interaction with the contaminants. On the other hand, column tests are performed with intact solids, i.e., samples which have a definite matrix and structure. The sorption characteristics obtained from the experiments are the result of contaminant interaction with a structured system

Tab. 3.1 Physico-chemical properties of test chemicals (most data from Verschueren, 1996 except noted)

Chemicals	MW [g mol^{-1}]	VP [mm Hg]	Aqueous Solu. [mg L^{-1}]	Subcool. Solu. [mg L^{-1}]	Log K_{ow} [-]	[b] D_{aq} [cm² s^{-1}]	Drinking water lim. [mg L^{-1}]	Sources of contam. in groundwater	Potential health effects
Phenan-threne	178.2	6.8×10^{-4}	1.29	6.2	4.57	6.6×10^{-06}	0.002	Gas manufac. plant	Cancer risk
1,2-DCB	147.01	1	145	-	3.38	8.4×10^{-06}	0.6	Chem. factories	Liver problem
Carbofuran	221.25	4.8×10^{-6}	320	3100 [a]	2.32	6.8×10^{-06}	0.04	Agriculture field	Nervous system difficul.
Trichloroe-thene (TCE)	131.5	60	1100	-	2.42	8.9×10^{-06}	0.005	Petroleum refineries	Cancer risk

[a] Estimated after Lane and Loehr, 1992, [b] Estimated after Worch, 1993

where not all the particles are exposed to or available for the interaction with the chemical, thus often resulting in nonequilibrium conditions. However, the main objectives of the two aforementioned experiments are: to study the sorption and attenuation of contaminants; to determine (estimate) the number of pore volumes required to achieve breakthrough of a contaminant; to provide the information necessary for the calculation of the retardation parameter(s) required in the contaminant transport equation and to determine (estimate) the transport parameters (dispersion/diffusion and diffusion coefficients) which control the migration of contaminants through soils.

3.4 Batch sorption experiments

Batch experiments in an aqueous system are performed to determine the sorption coefficients (e.g., K_d) by mass balance considerations. Usually, water already containing a given amount of solute (sorbate) is added to the sample or the water is spiked with the solute. By monitoring the decrease of the aqueous concentration of the solute, the sorbed amount is determined. The prerequisite is that the reduction of the aqueous concentration is solely due to sorption of the compound by the soil or sediment samples. If volatilisation, degradation (biotic and abiotic) or sorption of the solute onto glass surfaces or liners occur, a correction term in the mass balance equation is necessary. The decrease of the aqueous concentration due to sorption should be significantly higher than the analytical errors of the measurement of the aqueous concentration (which are typically between 5 % and 15 %). For example, the water to solid ratio (volume/mass) required in a batch system to achieve a decrease of the initial aqueous concentration of 50 % under equilibrium conditions (50 % of the initial mass of solute is sorbed and 50 % is in aqueous solution) equals K_d:

$$K_d = \frac{V_w}{m_d} \tag{3.1}$$

where V_w and m_d denote the volume of water [L³] and the dry mass of the solids [M] in the batch system, respectively. Fig. 3.3 shows a conceptual set-up of conventional batch experiments performed in the laboratory.

3.4.1 Preparation of test water and stock solution

It has been observed from many studies that there is an effect of using mineralised water (salting out effect) on the sorption capacity. Karickhoff (1984) found an increase of about 20 % of K_d with highly mineralised water. In the present study synthesised deionised water (Milli-Q water) was used instead of deionised water (EC < 2 µS/cm).

At first the deionised water allows to enter the Milli-Q system and is pumped through the Q-guard cartridge for an initial purification step. The water is then exposed to UV light at both 185 and 254 nm wavelength. This oxidises organic compounds and kills bacteria. The function of the quantum activated carbon cartridge is to remove trace ions and oxidation

by-products produced by the action of UV light. Purified water then passes through an ultrafiltration module that acts as a barrier to colloids, particles and organic molecules. Finally a manual 3-way valve directs ultrapure water through a final filter made up of a 0.22 µm membrane. Concentrated methanol stock solutions were prepared for each chemical. Methanol was used because it is completely miscible in water. The concentration of each chemical in methanol was determined according to the 50 % of K_{ow} of the chemical concerned.

Air bubbles were removed by completely mixing the solid-solute suspension and then allowed to sit in the dessicator to pump out the bubbles for phenanthrene and carbofuran experiments. Then the caps were sealed and the vials were stored at 20 °C in the dark and shaken by hand routinely. In order to investigate the influence of temperature on sorption processes some experiments were carried out at controlled 4 °C and 40 °C. Reference vials containing no solids were treated in the same way in order to check and correct losses of the compound in the

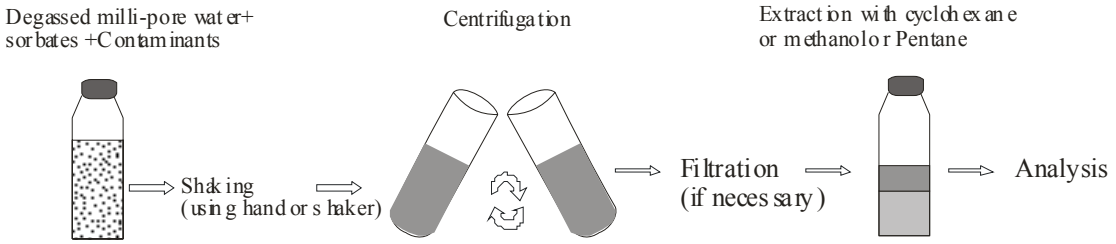

Fig. 3.3: Conventional batch experiment set-up

3.4.2 Experimental set-up and procedure

All batch experiments were carried out in triplicate in 10 ml to 100 ml crimp top reaction glass vials (batch reactor) sealed with PTFE-lined butyl rubber septa (Alltech). The reactors were filled to have minimum headspace and to have approximately constant solid/solution ratios. Solid/solution ratios (M L^{-3}) were in the range of 1:600 to 1:2 depending on the solutes in order to achieve 30 - 70 % reduction in the initial solute concentration after equilibration. The methanol stock solution containing the contaminant was spiked into milli-Q water such that the methanol was always less than 0.5 % in aqueous solution, a level at which methanol has no measurable effect on sorption (Nkedi-Kizza et al., 1987). In addition to the organic solutes, the background solution also contained 200 mg L^{-1} sodium azide (NaN_3). In the carbofuran batch experiments the background solution was also buffered at pH 6.0 and 7.0 in order to prevent hydrolysis which is very rapid at high pHs (Howard, 1991). Initial aqueous phase concentrations were selected to yield a set of isotherms for each sorbent that was distributed evenly on a log-log scale plot and spanned approximately 2 - 4 orders of magnitude in residual aqueous phase solute concentration.

system. The equilibration time was controlled by doing the parallel kinetic experiments.

After equilibration (7 - 100 days: short equilibration time for carbofuran and long equilibration time for phenanthrene), the solids were separated from the aqueous solution (except TCE) through centrifugation (1800 rpm for 30 min). For the phenanthrene, 1,2-DCB and carbofuran, an aliquot of 0.5 ml – 10 ml of the supernatant water was withdrawn, filtered using a syringe filter unit with aluminumoxide filters (Anodisk). The water samples were immediately transferred to 2 - 4 ml amber hypo vials containing already 1 – 2 ml cyclohexane and internal standard. Internal standards were chosen such that the physico-chemical properties were comparable to (or similar to) the chemicals of interest. In case of TCE, the headspace of the vials was sampled and analyzed directly. Detection and quantification of 1,2-DCB was done by gas chromatography (GC) equipped with MSD (mass selective detector, quadrupol), TCE by GC-FID (flame ionization detector). Phenanthrene and carbofuran were analyzed by HPLC (high performance liquid chromatography) equipped with UV (ultraviolet) and fluorescence detectors.

Sorption kinetics experiments were also carried out in batch reactors with the same solids and solutes. After distinct time intervals (1, 3, 7, 10, 30 and 100 days) the aqueous phase was sampled by opening the vials and withdrawing a small amount (0.25 – 2 ml) of the supernatant water. Afterwards, the vials were recapped immediately with new septa for subsequent sampling.

For selected samples mass balances were conducted by extracting phenanthrene in hot methanol. At first, sample vials containing phenanthrene solution and solid were centrifuged at 1800 rpm for about 20 min to separate the solid and liquid phase. Supernatant was collected with caution in order to avoid solid particles and then weighed. 1 - 2 ml of supernatants were transferred to amber hypovials already containing 1 - 2 ml cyclohexane and a known concentration of naphthalene as an internal standard and measured aqueous phase solute concentration in HPLC equipped with UV/fluorescence detector. Vials containing the rest of phenanthrene solution and solid were reweighed to determine the amount of water and solid. 2 - 6 ml of methanol was added in each vial and mixed properly for about 10 minutes. After sealing the vials with a teflon lined cap, the vials were placed in a hot sand bath (70 °C) for about a week to promote phenanthrene migration towards methanol. As an extraction material methanol was chosen over other hydrophobic solvents because it is completely miscible with water and therefore it can enhance the rate of desorption for sorbed analyte (Ball et al., 1997). Following extraction, the vials were centrifuged again at 1800 rpm for about 30 min. Extracted phenanthrene in the supernatant water (supernatant methanol solution) were then transferred to 1 – 2 ml of cyclohexane and sealed and centrifuged once again at 1500 rpm for 10 min in order to facilitate separation of the cyclohexane phase. Quantification was done as described before. The recovery rate (%) was calculated as follows:

Recovery rate (%) =

$$\frac{C_{w+m}\left(V_{w,soil}+V_{methanol}\right)-\left(C_w V_{w,soil}\right)}{C_s m_d} * 100 \quad (3.2)$$

where C_{w+m} , $V_{methanol}$, $V_{w,soil}$, C_w, C_s and m_d denote the concentration of extracted phenanthrene from solid plus phenanthrene solution remained in soil [M L^{-3}], the volume of methanol [L^3], the volume of water retained in soil [L^3], the concentration of phenanthrene solution separated before extraction [M L^{-3}], the sorbed phase concentration obtained from batch experiments [M M^{-1}] and the mass of solid [M], respectively.

3.4.3 Evaluation of batch data

For equilibrium conditions, the distribution coefficient $K_{d,eq}$ [L^3 M^{-1}] i.e., the ratio of the amount C_s of solute sorbed per unit mass of solid [M M^{-1}] and the aqueous concentration C_w in equilibrium with the solids [M L^{-3}], was determined from the concentration in reference vials C_{ref} [M L^{-3}], the volume of water in the reference vials V_{ref} [L^3], the volume of water V_w [L^3] in sample vials containing solids and the mass of solid m_d [M] as:

$$\frac{C_s}{C_w} = K_{d,eq} = \frac{C_{ref}V_{ref} - C_w V_w}{C_w m_d} \quad (3.3)$$

For sorption kinetics experiments, the system loss due to partitioning of solutes to the head space and onto the glass surface were taken into account for calculating the sorbed phase concentration by carefully monitoring the reference vials (containing solutes and water but no solids) on a routine base:

$$C_s(t) = \frac{C_{ref}V_{ref} - C_w V_w - C_w K_{sys}}{m_d} \quad (3.4a)$$

$$\rightarrow K_{sys} = V_{ref}\left(\frac{C_{input,measured}}{C_{ref,t}} - 1\right) \quad (3.4b)$$

where K_{sys} [L^3], $C_{input,measured}$ [M L^{-3}] and $C_{ref,t}$ [M L^{-3}] denote the system loss, measured input concentration and concentration in a reference vial containing no solid at any time, respectively.

3.5 Modelling of sorption kinetics experiments

Sorption of hydrophobic organic chemicals by natural particles can be limited by slow diffusion. Some recent examples show that the apparent sorption distribution coefficient ($K_{d,app}$)

can increase by 30 % to as much as 10 fold (Pignatello 1989; Rounds et al., 1993) between short contact and long contact times and the times required to reach true equilibrium can be months to years (Ball and Roberts, 1991a,b; Rügner et al., 1999). Most important limiting processes are hypothesised to be retarded diffusion in the intraparticle pore space (Wu and Gschwend, 1986; Grathwohl and Reinhard, 1993) or diffusion into the soil organic matter (Nkedi-Kizza et al., 1989; Brusseau et al., 1991).

It is quite likely that both organic matter diffusion and retarded intraparticle diffusion mechanisms often operate in the environment simultaneously. Organic matter diffusion may predominate in soils/sediments that are high in organic matter/organic carbon and low in aggregation while the retarded intraparticle diffusion may predominate in the soils or sediments when the opposite conditions exist.

Diffusion rate constants were estimated as fitting parameters from batch experimental results using the diffusion model which actually reflects the processes active at the grain scale. The following assumptions are made for the modelling of kinetic experiments which are analogous to Wu and Gschwend (1986, 1988) and Ball and Roberts (1991b):

- Molecular diffusion controls the kinetics in the intraparticle region.
- Particles are considered to be of spherical shape with an average (effective) radius.
- The apparent diffusion coefficient is considered to be constant, i.e., independent of concentration.
- Physical characteristics of the spherical particles are homogeneously distributed throughout their volume.
- The concentration gradient exists only in the radial direction towards or away from the centre of the particle.

Under the above considerations sorptive uptake in the spherical particles can be modelled based on the analytical solution of Fick's 2nd law in spherical co-ordinates. For a constant D_a (e.g., linear sorption isotherm) and a variety of initial and boundary conditions analytical solutions of Fick's 2nd law in spherical co-ordinates, eq. (2.11), are available which allow the calculation of solute mass after a time t as well as sorption and desorption rates (bath of limited volume).

If the particles are free of solute initially, the following initial and boundary conditions can be applied:

(IC) $C = 0$ $t = 0$ $0<r<a$

(BC) $C = C_{eq}$ $t =>0$ $r = a$

(BC) $\partial C/\partial r = 0$ $t>0$ $r = 0$

The analytical solution in this case (Crank, 1975) is:

$$\frac{M_t}{M_{eq}} = 1 - \sum_{n=1}^{\infty} \frac{6\beta(\beta+1)}{9+9\beta+q^2{}_n\beta^2} \exp\left[-q^2{}_n \frac{D_a t}{a^2}\right] \tag{3.5}$$

where M_t/M_{eq}, β and q_n denote the ratio of mass which has diffused into or out of the sphere (sorbed or desorbed) after time t to the mass at equilibrium [-], the ratio of mass of solute dissolved in the aqueous phase to the mass in the solids [-] and the positive roots of:

$$\tan\ q_n = \frac{3q_n}{3+\beta q_n{}^2} \tag{3.6}$$

respectively.

In illustrating modelling fits of data from samples having different solid/liquid ratios (and thus different ultimate uptake) it is useful to plot the uptake curves with $K_{d,app}/K_{d,eq}$. In this case, the sorptive uptake at different solid to water ratios under nonequilibrium conditions ($K_{d,app}$) relative to equilibrium $K_{d,eq}$ can be expressed as:

$$\frac{K_{d,app}}{K_{d,eq}} = \frac{\beta}{\frac{1+\beta}{M_t/M_{eq}} - 1} \tag{3.7}$$

In the two-site two-region model, sorption is considered as the contribution of both rate limited (e.g., diffusion controlled) and instantaneous sorption. To fit the measured data, again it is useful to include a fast sorbing fraction X_i, which is assumed to reach sorption

equilibrium instantaneously. The analytical solution in this case is:

$$\frac{M_t}{M_{eq}} = (1 - X_i)\left(1 - \sum_{n=1}^{\infty} \frac{6\beta(\beta+1)}{9 + 9\beta + q^2{}_n\beta^2} exp\left[-q_n{}^2 \frac{D_a t}{a^2}\right]\right) + X_i \quad (3.8)$$

From the model, the diffusion rate constant D_a/a^2 [T^{-1}] was estimated as a fitting parameter. The best fit X_i value was determined by trial and error. Best fit values of D_a/a^2 and the corresponding Mean Weighted Square Error (MWSE) were determined for a range of X_i values until an X_i value corresponding to the minimum MWSE was found. The MWSE was calculated based on a least square approximation of model data and experimental results as:

MWSE =

$$\sum \left[\frac{\text{Exp. data } (K_{d,app}/K_{d,eq}) - \text{Mod. data } (K_{d,app}/K_{d,eq})}{\text{Experiment data } (K_{d,app}/K_{d,eq})}\right]^2 \quad (3.9)$$

3.6 Column experiments

The classical laboratory experiment for the simulation of flow and transport of a contaminant in the subsurface environment is the column experiment. Generally a column is filled with soil/sediments and water is allowed to flow through the column from a water reservoir which is connected by a pump. The packed columns are equilibrated with unspiked deionised water / electrolyte solution prior to experiment passing some pore volumes slowly through the column. The concentration, C, of a chemical species appearing in the effluent reservoir is measured over time and the results are plotted in the form of solute breakthrough curves, or relative concentration, C/C_0, versus time or pore volumes of flow (Fig. 3.4). One pore volume is the cross-sectional area of the column times the length times the porosity.

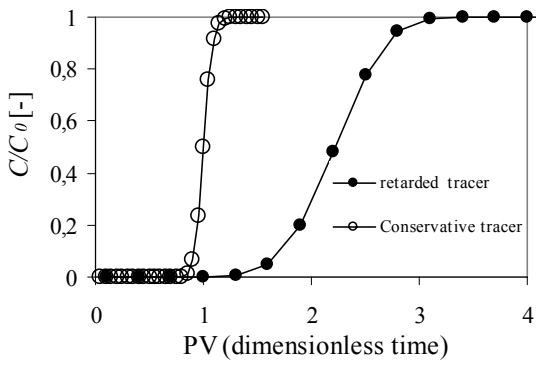

Fig. 3.4: Scheme of typical breakthrough curves for a conservative (R_f = 1) and retarded tracer (R_f = 2.2) which can be obtained from laboratory column experiments

3.6.1 Column apparatus, packing and experimental set-up

One dimensional column experiments under water saturated conditions were performed using a stainless steel column having an internal diameter of 0.5 cm and a length of 9 cm. Stainless steel capillaries were used with an inner diameter of 0.5 mm (Alltech). Stainless steel frits of 2-µm pore size were used to prevent migration of fine particles of the aquifer materials and soils. The system was designed so that the solute contacted only stainless steel or glass. This was done to eliminate problems associated with the use of Teflon® and other such materials which have been shown to interact with some organic chemicals (Lion et al., 1990; Reynolds, 1990).

Deltaic aquifer sediments with a grain size fraction of 0.01 - 0.3 mm and deltaic soils were used for the column experiments. The solutes used for the column experiments were the same as used in the batch experiments. Additionally fluorescein was used as a conservative tracer. Each column was packed as uniformly as possible by flooding from below and filling in the solids from above at the same time. During the procedure the column was slightly shaken. In that way the column could be homogeneously packed which minimised entrapped air bubbles and grain size separation due to gravity in the supernatant aqueous phase. The breakthrough of the conservative tracer (fluorescein) and retarded compounds (phenanthrene and carbofuran) were measured using an on-line fluorescence detection set-up (Fig. 3.5A) which consists of

the inlet solution reservoir, the stainless steel column containing the aquifer solids or soils, a fluorescence detector (Merck-Hitachi, F-1080), the peristaltic pump and the effluent reservoir in that order. The fluorescence detector was coupled to a personal computer through the system interface module (SIM). Optimised excitation and emission wavelengths were obtained by means of scanning the reference solution. The maximum signal was obtained at excitation/emission wavelengths (nm) of 487/512, 280/312 and 249/345 for fluorescein, carbofuran and phenanthrene, respectively. The chromatographic software Waters Maxima 820 was used to record breakthrough curves in real time. The system dead volume of the connecting tubing, fittings etc. between the influent solution bottle and the detector which was not filled by the porous medium was kept minimum. The column experimental set-up for 1,2-DCB and TCE is also shown in Fig. 3.7B-C.

3.6.2 Experimental procedure

After completing the packing, deionised water containing 0.02 % NaN_3 used to prevent a biotransformation was pumped through the column. The columns were operated at room temperature of about 22 °C corresponding approximately to the Bangladesh groundwater temperature.

During the on-line experiments, deionised water was pumped until a stable baseline signal was observed in the fluorescence detector. For TCE and 1,2-DCB experiments deionised water was pumped until steady-state water saturation conditions were established, which required about 1 day and confirmed by weighting the column. The constancy of column weights was monitored periodically throughout the miscible

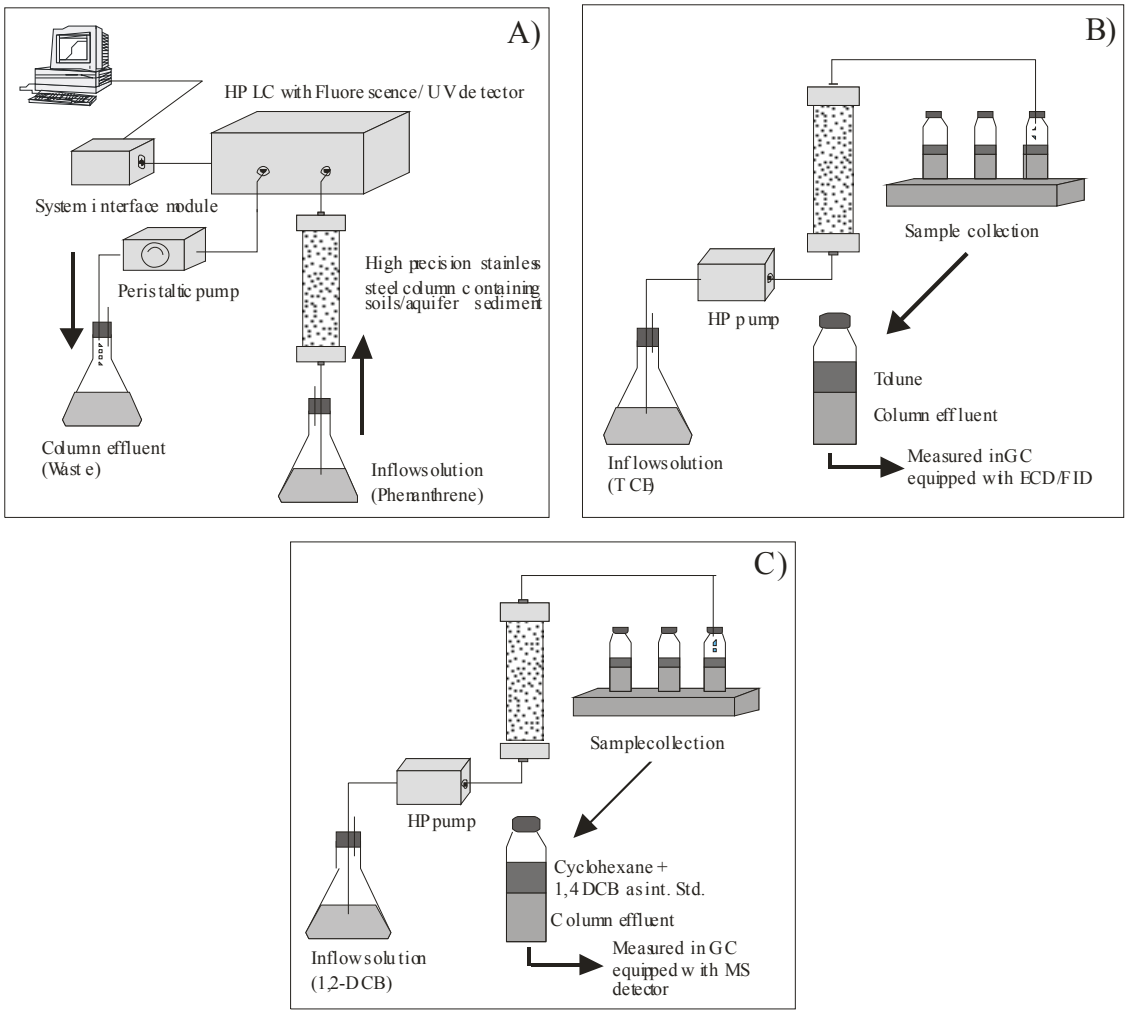

Fig. 3.5: Experimental set-up for the determination of breakthrough curves (BTCs) of A) fluorescein, phenanthrene and carbofuran, B) TCE and C) 1,2-DCB

displace studies. Solutions for each solute were prepared in the concentration range of generally 10 - 25 % water solubility.

Deionised water spiked with specific organic compounds was fed to the column inlets from the reservoir either at flow rates of about 0.1 ml/min that mimic the recharge rate of seepage water in the subsurface or at a flow rate of 0.5 ml/min. Constancy of flow was periodically checked by collecting fractions. These measured flow rates were occasionally checked against the average flow rate determined by collecting and measuring all effluent over the injection period and they compared well in all cases. On-line fluorescein, phenanthrene and carbofuran experiments involved continuous injection of the solution until $C/C_0 = 1$ was reached or the effluent concentration reached a constant signal (C and C_0 are the concentrations of solute in the effluent and influent solutions, respectively). Column effluents of TCE were collected in vials containing toluene as extracting solvent, capped immediately and removed for storage at 4 °C. The samples were analyzed next day and quantification was made by injecting a toluene aliquot into a GC equipped with ECD/FID which was calibrated by a known TCE standard solution. Effluents of 1,2-DCB were trapped in vials containing cyclohexane as extracting solvent and 1,4-DCB as internal standard and detection and quantification was done as described before.

In each experiment at first fluorescein tracer experiments were conducted in all columns to control the packing of the sediments and to determine the hydrodynamic parameters. Following the tracer experiments, a solution of specific chemicals was displaced through the column at each of the aforementioned two velocities. Columns were cleaned, repacked with fresh materials, conditioned and investigated following the same procedure for each experiment. Some details of the experimental conditions for the breakthrough curves of phenanthrene, as an example, are given in Tab. 3.2.

Tab. 3.2: Experimental conditions during the column studies of tracer and sorbed solutes

Column Length [cm]	9
Radius [cm]	0.495
Pore volume [ml]	2.5
Porosity [-]	0.30 - 0.40
Flow rate [ml min^{-1}]	0.1 - 0.5
Pore water velocity [cm min^{-1}]	0.4 - 1.5

3.6.3 Evaluation of experimental data

The column experimental data were evaluated for determining the hydrodynamic properties such as porosity, average linear velocity and dispersivity from tracer experiments. By using the available information it is possible to determine the distribution coefficient and retardation factor from the breakthrough curve of a sorbing solute which are important parameters in solute transport models.

3.6.3.1 Conservative tracer

To compute the shape of tracer breakthrough curves and concentration profiles, an analytical solution of the differential equation for advective and dispersive transport with the respective initial and boundary conditions can be used (Chapter 2, Section 2.4.1, eq. (2.26)). For the sake of explanation the analytical solution is again mentioned here:

$$\frac{C}{C_0} = 0.5\left[\operatorname{erfc}\left(\frac{x-v_a t}{2\sqrt{D_H t}}\right) + \exp\left(\frac{v_a}{D_H}\right)\operatorname{erfc}\left(\frac{x+v_a t}{2\sqrt{D_H t}}\right)\right] \tag{3.10}$$

The terms in the above equation are described before.

C/C_0 was calculated from fluorescence signals, which represent the effluent concentration normalised to influent concentration according to:

$$\frac{C}{C_0} = \frac{S_{i,t} - S_{i,\min}}{S_{i,\max} - S_{i,\min}} \tag{3.11}$$

where $S_{i,t}$, $Si_{,min}$ and $S_{i,max}$ denote the fluorescence signal at any time t, background or minimum fluorescence signal and maximum fluorescence signal, respectively.

The average linear velocity of the water in the column was determined from the quantity of water discharging per unit time, Q [L³ T^{-1}], divided by the cross-sectional area, A [L²] and the flow effective porosity, n_e [-] as:

$$v_a = \frac{Q}{n_e A} \tag{3.12}$$

For the determination of porosity it is assumed that a pore volume is exchanged, if the effluent concentration achieves 50 % of the input /influent concentration. On this assumption applies:

$$n_e = \frac{Q t_{0.5}}{V} \tag{3.13}$$

where V [L³] is the volume of the column, $t_{0.5}$ is the time required for the effluent concentration to reach $C/C_0 = 0.5$. The time $t_{0.5}$ was determined according to the following linear assumption:

$$t_{0.5} = \frac{(0.5 - (C/C_0)_{n-1})(t_n - t_{n-1})}{(C/C_0)_n - (C/C_0)_{n-1}} + t_{n-1} \tag{3.14}$$

where t_n is the corresponding time to the first measured data point of $C/C_0 > 0.5$.

The longitudinal dispersion coefficient (D_H in eq. 2.26) can be calculated either from the temporal delay, in that the relative effluent concentration rises from 0.159 to 0.841 (assuming an integrated Gauss or normal distribution with in each case considering a standard deviation from the average value):

$$D_H = \frac{v_a (t_{0.841} - t_{0.159})}{8 t_{0.5}} \tag{3.15}$$

where $t_{0.841}$, $t_{0.5}$ and $t_{0.159}$ are the actual time at effluent relative concentration of 84.1 %, 50 % and 15.9 %, respectively. Alternatively, D_H can be obtained as a fitting parameter from the comparison of model results with measured data.

3.6.3.2 Reactive solutes

With the help of a tracer breakthrough curve, it is also possible to assess the breakthrough curve of a reactive/sorbing compound. The two most important parameters which can be determined from a breakthrough curve of a reactive solute are the retardation factor (R_f) and the distribution/partition coefficient (K_d). Two methods were used to quantify the retardation factor of a reactive solute (Nkedi-Kizza et al., 1987). In method 1, R_f was obtained from moment analysis according to:

$$R_f = \frac{\mu_{rs}}{\mu_{ct}} \tag{3.16}$$

where μ_{rs} and μ_{ct} denote the first moment of reactive solute [T] and conservative tracer [T], respectively.

The first moment of a breakthrough curve can be calculated as (conservative tracer, for example):

$$\mu_{ct} = \int_0^\infty (1 - C/C_0)\,dt \tag{3.17}$$

By numerical integration, the above equation yields ,

$$\mu_{ct} = \sum_{n=0}^{\infty} \left[\left(1 - \frac{(C/C_0)_{n+1} + (C/C_0)_n}{2} \right) (t_{n+1} - t_n) \right] \tag{3.18}$$

Based on the principle of mass conservation the retardation factor can be visualised as the total mass of reactive solute in the system compared to the mass in the mobile phase. For conservative tracers these masses are equal resulting in $R_f = 1$.

According to method 2, the retardation factor is given by a ratio of arrival times, i.e.,

$$R_{0.5} = \frac{t_{0.5(rs)}}{t_{0.5(ct)}} \tag{3.19}$$

The indices *rs* and *ct* correspond to reactive solute and conservative tracer, respectively.

For practical purposes, the arrival of a contaminant, e.g., given by $R_{0.5}$, may be more important. For theoretical considerations, R_f derived from the mass balance is more important for the comparison of nonequilibrium column results to equilibrium batch systems. Both retardation factors are afflicted with an uncertainty due to the experimental and parameter identification methods. R_f is very sensitive to uncertainties in the influent concentration and may generally be overestimated by numerical integration of the area left of the breakthrough curve since it is difficult to distinguish between 99 % and 100 % breakthrough. $R_{0.5}$ is more reliable to determine but it is more sensitive to the flow velocity and generally underestimates the mass of solute absorbed in the column. Due to this fact, it is recommended to determine the retardation factor by both ways. The equilibrium transport of a sorbing compound through a column yields a fairly symmetrical breakthrough curve. A high degree of asymmetry or skewness of the breakthrough curve may indicate sorption nonequilibrium (Nkedi-Kizza et al., 1987). A measure for the skewness can be obtained by the ratio $R_{0.5}/R_f$ which compares the retardation factor on the first moment analysis (R_f) and the retardation factor at 50 % breakthrough ($R_{0.5}$). For ideal equilibrium breakthrough curves this becomes 1 indicating sorption equilibrium within the column transport experiment.

The apparent (non-equilibrium) distribution coefficients $K_d(t)^*$ and $K_{0.5}(t)^*$ in the column systems can be calculated from the retardation factors according to:

$$K_d(t)^* = \frac{(R_f - 1)n_e}{\rho_b} \quad \text{and}$$

$$K_{0.5}(t)^* = \frac{(R_{0.5} - 1)n_e}{\rho_b} \qquad (3.20)$$

3.7 Macropore column experiments

Soluble contaminants are often transported from the soil surface to the groundwater much faster than predicted by the advection-dispersion equation and the mean annual recharge rate (Rao et al., 1974; Jury et al., 1986; Roth et al., 1991). There are several reasons for this. One explanation is that only a "preferred" fraction of the water filled pore space contributes to the advective transport volume.

Soil as well as unweathered subsoil is structured to various degrees and exhibits an uneven or multimodal pore size distribution. Aggregation and continuous macropores are limiting cases of such structures with a distinct bimodal pore size distribution. Only the water filled macropores are considered to contribute to the advective transport, whereas in most cases transport into and out of the micropores is assumed to occur by diffusion only. Solute transport in aggregated porous media is therefore characterised by an early arrival of solutes displaced through the macropores and a slow approach to the final concentration caused by the slow diffusion within aggregates.

In this section a column experiment is presented which has been performed to estimate the diffusion coefficient in an aquitard material by conducting miscible solute transport experiments through a specially constructed column having both the macropore and micropore region. Initial and boundary conditions were set in such a way that analytical solutions of the corresponding model equations are available.

3.7.1 Column construction and determination of parameter values

The packing and construction procedure of the column followed the scheme of Young and Ball (1998). A stainless steel HPLC column with a length of 12.1 cm and an internal diameter of 2.94 cm (Alltech) with mirror finished walls and very minimal dead volume in the end fittings was used (Fig. 3.6). Prior to the column packing, the dry aquitard material (silty loam soil) was moistened with about 20 % (by weight) of solution (0.005 M $CaCl_2$) and 0.02 % NaN_3 in Milli-Q water. The moistened material was divided into 5 g units of moist material.

The column was then packed in lofts. Each loft was pressed into place using a flat-tipped rod, which was of nearly the same diameter as the interior of the column. Following complete packing of the column in this manner, a cylindrical section was removed by slowly pushing a brass tube (0.422 cm outer diameter) entirely through the centre of the column. Another previously prepared solid rod was

pressed through the brass tube to remove the aquitard material from the brass tube.

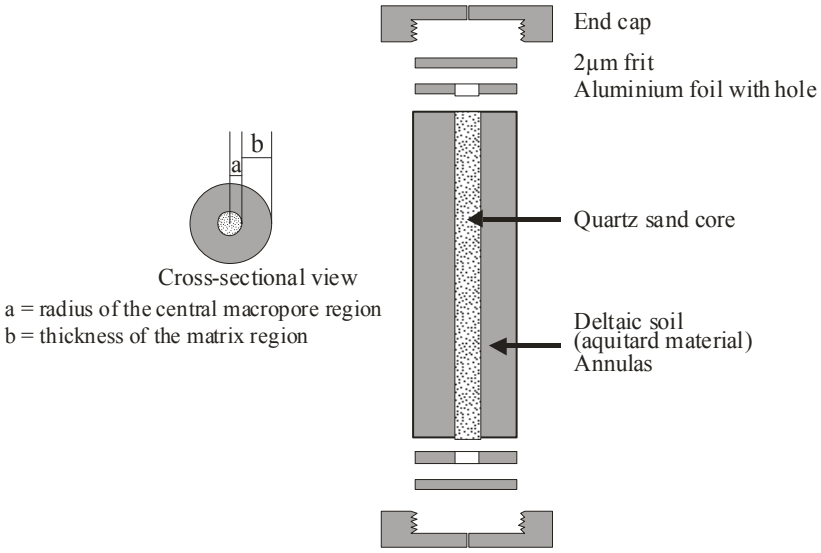

Fig. 3.6: Macropore column construction (following Young and Ball, 1998)

After being thoroughly cleaned, the brass tube was slowly withdrawn by about 1 cm and quartz sand (grain size 0.1 – 0.4 mm, heated at 550 °C for 24 h to remove organic carbon residues and thus to minimize the sorption of organic chemicals) was poured down the tube so that the 1 cm evacuated space was filled. The quartz sand was lightly tamped by inserting a glass rod through the brass tube. The tube was then withdrawn another 1 cm and the procedure was repeated until the brass tube was completely removed and the inner core completely filled with quartz sand. A piece of aluminum foil (cut to match the shape of the annulus) was placed at each end of the column. This piece of foil was intended to direct flow into the quartz sand filling the core of the column. A 2-µm frit was placed over the foil on each end and the column was capped. The resulting column thus contained the central macropore region consisting of quartz sand, surrounded by the soil material forming the matrix region (Fig. 3.6). The column was then saturated by flowing a degassed electrolyte solution (0.005 M $CaCl_2$) until a constant weight of the column was achieved that needed about 5 days. Some important properties of the column are given in Tab. 3.3.

The mass of quartz sand put into the column was determined by the difference in weight before and after packing the column. Since the aquitard material was packed wet, the total mass of solids was determined after completion of the experiments by removing the solids from the column, drying the solids over night at 105 °C, and then weighing the solids. The total water content of the packed column (V_w) was found by the difference between saturated column weights and the weight of dried materials. Dimension "b" was taken from a vernier-caliper measurement of the inside diameter of the column and "a" was measured for the outside diameter of the coring tube (Fig. 3.6).

Tab. 3.3: Experimental conditions of the macropore column studies

Length of column [cm]	12.1
Inner radius [cm]	0.422
Outer radius [cm]	1.05
Mobile (macropore) solid mass [g]	11.4
Immobile (matrix) solid mass [g]	62.0
Mobile region porosity [-]	0.37
Immobile region porosity [-]	0.45
Mobile region solid density [g cm^{-3}]	2.65
Immobile region solid density [g cm^{-3}]	2.69
Immobile region bulk density [g cm^{-3}]	1.47
Total pore volume [cm^3]	21.65

All other column properties were either easily measured or easily calculated given the above measurements and a solid density of 2.69 g cm^{-3} for the aquitard material and 2.65 g cm^{-3} for the quartz sand. The hydrodynamic dispersion coefficient (D_H) for the macropore region was estimated from packing a column with just the quartz sand and fitting the advection-dispersion model of Ogata and Banks (1961). The Peclet number was found to be sufficiently high (> 400) for the macropore region such that dispersion was relatively small.

3.7.2 Experimental design, procedure and analysis

After packing, deionised water containing 0.02 % NaN_3 was pumped through the column to minimize biotransformation of the organic compounds. The column was operated at room temperature of about 22 °C. The mean water velocities in the central quartz sand core ranged from 0.2 - 0.3 cm min^{-1} and were checked continuously in the effluent gravimetrically. The pumps were connected to the column with a 3-port control valve (Valco, Switzerland) in order to switch between solute solution and degassed water without flow interruption. An HPLC pump was used to control the finite pulse injection of solute solution and a peristaltic pump was used to feed the column continuously with degassed and deionised water until the end of the experiment. Before the finite pulse injection was made, the corresponding valve and tubings were purged in order to equilibrate it with the solution. The breakthrough of fluorescein, phenanthrene and carbofuran, was measured using the on-line fluorescence detection set-up shown in Fig. 3.7.

In the case of TCE and 1,2-DCB, the size of the collected effluent samples was varied over the course of the experiment so that maximum information could be achieved. During breakthrough when concentrations were changing rapidly, samples as small as 60 µl were taken. For the very low concentrations in the tailing, samples as large as 600 µl were taken. Detection and quantification of fluorescence, phenanthrene, carbofuran, TCE and 1,2-DCB was done in the same way mentioned previously.

3.7.3 Mass balance

In the pulse experiment, the solute recovery rates determine whether the breakthrough curves were measured for a period long enough to allow for the application of the methods of temporal moments which is sensitive to incomplete breakthrough curves. Mass balance is carried out by evaluating the ratio of eluted mass at time t and total mass injected. The ratio is computed via the trapezoidal rule yielding:

$$\frac{M(t)}{M_{total}} = \frac{1}{t_0}\int_0^t \frac{C(t)}{C_0}dt = \frac{1}{t_0}\sum_{n=1}^{n=k-1}\left[\left(\frac{C_n/C_0 + C_{n+1}/C_0}{2}\right)\left(t_{n+1} - t_n\right)\right] \quad (3.21)$$

where the first term of eq. (3.21) refers to the ratio of mass at time t to the total mass [-]. k, C_n/C_0, t and t_0 denote the number of observed data points, the effluent concentration normalized to the influent concentration [-], the time [T] and the pulse duration [T].

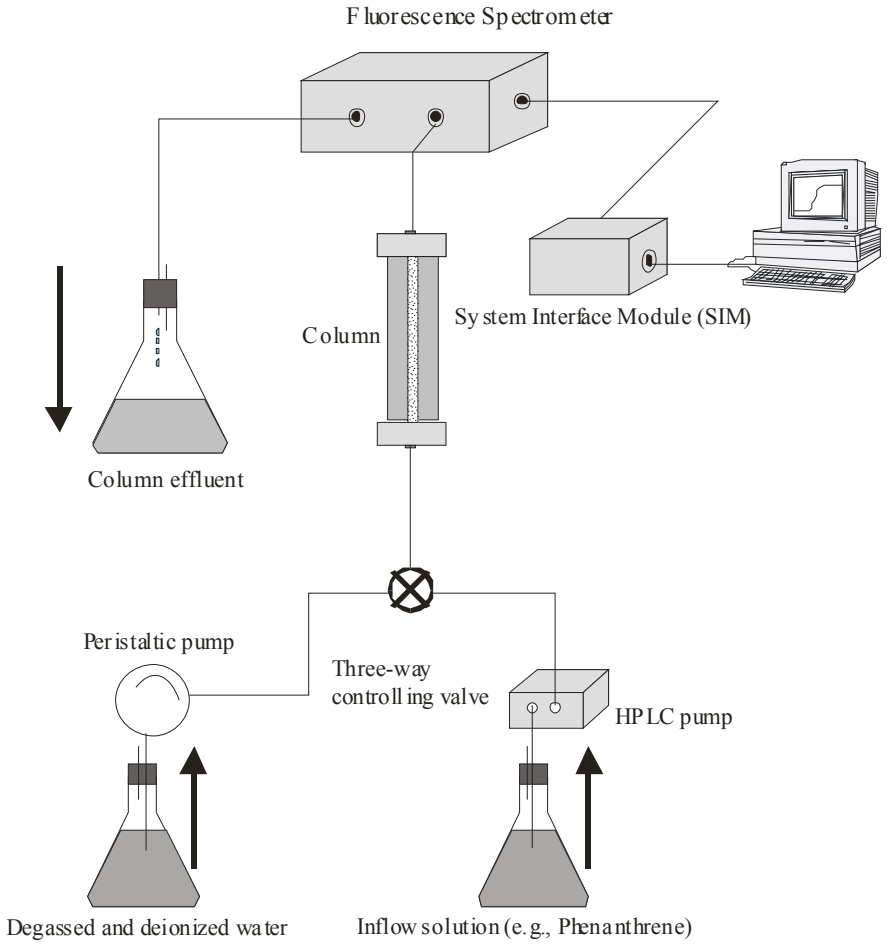

Fig. 3.7: On-line experimental set-up for the detection of breakthrough curves of fluorescein, carbofuran and phenanthrene.

4. RESULTS AND DISCUSSIONS

4.1 Sample Characterization

In order to evaluate the batch sorption and column experimental data and finally draw conclusions for groundwater risk assessment soil/sediments samples were characterized in terms of grain size distribution, particle density and organic carbon content. The effect of particle size on non-ionic organic solutes (NOS) sorption has been reported by Karickhoff et al. (1979) and Schwarzenbach and Westall (1981), who observed that soil/sediment organic carbon (SOC) and sorption increased with decreasing particle size. In contrast, Ball and Roberts (1991), observed that sorption, SOC and surface area increased with increasing particle size. Studies of sorption of non-ionic organic solutes from water to natural soil/sediments have proved that organic carbon is the major soil/sedimentary property controlling sorption. The value of particle density, which can be assumed to be almost constant in space is required when calculating the retardation factor of a sorbate-sorbent system.

4.1.1 Grain size distribution, particle density and organic carbon content

The grain size distribution of studied soil/sediments is shown in Fig. 4.1a-c. Tab. 4.1 summarizes the characterization results for sediment and soil materials collected from different horizons. The aquifer sediments consist of well sorted (uniformity coefficient < 4) 40 – 56 % sand (70 - 250 µm) to 40 — 60 % silt (2 - 70 µm) whereas soils consist of poorly sorted (uniformity coefficient > 4) 0.35 - 12.5 % sand (70 – 150 µm), 45 - 76 % silt (2 – 70 µm) and 2.7 – 49 % clay (< 2 µm). Grain size distribution does not show significant variation over depth from the A-horizon to the C-horizon.

Particle densities measured for soils and aquifer sediments were in the range of 2.66 to 2.69 g cm^{-3}. Soil/sediment organic carbon (SOC) decreases with increasing depth (A - C horizon). The organic carbon (OC) content within the soil horizons in the deltaic area (SatDs A-C horizons) varied from 0.46 to 1.58 % while the OC content of the floodplain soil horizons varied from 0.15 - 0.61 % and that of the residuum soil horizons varied from 0.12 - 0.67 % (Tab. 4.1). OC content of the deltaic soils (KhDs A-C horizons) does not show variation with depth. The deltaic aquifer sediment (Kh Aqfr) contains a higher percentage of OC (0.18 %) than that of the floodplain aquifer sediment (Raj Aqfr) (0.09 %). The deltaic soil has higher percentage of organic carbon than that of the residuum and floodplain soils both spatially and with depth (Fig. 4.1d). Peat (collected from the Bildakatia regio, Khulna district, from a depth range of 0.5 - 1.1 m) seems to have formed from reeds growing in fresh water swamps and shows the highest percentage of OC content (31.66 %) within the samples studied. Fig. 4.1e shows the plot of OC content measured using dry combustion and wet oxidation methods. OC content measured using the dry combustion method is ca. 50 % higher than measured using wet oxidation method.

4.1.2 Summary and discussion

From field observations it is concluded that the depth from the ground surface to the soil C-horizon varies from 1.2 m to 1.5 m, then followed by the substratum of very fine sandy and clayey loam and the aquitard material (Fig. 3.2). Grain size distribution data of soil and sediments reflect that soils/sediments are composed of fine grained sand, silt and clay sized particles. Soils are poorly sorted and are mainly composed of silty loam to silty clay in texture. Aquifer sediments are well sorted and mainly composed of fine grained sand and silty materials. Soil horizons do not show significant variation in particle size over depth but upon comparison to aquifer sediments a fining upward sequence is observed. The results of organic carbon analysis show that the soil horizons are lower in OC content with depth. The deltaic soils contain a higher percentage of organic carbon compared to floodplain and terrace soils both spatially and with depth.

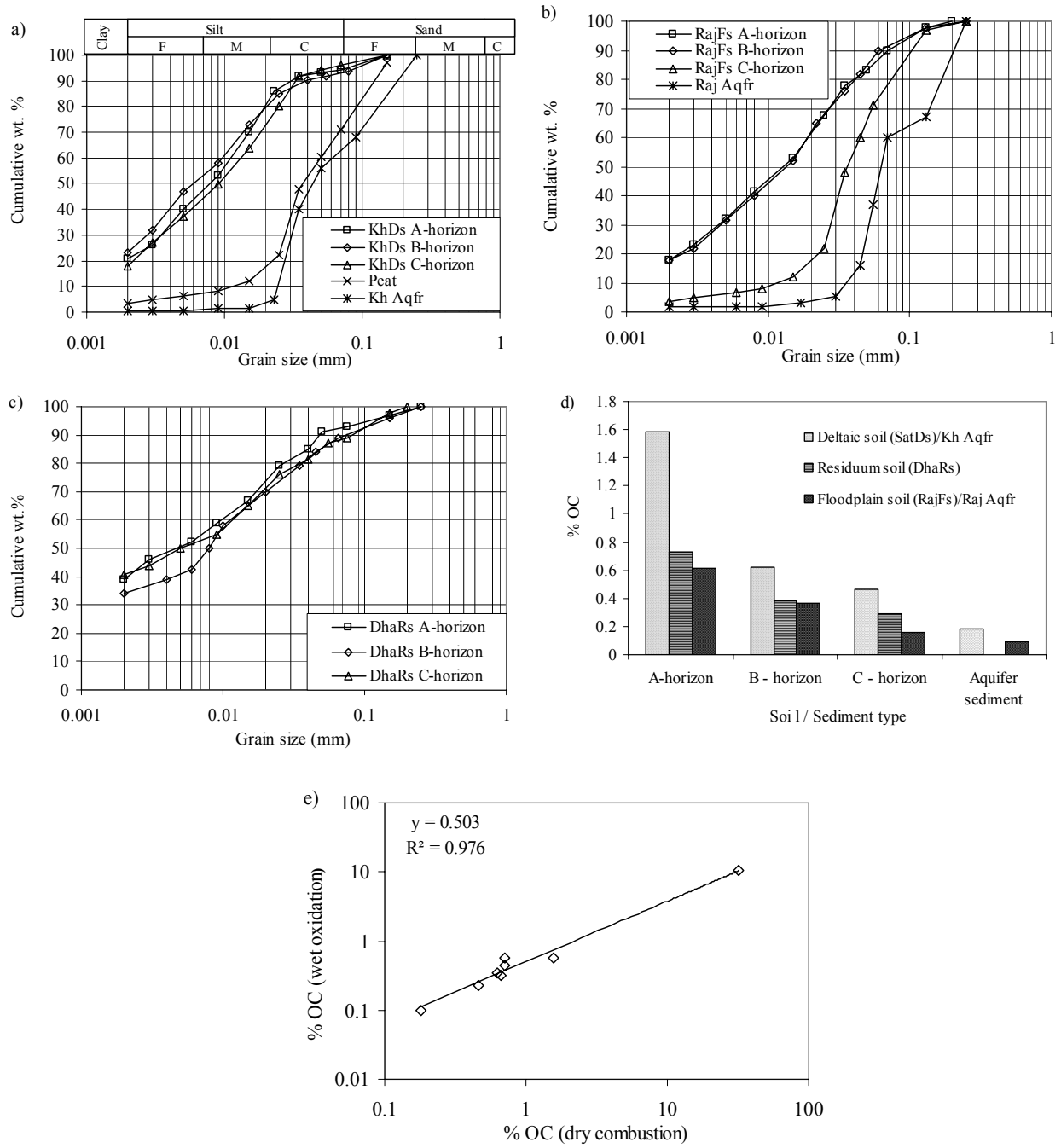

Fig. 4.1: Physico-chemical properties of soil/sediments. a) grain size distribution of deltaic soil (KhDs A, KhDs B and KhDs C-horizon), aquifer sediment (Kh Aqfr) and peat, b) floodplain soil and (RajFs A, RajFs B and RajFs C-horizon) and aquifer sediment (Raj Aqfr); c) residuum soil (DhaRs A, Dha Rs B and DhaRs C-horizon); d) soil/ sediment organic carbon as a function of soil/sediment type; e) difference of OC content measured using dry combustion and wet oxidation method. For sample notations also see Tab. 4.1.

Tab. 4.1: Summary of data of sample characterization: soils and sediments

Sample identifi-cation	Depth (m)	% of			Soil texture class	Uniform. Coeffi. (D_{60}/D_{10})	% OC		% $CaCO_3$	Par. den. [g cm^{-3}]
		Sand	Silt	Clay			Dry comb.	Wet oxidati.		
KhDs A	0.00-.20	5.00	74.0	21.0	SiL	30	0.71	0.56	4.80	2.69
KhDs B	0.20-.65	7.30	67.7	25.1	SiL	26	0.67	0.32	2.92	2.67
KhDs C	0.65-1.5	3.30	76.0	20.6	SiL	28	0.71	0.44	1.95	2.69
Kh Aqfr	2.90-20	40.0	59.6	0.32	SaSi	2.5	0.18	0.10	2.82	2.68
Peat	0.50-1.1	33.0	65.0	2.0	Peat	4	31.66	10.38	0.77	ND
SatDs A	0.00-.30	0.94	49.5	49.5	ClSi	>100	1.58	0.57	2.30	ND
SatDs B	0.30-.75	0.78	52.1	47.0	ClSi	>100	0.62	0.34	5.00	ND
SatDs C	0.75-1.2	0.35	60.9	38.7	ClSi	>100	0.46	0.23	8.13	ND
DhaRs A	0.00-.15	8.00	52.0	40.0	ClSi	>100	0.72	ND	0.67	2.68
DhaRs B	0.15-.80	11.5	52.7	35.9	ClSi	>100	0.38	ND	0.32	ND
DhaRs C	0.80-1.5	12.8	45.1	42.0	ClSi	>100	0.29	ND	0.12	ND
RajFs A	0.00-.18	12.5	68.2	19.3	SiCL	46	0.61	ND	2.35	ND
RajFs B	0.18-.70	11.4	69.6	19	SiCL	38	0.36	ND	9.33	ND
RajFs C	0.70-1.2	27.1	70.2	2.70	SiCL	3.40	0.15	ND	11.16	ND
Raj Aqfr	1.2-2.0	56.7	41.5	1.8	SaL	1.8	0.09	ND	6.30	2.66

Notes: In the sample identification prefix stands for location, middle unit for physiographic location and the suffix for soil horizon/aquifer sediments, if applicable. SiL: silt loam , SaSi: sandy silt, ClSi: clayey silt, SiCL: silt clay loam, SaL: sandy loam, ND: not determined. Kh: Khulna, Ds: Deltaic soil, Sat: Satkhira, Dha: Dhaka, Rs: Residuum soil, Raj: Rajshahi, Fs: Floodplain soil, Aqfr: Aquifer sediment. A, B and C represent the A, B and C horizon, respectively.

4.2 Equilibrum sorption isotherms

Equilibrium sorption isotherm experiments were carried out with all the collected soils/sediments using phenanthrene as a chemical probe for an initial screening assessment. Following the result with phenanthrene only deltaic soil (KhDsABC; mixture of KhDa A, KhDs B and KhDs C-horizon samples), aquifer sediment (KhAqfr) and peat samples were selected for further sorption experiments with 1,2-DCB, TCE and carbofuran in order to cover a wide variety of organic compounds with different water solubility.

4.2.1 Sorption of phenanthrene with all the collected samples

Sorption isotherm results of phenanthrene with pulverized deltaic, floodplain and residuum soils and aquifer sediments are shown in Fig. 4.2 a - d. Sorption experimental conditions are summarized in Tab. 4.2. Fitted Freundlich parameters, distribution coefficients (K_d) obtained through linear regression and average K_d (obtained by arithmatic average of each data point)by are given in Tab. 4.3. Isotherm data cover almost three to four order of magnitude range in solute concentration with equilibrium aqueous concentration to aqueous solubility ratios ranging from 0.001 to 0.28. Solid:water ratios were in the range of 1:2 – 1:5000.

The isotherms of phenanthrene with all the solids are approximately linear ($1/n$ = 0.7 - 1). A Freundlich exponent ($1/n$) as low as 0.82 was obtained for the peat sample. The increase in sorption is consistent with the increase in organic carbon content. The sorption distribution coefficient (K_d or K_{fr}) is found to decrease roughly 2 fold for the deltaic soils (SatDs A, SatDs B and SatDs C), 2 - 9 fold for the residuum soils (DhaRs A, DhaRs B and DhaRs C) and 2 - 3 fold for floodplain soils (RajFs A, RajFs B and Raj Fs C) down the soil profile. Hydrophobic partitioning is believed to be the dominant sorption mechanism as almost linear isotherms were observed over a wide range of solute concentration. The non-linearity of the deltaic soil ($SatD_s$ A-C horizons), although slight ($1/n$ = 0.72 - 0.86), may be related to the heterogeneity of NOM and the presence of HSACM (e.g., charcoal).

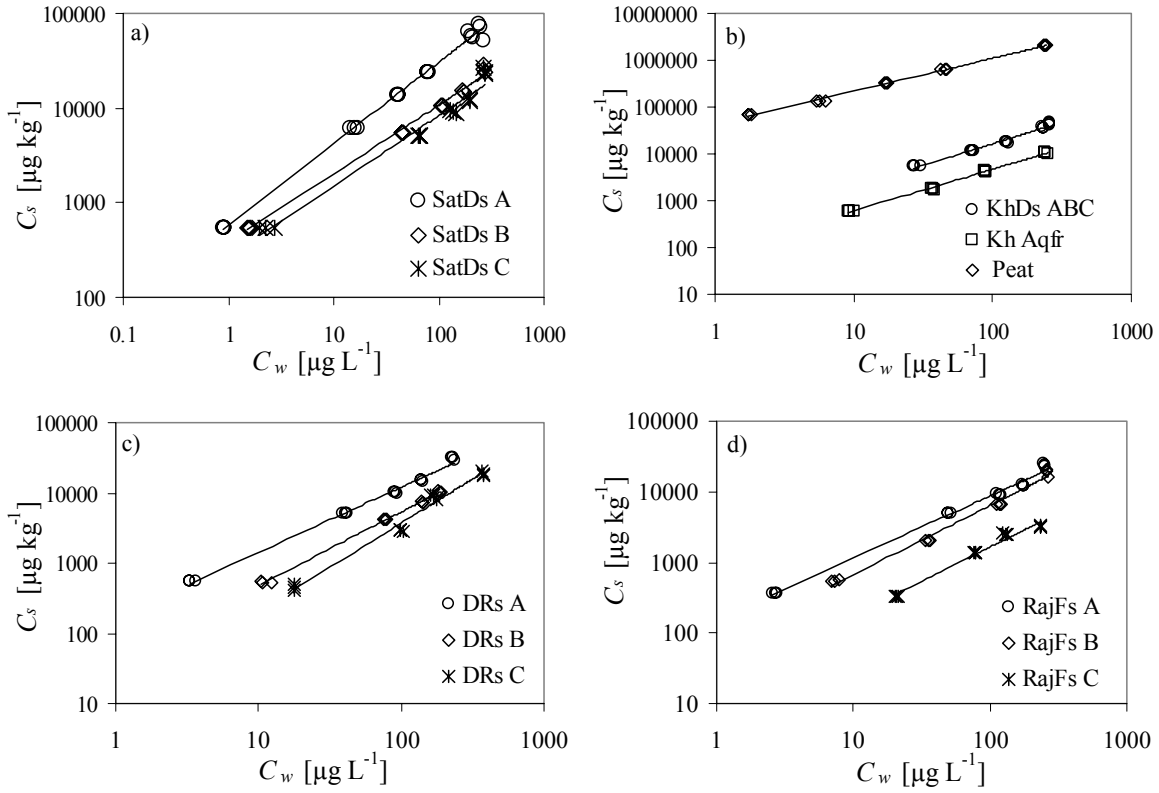

Fig. 4.2: Experimental equilibrium sorption isotherm data (symbols) and Freundlich isotherms models (solid lines) for phenanthrene with a) deltaic soils (SatDs A, SatDs B and SatDs C), b) deltaic soil (KhDs ABC), aquifer sediment (Kh Aqfr) and peat), c) residuum soils (DhaRs A, DhaRs B and DhaRs C) and d) floodplain soils (RajFs A, RajFs B and Raj Fs C). Parameters for model fits are given in Tab. 4.3. For the notation of samples name see Tab. 4.1. The notation KhDsABC corresponds to the name of the sample collected from three soil horizons A, B and C and mixed together subsequently for sorption experiments as the individual samples donot show variation in OC content with depth.

Tab. 4.2: Summary of sorption experimental condition (chemical: phenanthrene)

Sorbent name	Sorbent descrip.	Equili. Time [day]	Solid: Water	C_w/S [-]	Comments
Deltaic soil	SatDs A	30	1:2-500	0.001-0.16	3 ref. conc.
	SatDs B	30	1:5-500	0.001-0.20	Single conc.
	SatDs C	30	1:5-500	0.001-0.20	do
Deltaic soil	KhDs ABC	30	1:20-1000	0.02-0.20	2 ref. conc.
Aquifer sedi.	Kh Aqfr	30	1:2-150	0.007-0.20	do
Peat	Peat	30	1:100-5000	0.001-0.18	do
Residuum soil	DhaRs A	30	1:5-500	0.003-0.18	do
	DhaRs B	30	1:5-500	0.009-0.14	3 ref. conc.
	DhaRs C	30	1:2-160	0.07-0.28	4 ref. conc.
Floodplain soil	RajFs A	25	1:2-500	0.002-0.20	3 ref. conc.
	RajFs B	25	1:2-500	0.005-0.20	do
	RajFs C	25	1:17-50	0.01-0.18	4
Aquifer. sedi.	Raj Aqfr	25	1:2-8	0.009-0.18	4

Tab. 4.3: Summary of sorption isotherm analysis of phenanthrene with deltaic, floodplain and residuum soils, aquifer sediments and peat

Sorbent name	Sorbent description	f_{oc} (%)	Freundlich fit			Linear regression		Aver. K_d
			K_{fr} [L kg^{-1}]	*1/n*	R^2	K_d [L kg^{-1}]	R^2	[L kg^{-1}]
Deltaic soil	SatDs A	1.581	582	0.86	0.99	298	0.97	387
	SatDs B	0.622	380	0.72	0.99	95	0.97	151
	SatDs C	0.463	273	0.74	0.97	78	0.91	107
Deltaic soil	KhDsABC	0.698	232	0.92	0.98	161	0.97	163
Aquifer sedi.	Kh Aqfr	0.182	67	0.83	0.99	26	0.99	50
Peat	Peat	31.66	33136	0.82	0.97	19696	0.96	24411
Residuum soil	DhaRs A	0.727	166	0.92	0.99	125	0.97	127
	DhaRs B	0.385	43.6	1.04	0.99	54	0.99	53
	DhaRs C	0.290	11.3	1.05	0.98	49	0.96	39
Floodplain soil	RajFs A	0.613	155	0.87	0.99	86	0.95	96
	RajFs B	0.362	70	0.97	0.98	69	0.95	65
Aquifer sedi.	RajFs C	0.156	19.2	0.96	0.98	15.2	0.90	16.7
	Raj Aqfr	0.090	16.7	0.89	0.99	10.1	0.99	11.3

4.2.2 Sorption of 1,2-DCB with deltaic soil, aquifer sediment and peat

Sorption isotherm results of 1,2-DCB with deltaic soil, aquifer sediment and peat are shown in Fig. 4.3 and sorption experimental conditions are summarized in Tab. 4.4.

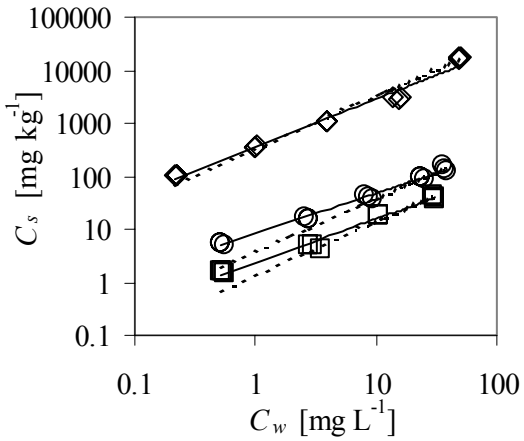

Fig. 4.3: Experimental equilibrium sorption isotherm data and Freundlich and linear isotherm model fit for 1,2-DCB with deltaic soil, aquifer sediment and peat. Circles: deltaic soil; squares: aquifer sediment; diamonds: peat; solid lines: Freundlich model; dotted lines: linear model. Parameters for model fits are given in Tab. 4.5.

Isotherm data with the solids cover three orders of magnitude in solute concentration with equilibrium aqueous concentrations between 0.2 mg L^{-1} to 48 mg L^{-1}. A Freundlich model fits these sorption data better than the linear model over the concentration range. Furthermore, the higher correlation coefficients (R^2) for the Freundlich fit (Tab. 4.5, for example) confirms that the Freundlich type model provides a better fit to the data than the linear model. The fitted Freundlich exponents (*1/n*) for deltaic soil, aquifer sediment and peat are roughly the same that is 0.8 - 0.9. Freundlich and linear model fit parameters are summarized in Tab. 4.5. Again the solids with the lowest organic carbon (aquifer sediment) exhibit the lowest sorption capacities while peat (highest organic carbon content) has the highest capacity.

Tab. 4.4: Summary of experimental conditions for sorption of 1,2-DCB on deltaic soil, aquifer sediment and peat

Sorbent name	Deltaic soil	Aqui. Sedi.	Peat
Sorbent description	KhDs ABC	Kh Aqfr	Peat
Equili. time [days]	15	15	15
Solid: Water	1:4-17	1:2-3	1:9-750
C_w/S [-]	0.003-0.26	0.003-0.21	0.001-0.34
Comments	Mul. ref. conc.	do	do

Tab. 4.5: Summary of sorption isotherm analysis of 1,2-DCB with deltaic soil, aquifer sediment and peat

Sorbent name	Sorbent descrip.	f_{oc} (%)	Freundlich fit			Linear regression		[1]Aver. K_d
			K_{fr} [L kg^{-1}]	*1/n*	R^2	K_d [L kg^{-1}]	R^2	[L kg^{-1}]
Deltaic soil	KhDs ABC	0.698	8.23	0.76	0.99	3.80	0.90	5.72 ± 2.5
Aqui. Sedi.	Kh Aqfr	0.182	2.38	0.81	0.98	1.35	0.97	1.89 ± 0.6
Peat	Peat	31.66	364	0.89	0.98	328	0.97	333 ± 101

[1] $K_d = C_s/C_w$ for each data point

4.2.3 Sorption of TCE with deltaic soil, aquifer sediment and peat

Sorption isotherm results of TCE with deltaic soil, aquifer sediment and peat are shown in Fig. 4.4 and experimental conditions are summarized in Tab. 4.6.

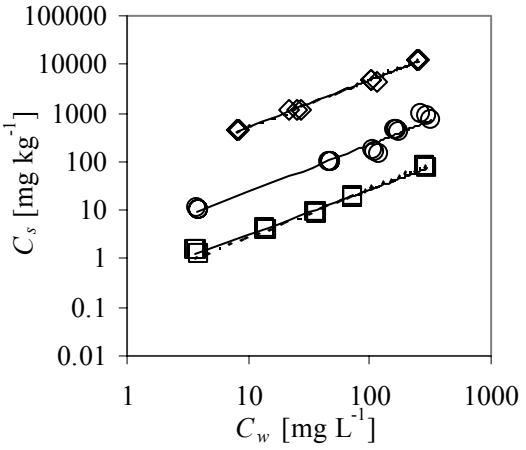

Fig. 4.4: Experimental equilibrium sorption isotherm data and Freundlich and linear isotherm model for TCE with deltaic soil, aquifer sediment and peat. Circles: deltaic soil; squares: aquifer sediment; diamonds: peat; solid lines: Freundlich model; dotted lines: linear model. Parameters for model fits are given in Tab. 4.7.

Isotherm data with the solids covered almost three orders of magnitude in solute concentration with equilibrium aqueous concentrations between 3 mg L^{-1} to 300 mgL^{-1}. Over this full range of equilibrium aqueous concentrations, both the Freundlich and the linear model show the same quality of fit with the data points. Solid to water ratios ranged from 1:2 - 5 for deltaic soil, 1:2 for aquifer sediment and 1:10 - 50 for peat. Because of the comparatively low K_{ow} and the low organic carbon content, a solid water ratio as low as 1:2 was used for the aquifer sediment. Sorption isotherms are almost linear (*1/n* = 0.96 - 0.99) with all the solids. The fitted Freundlich isotherm parameters together with the fraction of organic carbon (f_{oc}) are summarized in Tab. 4.7. The increase in sorption is consistent with the increase in organic carbon content.

Tab. 4.6: Summary of sorption experimental conditions of TCE with deltaic soil, aquifer sediment and peat

Sorbent name	Deltaic soil	Aqui.Sedi.	Peat
Sorbent description	KhDs ABC	Kh Aqfr	Peat
Equili. time [days]	20	20	20
Solid: Water	1:2-5	1:2	1:10-50
C_w/S [-]	0.003-0.22	0.003-0.26	0.007-0.26
Comments	Mul. ref. conc.	do	do

Tab. 4.7: Summary of sorption isotherm analysis of TCE with deltaic soil, aquifer sediment and peat

Sorbent name	Sorbent descrip.	f_{oc} (%)	Freundlich fit			Linear regression		[1]Aver. K_d
			K_{fr} [L kg^{-1}]	*1/n*	R^2	K_d [L kg^{-1}]	R^2	[L kg^{-1}]
Deltaic soil	KhDs ABC	0.698	2.46	0.98	0.96	2.67	0.89	2.35 ± 0.6
Aqui. Sedi.	Kh Aqfr	0.182	0.37	0.93	0.99	0.28	0.99	0.29 ± 0.05
Peat	Peat	31.66	56.4	0.96	0.99	49.3	0.98	49 ± 6

[1] $\boldsymbol{K_d} = C_s/C_w$ for each data point

4.2.4 Sorption of carbofuran with deltaic soil, aquifer sediment and peat

Sorption isotherm results of carbofuran with deltaic soil, aquifer sediment and peat are shown in Fig. 4.5 and experimental conditions are summarized in Tab. 4.8.

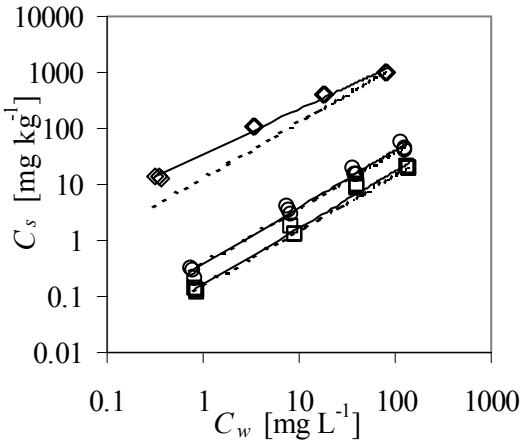

Fig. 4.5: Experimental equilibrium sorption isotherm data and Freundlich and linear isotherm model fit for carbofuran with deltaic soil, aquifer sediment and peat. Circles: deltaic soil; squares: aquifer sediment; diamonds: peat; solid line: Freundlich model; dotted line: linear model. Parameters for model fits are given in Tab. 4.9.

Isotherm data with the solids cover almost four orders of magnitude in solute concentration with equilibrium aqueous concentrations between 0.3 mg L^{-1} to 136 mg L^{-1}. Soil and aquifer sediments exhibit linear sorption isotherms while peat has a Freundlich exponent of 0.8. Solid to water ratios used for this system ranged roughly from 1:2 for soil and aquifer sediment and 1:10 – 1:20 for peat. Freundlich and linear model fit parameters as well as average K_d values are shown in Tab. 4.9.

Tab. 4.8: Summary of experimental conditions for sorption of carbofuran on deltaic soil, aquifer sediment and peat

Sorbent name	Deltaic soil	Aqui.Sedi.	Peat
Sorbent description	KhDs ABC	Kh Aqfr	Peat
Equili. time [days]	7	7	7
Solid: Water	1:2	1:2	1:10-20
C_w/S [-]	0.002-0.40	0.003-0.43	0.001-0.25
Comments	Mul. ref. conc.	do	do

Tab. 4.9: Summary of sorption isotherm analysis of carbofuran with deltaic soil, aquifer sediment and peat

Sorbent name	Sorbent descrip.	f_{oc} (%)	Freundlich fit			Linear regression		[1]Aver. K_d
			K_{fr} [L kg^{-1}]	*1/n*	R²	K_d [L kg^{-1}]	*R²*	[L kg^{-1}]
Deltaic soil	KhDs ABC	0.698	0.37	1.01	0.98	0.38	0.94	0.40 ± 0.08
Aqui. Sedi.	Kh Aqfr	0.182	0.16	1.01	0.98	0.15	0.95	0.17 ± 0.04
Peat	Peat	31.66	35.3	0.80	0.99	13.25	0.95	26.40 ± 10

[1] $K_d = C_s/C_w$ for each data point

4.2.5 K_d - f_{oc} and K_d - S correlation

If all observed sorption is attributable to organic partitioning, good correlation between K_d and f_{oc} might be expected (Karickhoff, 1984 and Voice and Weber, 1983). In general, the sorption coefficients (e.g., K_d) increase with increasing organic carbon content. Added to that, for a given organic chemical, K_d can vary considerably from soil to soil or sediment to sediment, depending upon the properties of sorbent such as type and maturity of organic matter. Therefore, it is not always useful to use a regression equation cited in the literature for the accurate estimation of the K_d value.

In Fig. 4.6 the distribution coefficient K_d for phenanthrene with all the collected soils/sediments calculated from the fitted Freundlich parameter (K_{fr}) at an aqueous concentration of 1 µg L^{-1} is plotted against the measured organic carbon content (f_{oc}). Values are compared with the results from the regression equation of Karickhoff et al. (1979) (line 1). It is apparent from the diagram that for the sorbents such as floodplain aquifer sediments, K_d can be perfectly predicted by the correlation from Karickhoff et al. (1979), which was established for soils (e.g., humic substances, humic and fulvic acid). For other sorbents like deltaic aquifer sediment and soils and peat, the use of Karickhoff's regression equation may lead to an underestimation of the K_d value.

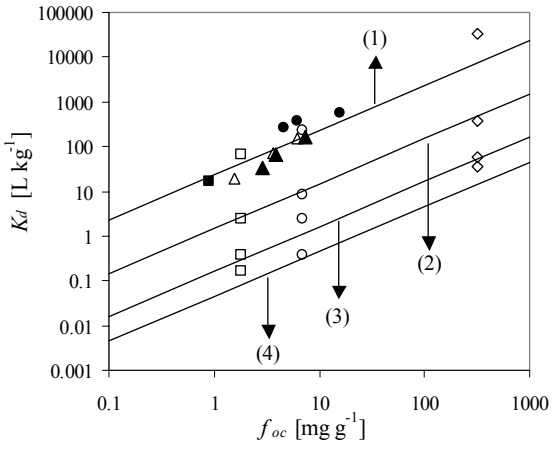

Fig. 4.6: K_d values vs. f_{oc} for the studied sorbents in comparison with regression correlation from Karickhoff et al. (1979) (lines): (1) for phenanthrene, (2) for 1,2-DCB, (3) for TCE and (4) for carbofuran. Open circles: deltaic soil (KhDs ABC); open squares: aquifer sediment (Kh Aqfr); diamonds: peat; filled circles: deltaic soils (Sat DsA, SatDs B and SatDs C); filled squares: aquifer sediment (Raj Aqfr); open triangles: floodplain soils (RajFs A, RajFs B and RajFs C); filled triangles: residuum soils (DhaRs A, DhaRs B and DhaRs C). K_d was calculated at C_w = 1 µg L^{-1} for phenanthrene and at C_w = 1 mg L^{-1} for 1,2-DCB, TCE and carbofuran.

K_d (calculated from the fitted Freundlich parameter, $K_{fr,}$ at an aqueous concentration of 1 mg L^{-1}) was also determined with the selected deltaic soil, aquifer sediment and peat (as these solids show deviation of K_d values from Karickhoff) and using the solutes 1,2-DCB (line 2), TCE (line 3) and carbofuran (line 4). As shown in Fig. 4.6 Karickhoff's regression equation can better fit the data points for these chemicals than for phenanthrene.

Experimentally obtained K_d values and the observed and predicted K_{oc} values of phenanthrene, 1,2-DCB, TCE and carbofuran with deltaic soil, aquifer sediment and peat are summarized in the upper part of Tab. 4.10. The variations of K_d or K_{oc} for phenanthrene with soil depth are summarized in the lower part of the Tab. 4.10. K_{oc} values of phenanthrene with deltaic soil, aquifer sediment and peat are found to be 1.4, 1.6 and 4.5-fold higher than the predicted K_{oc} values based on Karickhoff's regression equation. A similar trend is observed for carbofuran with the highest K_{oc} variation in peat (4.4-fold) and lowest in deltaic soil and aquifer sediment (2.2 and 3.6-fold, respectively). 1,2-DCB and TCE do not show significant variations in K_{oc} for most experiments except for the TCE with deltaic soil where the observed K_{oc} is ca. 2-fold higher than the predicted value.

It is also evident from Tab. 4.10 that K_d as well as K_{oc} values decrease monotonically with depth in all soil horizons especially in residuum (DhRs A-C) and floodplain soils (RajFs A-C). K_{oc} of phenanthrene for the residuum soil A-horizon is half an order of magnitude higher than in the C-horizon. K_{oc} of the C-horizon of residuum soil (DhRsC) is also half an order of magnitude lower than the predicted K_{oc} value. Variations in K_{oc} of

Tab. 4.10: Observed and estimated K_{oc} values

Chemicals	Soil/Sediment	f_{oc}	[a] K_d	Observed K_{oc}	[b] Estimated K_{oc}
Phenanthrene	Deltaic soil	0.00698	232.46	33303	23035
	Aqui. sediment	0.00182	67.51	37073	
	Peat	0.3166	33136	104662	
1,2-DCB	Deltaic soil	0.00698	8.23	1179	1487
	Aqui. sediment	0.00182	2.38	1306	
	Peat	0.3166	364.46	1151	
TCE	Deltaic soil	0.00698	2.46	352	163
	Aqui. sediment	0.00182	0.36	197	
	Peat	0.3166	56.47	178	
Carbofuran	Deltaic soil	0.00698	0.38	54	25
	Aqui. sediment	0.00182	0.163	89	
	Peat	0.3166	35.31	111	
	f_{oc}-K_{oc} variation with depth				
Phenanthrene	SatDs –A horizon (0-0.2)[c]	0.0158	582.03	36837	23035
	SatDs –B horizon (0.2-0.65)[c]	0.00622	380.68	61113	
	SatDs –C horizon (0.65-1.5)[c]	0.00463	273.75	59099	
	DhaRs-A horizon (0-0.15)[c]	0.00727	166.85	22947	
	DhaRs-B horizon (0.15-0.80)[c]	0.00385	43.6	11318	
	DhaRs-C horizon (0.8-1.5)[c]	0.00290	11.35	3907	
	RajFs-A horizon (0-0.20)[c]	0.00613	155.3	25330	
	RajFs-B horizon (0.2-0.7)[c]	0.00362	70.87	19557	
	RajFs-C horizon (0.7-1.2)[c]	0.00157	19.22	12265	

[a] K_d was calculated using C_w = 1 µg L^{-1} for phenanthrene and for the rest of the chemicals using 1 mg L^{-1}. [b] K_{oc} was estimated based on the regression equation given by Karickhoff et al., (1979) and using the K_{ow} values given in Tab. 3.1. The unit of K_{oc} is the same as for K_d. [c] thickness of soil horizon in meter.

phenanthrene for deltaic soil (SatDs A-C) and floodplain soil (RajFs A-C) are also observed but are not as significant as in residuum soil. Changes in K_{oc} with soil depth are believed to occur due to structural variations, maturity and chemical composition of natural organic matter (NOM) in soils and sediments which are in coincidence to findings from others (e.g., Njoroge et al., 1998).

Sorption or distribution coefficients of non-polar and hydrophobic organic compounds tend to decrease with increasing water solubility. K_d was therefore calculated at 10 % of the compounds water solubility from experimental data as the data are available in this concentration range which is not so much affected by adsorption. K_d values calculated at 10 % water solubility are summarized in Tab. 4.11.

Fig. 4.7a shows an inverse linear relationship (slope: -1) between measured K_d (calculated at 10 % S) and water solubility S [mg L^{-1}]. In such a case (log linear relationship), the product of K_d and S is then a constant for a given sorbent. Consequently, the sorption coefficients (K_d) at a given concentration relative to the solubility of various compounds are also expected to be inversely linear to the water solubility and this allows the prediction of sorption of compounds similar to compounds investigated in this study. If K_d is normalized to the organic carbon fraction (K_d/f_{oc} = K_{oc}) then all compounds and all samples yield similar inverse linear relationships to S, as expected from eqs. (2.1).

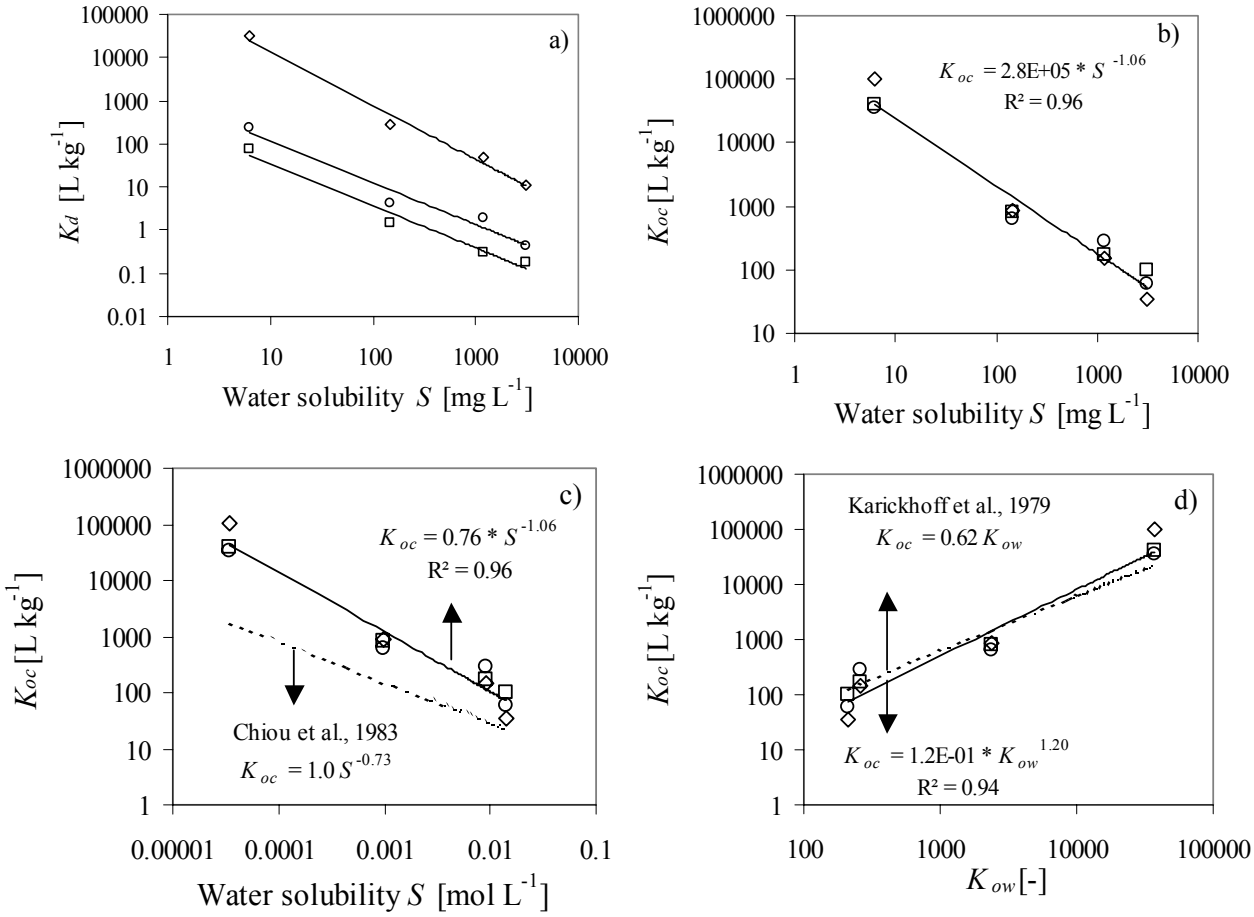

Fig. 4.7: Relationship of a) measured K_d vs. S in mg L^{-1}, b) K_{oc} vs. S in mg L^{-1}, c) K_{oc} vs. S in mol L^{-1}, d) K_{oc} vs. K_{ow} and comparison with literature regression correlations. K_{oc} was calculated as the ratio of K_d (at 10 % of S) to f_{oc}. Circles: deltaic soil; squares: aquifer sediment and diamonds: peat.

Tab. 4.11: Distribution coefficient (K_d) at 10 % water solubility (C_w/S = 0.1)

Chemicals	Water solubility S (mg L^{-1}]	K_d at 10 % water solubility [L kg^{-1}]		
		Deltaic soil	Aquifer sediment	Peat
Carbofuran	3100[a]	0.41	0.17	11
TCE	1198	1.93	0.31	47
1,2-DCB	145	4.35	1.46	276
Phenanthrene	6.2[a]	241	73	31754

[a] subcooled liquid solubility

and (2.6) (Fig. 4.7b). The K_{oc} vs. S relationship (Fig. 4.7c) fits better if S is expressed in the units mol L^{-1} compared to S in mg L^{-1} as expected from eq. (2.2) (partitioning). Interestingly the slope of the relationship determined here is close to -1, which is in contrast to earlier literature relationships where slopes of typically -0.6 to - 0.7 are reported. Fig. 4.7d shows in addition the correlation between K_{oc} and K_{ow}, which is slightly worse than K_{oc} - S.

4.2.6 Solubility normalized sorption isotherms

Figs. 4.8 a-c show the sorptive uptake vs. the solubility normalized aqueous concentration of phenanthrene, 1,2-DCB, TCE and carbofuran with deltaic soil, aquifer sediment and peat. These data were also fitted (fitting is not shown) using the linear model ($C_s = K_d\, C_w$) and the Freundlich equation ($C_s = K_{fr}\, C_w^{1/n}$). Freundlich coefficients K_{fr} and exponents $1/n$ were determined by a linear least square fit of the log transformed concentrations. Solubility

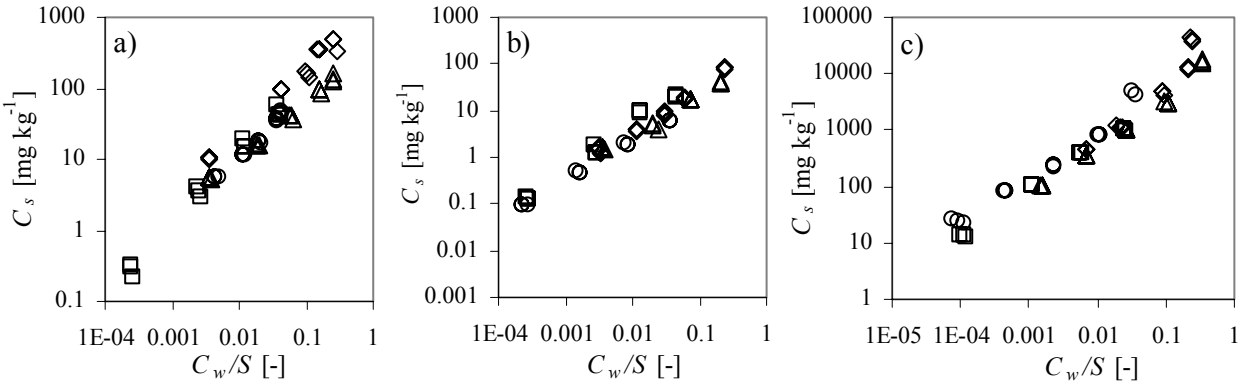

Fig. 4.8: Solubility normalized equilibrium sorptive uptake of phenanthrene, 1,2-DCB, TCE and carbofuran with a) deltaic soil, b) aquifer sediment and c) peat. Circles: phenanthrene; triangles: 1,2-DCB; diamonds: TCE and squares: carbofuran. In case of solid chemicals the subcooled liquid solubility (S_{scl}) is used.

Tab. 4.12: Freundlich, linear, normalized and overall sorption isotherm parameters. For phenanthrene and carbofuran subcooled liquid solubility (S_{scl}) was used instead of solid solubility.

Freundlich parameters	Deltaic soil (f_{oc} = 0.007)	Aquifer sediment (f_{oc} = 0.0018)	Peat (f_{oc} = 0.317)
	Phenanthrene		
log K_{fr} [L kg^{-1}]	2.23 ± 0.04	1.31 ± 0.02	4.06 ± 0.09
1/n [-]	0.92 ± 0.03	0.83 ± 0.01	0.82 ± 0.04
K_d at 10 % of S [L kg^{-1}]	241	73	31754
log K_{fr}^* [-]	2.87 ± 0.06	1.96 ± 0.03	4.63 ± 0.11
	Carbofuran		
log K_{fr} [L kg^{-1}]	-0.42 ± 0.04	-0.46 ± 0.04	1.54 ± 0.02
1/n [-]	1.01 ± 0.03	1.01 ± 0.02	0.80 ± 0.01
K_d at 10 % of S [L kg^{-1}]	0.41	0.17	11
log K_{fr}^* [-]	3.12 ± 0.08	2.75 ± 0.08	4.33 ± 0.05
	1,2-DCB		
log K_{fr} [L kg^{-1}]	0.91 ± 0.02	0.38 ± 0.03	2.56 ± 0.03
1/n [-]	0.76 ± 0.02	0.82 ± 0.03	0.89 ± 0.03
K_d at 10 % of S [L kg^{-1}]	4.35	1.46	276
log K_{fr}^* [-]	2.56 ± 0.03	2.14 ± 0.05	4.50 ± 0.06
	TCE		
log K_{fr} [L kg^{-1}]	0.39 ± 0.09	-0.43 ± 0.04	1.75 ± 0.05
1/n [-]	0.97 ± 0.05	0.93 ± 0.02	0.96 ± 0.02
K_d at 10 % of S [L kg^{-1}]	1.93	0.31	47
log K_{fr}^* [-]	3.40 ± 0.07	2.41 ± 0.04	4.71 ± 0.04
	Overall *S*-normalized sorption isotherm including all compounds		
log K_{fr}^* [-]	2.98 ± 0.04	2.40 ± 0.10	4.47 ± 0.10
1/n [-]	0.97 ± 0.02	0.93 ± 0.03	0.80 ± 0.03
R^2 [-]	0.98	0.95	0.95
[1]log (K_d S)	3.03 ± 0.35	2.51 ± 0.27	5.38 ± 0.26

[1]K_d was calculated at 10 % of S: $K_d = K_{fr}(S*0.1)^{1/n-1}$

normalized Freundlich coefficients K_{fr}^* ($K_{fr}^* = K_{fr} S^{1/n}$) were calculated based on the Freundlich parameters. The fitted Freundlich parameters together with K_{fr}^* are summarized in Tab. 4.12

Compared to the traditional Freundlich sorption isotherms (Figs. 4.3, 4.4 and 4.5), the solubility normalized data (Fig. 4.8a-c) demonstrate how the simple normalization procedure yields a "collapsing" sorption isotherms. Sorption of all compounds generally increases with increasing f_{oc} (from the aquifer sediment, to the soil, and to the peat sample). K_{Fr} and K_d increase with decreasing water solubility of the compounds. K_{fr}^* of all compounds is reasonably constant in each sample. For a given sample the error of the average log K_{fr}^* is just 0.04 - 0.1. As expected from the solubility normalized Freundlich isotherms (eq. 2.5) the product $K_d S$ is also reasonably constant (Table 4.12)

4.2.7 Composite adsorption partitioning with the Polanyi-Manes approach

As with other partitioning models (Freundlich or linear model), the Polanyi-Manes based composite adsorption-partitioning model(eq. 2.4) can also be used to fit observed sorption isotherms. This model has both the partitioning and adsorption component which allows to separate the contribution of each component individually. Sorption experimental results and the model fits are shown for all chemicals studied with the deltaic soil (Fig. 4.9), deltaic aquifer sediment (Fig. 4.10) and peat (Fig. 4.11). Also shown are the calculated adsorption component after subtraction of the partitioning contribution as well as the fitted lines from the adsorption partitioning model. The fitted parameters K_p (L kg^{-1}) which is equal to ($f_{om} K_{om}$) in eq. (2.4), V_o (cm³ kg^{-1} soil) and E (kJ mol^{-1}) along with the calculated mean weighted square errors (MWSE) for all chemicals with deltaic soil, peat and aquifer sediment are summarized in Tab. 4.13. In general, the fitted lines are in good agreement with the overall observed sorption data and adsorption component. In other words, the total sorption data and the adsorption component can be modelled by the Polanyi-Manes based adsorption-partitioning model for all the geosorbents with the investigated chemicals.

For highly sorbing chemicals (e.g., phenanthrene) adsorption can contribute significantly to the overall sorption isotherms especially in the low concentration range with all the geosorbents investigated, while for less sorbing chemicals (e.g. TCE, carbofuran) partitioning is the dominant mechanism in the concentration range covered. An adsorption plateau is observed at very high relative concentrations. The fitted values of V_0 for the individual sorbents were similar within the compounds (0.01 cm³ kg^{-1} for deltaic soil; 0.001 – 0.003 cm³ kg^{-1} for aquifer sediment and 0.12 – 0.2 cm³ kg^{-1} for peat; see also Tab. 4.13). Values of E are in the order of 8-14 kJ mol^{-1} which is reasonable for sorptive uptake of hydrophobic compounds from water. Choma et al. (1993) reported 10-13 kJ mol^{-1} for adsorption of benzene from water on activated carbons.

Figs. 4.12a-c show the correlation of K_{oc} obtained by dividing K_p by the fraction of organic carbon (f_{oc}) with K_{ow} for all the chemicals investigated. Regression coefficients of deltaic soil and aquifer sediment show similar values to those obtained from the regression equation of Karickhoff (Tab. 2.1). Slope and intercept of the regression line for peat are higher than for deltaic soil and aquifer sediment suggesting that the peat may contain an organic matter phase for partitioning which is less polar than that of the deltaic soil and the aquifer sediment.

Tabs. 4.14 - 4.16 compare the distribution coefficient values obtained from Freundlich (K_{fr}), linear (K_d), average (K_d) model and partition coefficient values (K_p) from the composite Polanyi-Manes based adsorption-partitioning model. For low sorbing chemicals like TCE and carbofuran, different models result in almost the same sorption coefficients (K_d, K_{fr} or K_p) observed for deltaic soil and aquifer sediment. On the contrary, for highly sorbing chemicals e.g., phenanthrene, the sorption coefficients vary by a factor of 1.5 – 2 between the Freundlich model and the linear model/average K_d approach. Sorption coefficients K_p obtained from the combined adsorption-partitioning model are always lower than K_{fr} and K_d as K_p was used as a fitting parameter which is covering only the partitioning process.

Tab. 4.13: Fitted parameters of the observed sorption isotherms with deltaic soil, aquifer sediment and peat in the composite adsorption-partitioning model. $^{\pm}K_p$, V_0 and E were used as fitting parameters in the model. The exponent b in eq. (2.4) was set to 2

Composite parameters	Deltaic soil	Aquifer sediment	Peat
	Phenanthrene ($^{+}\rho_o$ = 1.063 g cm^{-3})		
K_p [Lkg^{-1}]	138	26	11000
V_0 [cm^3 kg^{-1}]	0.01	0.001	0.16
E [kJ mol^{-1}]	6.5	9.9	12.9
*MWSE [-]	0.16	0.15	0.16
	Carbofuran ($^{+}\rho_o$ = 1.18 g cm^{-3})		
K_p [Lkg^{-1}]	0.36	0.13	14
V_0 [cm^3 kg^{-1}]	0.015	0.003	0.2
E [kJ mol^{-1}]	7.5	8.5	11.8
*MWSE [-]	0.15	0.78	0.17
	1,2-DCB ($^{+}\rho_o$ = 1.063 g cm^{-3})		
K_p [Lkg^{-1}]	3.6	1.29	287
V_0 [cm^3 kg^{-1}]	0.013	0.002	0.12
E [kJ mol^{-1}]	10.8	12.1	14.0
*MWSE [-]	0.08	0.2	0.04
	TCE ($^{+}\rho_o$ = 1.465 g cm^{-3})		
K_p [Lkg^{-1}]	2.2	0.24	46
V_0 [cm^3 kg^{-1}]	0.013	0.001	0.2
E [kJ mol^{-1}]	9.3	13.7	10.6
*MWSE [-]	0.52	0.11	0.006

$^{\pm}K_p = (f_{om} K_{om})$ in eq. (2.4), * Mean weighted square error; $^{+}\rho_o$ density of organic compound

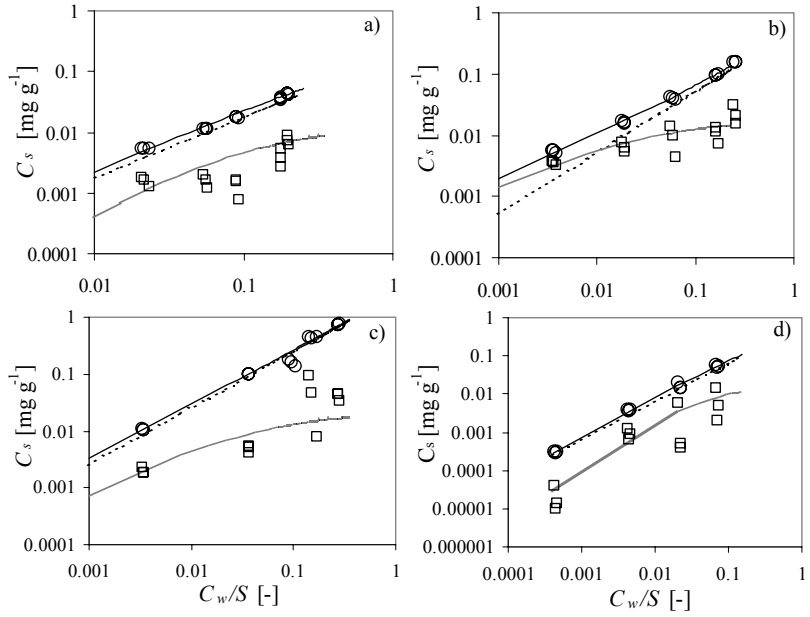

Fig. 4.9: Composite adsorption-partitioning isotherm with Polanyi-Manes based model fit for deltaic soil: a) phenanthrene, b) 1,2-DCB, c) TCE and d) carbofuran. For legends see Fig. 4.11.

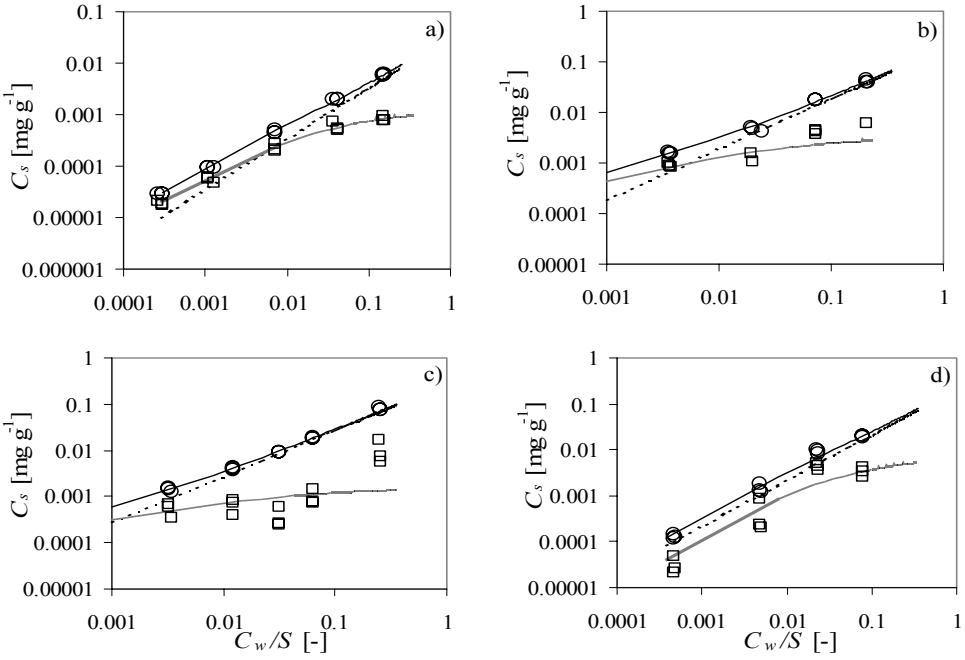

Fig. 4.10: Composite adsorption-partitioning isotherm with Polanyi-Manes based model fit for aquifer sediment: a) phenanthrene, b) 1,2-DCB, c) TCE and d) carbofuran. For legends see Fig. 4.11.

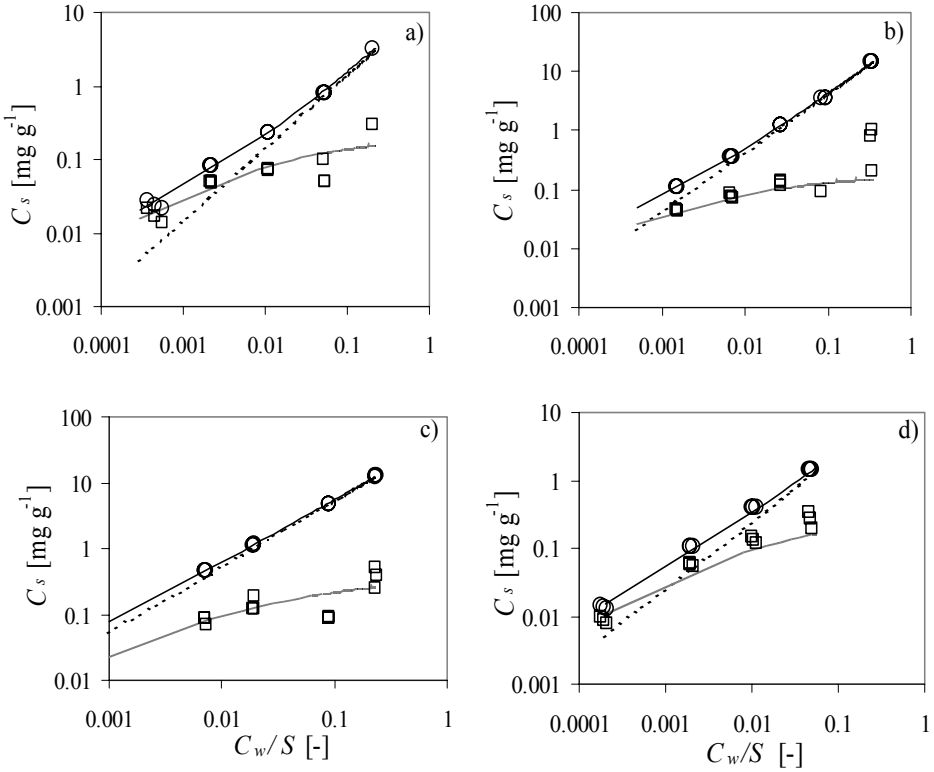

Fig. 4.11: Composite adsorption-partitioning isotherm with Polanyi-Manes based model fit for peat: a) phenanthrene, b) 1,2-DCB, c) TCE and d) carbofuran. Circles: partitioning plus adsorption (measured); squares: adsorption (calculated); solid lines: partitioning plus adsorption (fitted); dashed lines: adsorption (fitted); dotted lines: partitioning only (fitted)

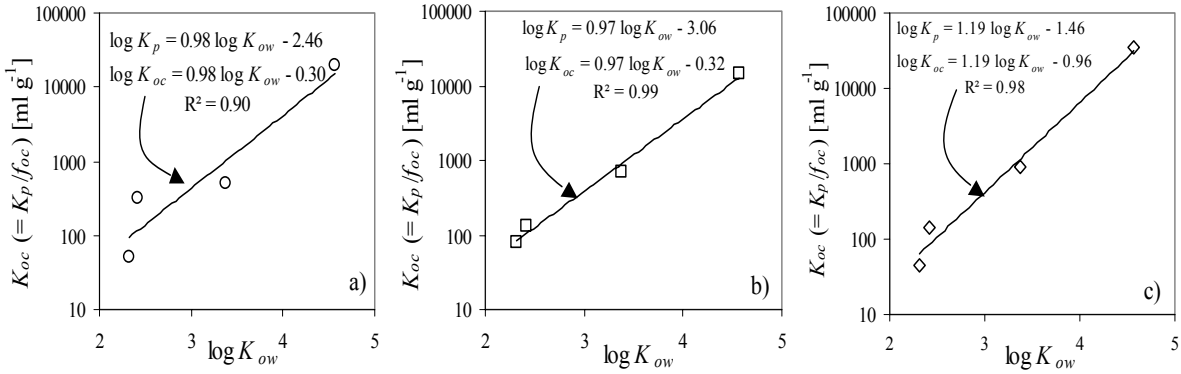

Fig. 4.12: Relationship between log K_{ow} and log K_{oc} ($K_{oc} = K_p / f_{oc}$) for the chemicals investigated with a) deltaic soil; b) aquifer sediment and c) peat, respectively. K_p(f_{om} K_{om}) values were obtained as a fitting parameter from the composite adsorption-partitioning model (Tab. 4.14-4.16).

Tab. 4.14: Comparison of K_d from different models (deltaic soil: KhDs ABC)

Chemicals	Freundlich model			Linear model		Average K_d	Composite model	
	K_{fr} [L kg^{-1}]	*1/n*	R^2	K_d [L kg^{-1}]	R^2	[L kg^{-1}]	K_p [L kg^{-1}]	MWSE
Phenanthrene	232	0.92	0.98	161	0.97	163	138	0.08
1,2-DCB	8.23	0.76	0.99	3.8	0.90	5.72	3.6	0.08
TCE	2.46	0.97	0.96	2.7	0.89	2.35	2.20	0.52
Carbofuran	0.37	1.01	0.98	0.38	0.94	0.40	0.36	0.15

Tab. 4.15: Comparison of K_d from different models (aquifer sediment: Kh Aqfr)

Chemicals	Freundlich model			Linear model		Average K_d	Composite model	
	K_{fr} [L kg^{-1}]	*1/n*	R^2	K_d [L kg^{-1}]	R^2	[L kg^{-1}]	K_p [L kg^{-1}]	MWSE
Phenanthrene	67	0.83	0.99	25.9	0.99	50	26	0.15
1,2-DCB	2.38	0.82	0.98	1.35	0.97	1.9	1.29	0.20
TCE	0.37	0.93	0.99	0.28	0.99	0.28	0.24	0.11
Carbofuran	0.16	1.01	0.98	0.15	0.95	0.17	0.13	0.78

Tab. 4.16: Comparison of K_d from different models (peat)

Chemicals	Freundlich model			Linear model		Average K_d	Composite model	
	K_{fr} [L kg^{-1}]	*1/n*	R^2	K_d [L kg^{-1}]	R^2	[L kg^{-1}]	K_p [L kg^{-1}]	MWSE
Phenanthrene	33136	0.82	0.97	19696	0.94	24411	11000	0.16
1,2-DCB	364	0.90	0.98	328	0.97	333	287	0.08
TCE	56	0.96	0.99	49	0.98	49	46	0.006
Carbofuran	35	0.79	0.99	13.2	0.95	26	14	0.17

4.2.8 Effect of temperature on the distribution coefficient

Sorption isotherm experiments of phenanthrene were carried out for deltaic soil, aquifer sediment and peat at three different temperatures such as 20 °C as reference temperature and 4 °C and 40 °C. The study of phenanthrene sorption at different temperatures aimed at predicting the phenanthrene partitioning ratio within a realistic range of environmental temperatures, validating experimental results by thermodynamic analysis and gaining insight onto the sorption mechanism. Fig. 4.13 shows the plot of the sorption coefficients (K_{fr}) versus *1/RT* and Tab. 4.17 presents the phenanthrene isotherm data at three different temperatures for the solids investigated.

The Freundlich coefficients were observed to be dependent on temperature. A decreasing temperature from 20 °C to 4 °C caused an

Tab. 4.17: Influence of temperature on sorption equilibrium and the values of sorption enthalpy.

Type of sorbent	$\Delta H°$ [a] [kJ mol^{-1}]	$\Delta H°$ [b] [kJ mol^{-1}]	K_{fr} [L/kg]			$K_{fr,4}/K_{fr,20}$ (batch)	$K_{fr,4}/K_{fr,20}$ [c] (predicted)
			4° C	20° C	40° C		
Deltaic soil	-16.59± 10	-16.33	557	232	239	2.4	1.96
Aqui. sediment	-16.05± 9.4	-16.91	149	67	66	2.22	
Peat	-5.93± 5.9	-6.08	47811	33136	35301	1.44	

[a] obtained as a slope from the plotting of ln K_{fr} vs. 1/RT (Arrhenius plot), [b] calculated using eq. (2.17), [c] calculated using eq. (2.18).

increase in the distribution coefficient by a factor of about 2 for deltaic soil and aquifer sediment but less than a factor of 2 for peat.

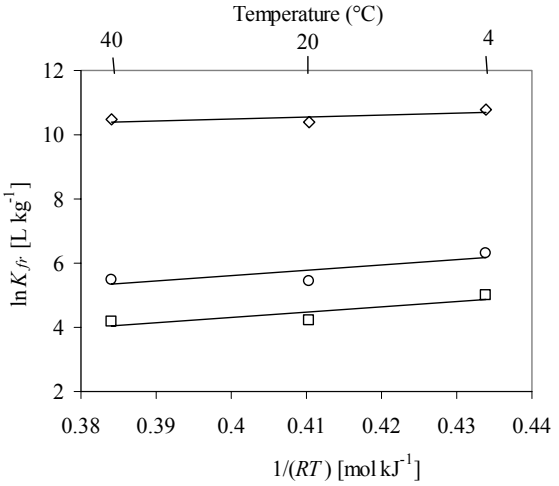

Fig. 4.13: Plot of sorption coefficients (K_{fr}) as a function of temperature for phenanthrene sorption on deltaic soil (circles), aquifer sediment (squares) and peat (diamonds).

The predicted ratio (eq. 2.18) of $K_{fr,4}$ / $K_{fr,20}$ (at 4 and 20 °C temperature, respectively) is about 2 (Tab. 4.17) which compares favourably well with the experimental ratios. The good agreement between the predicted and experimental ratios implies that the aqueous phase activity coefficient is a major factor controlling changes in the extent of sorption of phenanthrene especially on low f_{oc} solids with varying temperature.

Sorption enthalpy or standard enthalpy ($\Delta H°$) was obtained as a slope from the plotting of ln K_{fr} versus 1/RT (Fig. 4.13). The plot of ln K_{fr} versus 1/RT will give a straight line provided that $\Delta H°$ is constant over the range of temperatures. Sorption enthalpy was also calculated using an integrated form of the van't Hoff equation (eq. 2.17) which assumes that the $\Delta H°$ is constant over the temperature range of interest.

The $\Delta H°$ values of phenanthrene with deltaic soil, aquifer sediment and peat at the temperature of 4, 20 and 40 °C are –16.33, -16.91 and –6.05 kJ mol^{-1}, respectively. These values are comparable to other $\Delta H°$ for HOCs sorbed to natural solids with medium to large organic carbon contents in aqueous solution. Piatt et al. (1996) reported $\Delta H°$ = -3.3, -11 and –14 kJ mol^{-1} for phenanthrene, naphthalene and pyrene, respectively on medium grained sandy aquifer material (f_{oc} = 0.02 %). Wauchope et al. (1983) reported $\Delta H°$ = -6.2 to +3.1 kJ mol^{-1} for naphthalene sorbed to a silty loam (f_{oc} = 0.01). Mills and Biggar (1969) reported $\Delta H°$ = -12 kJ mol^{-1} for γ-hexachlorocyclohexane sorbed to a peat muck (f_{oc} = 0.22). In contrast, Woodburn et al. (1989) reported $\Delta H°$ = -19 kJ mol^{-1} for naphthalene and –38 kJ mol^{-1} for pyrene sorbed to a sandy clay loam (f_{oc} = 0.023). Szecsody and Bales (1991) reported $\Delta H°$ = +13 to +21 kJ mol^{-1} for sorption of chlorobenzenes on surface-modified silicas (f_{oc} = 0.016). The authors suggest that the large positive values are indicative of strong van der Waals forces due to site-specific binding. The magnitude of enthalpy values in this study are in the range of small to medium van der Waals forces, which are consistent with hydrophobic interactions and partitioning of the PAHs to soil organic matter (Chiou, 1989, Hassett and Banwart, 1989, Cancela et al., 1992).

4.2.9 Summary and discussion

The equilibrium sorption experiments were carried out for a variety of organic chemicals (PAH, Chlorinated solvents, Pesticides) covering a wide range of water solubility with different geosorbents of Bangladesh (soils, aquifer sediments and peat). Equilibrium sorption data were fitted by a linear and by a combination of a linear and a nonlinear sorption isotherm model (Freundlich model, 1909). Floodplain and residuum soils show almost linear sorption isotherms ($1/n$ = 0.9 -

1.05) with the chemicals investigated. In such cases (linear sorption isotherms) partition coefficients (K_d or K_{oc}) can well be predicted from the relations between K_{oc} and K_{ow} or S (e.g. Karickhoff et al., 1979; Chiou et al., 1983). Although hydrophobic partitioning is believed to dominate sorption for the solutes and solids investigated, variability in the K_{oc} content could not account for the variability of K_d in some cases. A 5-fold decrease of K_{oc} with soil depth (Tab. 4.10; residuum soil DhaRs A-C) than predicted by the Karickhoff regression correlation was observed and this may be attributable to the depth related changes in the composition, conformation and accessibility of soil organic matter.

Nonlinear sorption isotherms can be described by the combination of partitioning and pore-filling mechanisms. Both, the partitioning and the pore-filling models indicate to plot sorptive uptake vs. solubility normalized aqueous concentrations, which yields "collapsing" sorption isotherms for similar compounds (Grathwohl and Rahman, 2002). With that sorption of a variety of similar compounds can be predicted based on measured data of one probe chemical. The solubility normalized Freundlich model predicts an inverse linear relationship between the sorption coefficient measured at a given relative concentration vs. S that will allow the prediction of sorption of compounds similar to those investigated in the study. This simple normalisation (by water solubility/subcooled liquid solubility of the compound) procedure leads to similar sorption isotherms for various compounds in a specific sorbent, as to be expected as well from the partitioning and the pore filling mechanism, indicating that a given sorbent has the same capacity to sorb solutes at a given relative concentration.

K_d increases by a factor of ca. 2 when temperature decreases from 20 to 4 °C. The temperature dependence of K_d may not be of importance in comparison to subsurface heterogeneities especially when predicting solute transport.

4.3 Sorption kinetics

Generally, hydrophobic organic compounds (HOCs) often exhibit a slow sorption stage following an initial rapid sorption (Karickhoff, 1984). Both intraorganic matter diffusion (Brusseau et al., 1989, 1991) and intraparticle diffusion (McCall and Agin, 1985; Steinberg et al., 1987, and Ball and Roberts, 1991) have been proposed as the cause of the slow sorption. This can often result in a slow or incomplete desorption (Pignatello, 1990; Pignatello and Huang, 1991 and Pignatello et al., 1993). Such rate limitations (slow sorption process) can influence contaminant transport in the subsurface and may potentially hinder remediation efforts, where such remediation is attempted through vapour extraction or groundwater extraction and treatment (Mackay and Cherry, 1989). For a better understanding and prediction of the fate and transport of organic chemicals, accurate models are required not only for estimating the extent of sorption at equilibrium, but also for estimating the rate at which contaminants sorb to and desorb from the solid matrix.

4.3.1 Experimental results

Sorption kinetics was monitored in batch experiments both in reference vials and in sample vials. Reference vials containing no solids showed a higher percentage of mass loss compared to the sample vials (Fig. 4.14). Since the mass losses depend on the aqueous solute concentration thus are lower in the sample vials (triangle symbols) than in the reference vials (square symbols). The higher mass loss in the reference vials is attributed to sorption and diffusion into the septum (Rügner et al., 1999). Since losses in vials depend on the aqueous concentration, a decrease of about 3 % for phenanthrene and ca. 10 % for 1,2-DCB in the aqueous concentration in the reference vials will have minor effects in the sample vials. This was confirmed by solvent extraction from selected samples where ca. 100 % mass was recovered.

Fig. 4.15a-d shows the result of the sorption kinetics of phenanthrene, 1,2-DCB, carbofuran and TCE with the sorbents deltaic soil, aquifer sediment and peat, respectively. Sorptive uptake is shown in terms of the “apparent distribution coefficient” ($K_{d,app}$) calculated from mass balance considerations in relation to

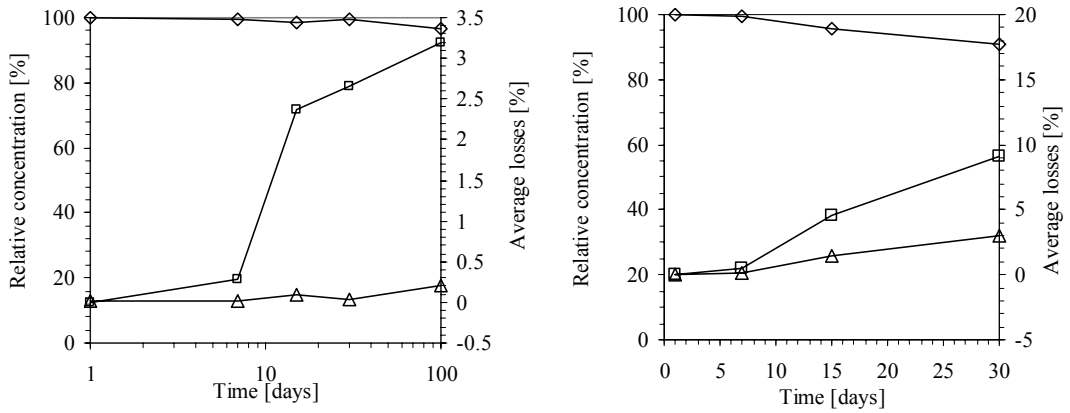

Fig. 4.14: Relative concentration in the reference vials and losses during the observation time. Left figure for phenanthrene with deltaic aquifer sediment and right figure for 1,2-DCB with deltaic aquifer sediment. Diamonds: relative concentration in reference vials; squares: average losses in reference and triangles: average losses in sample vials.

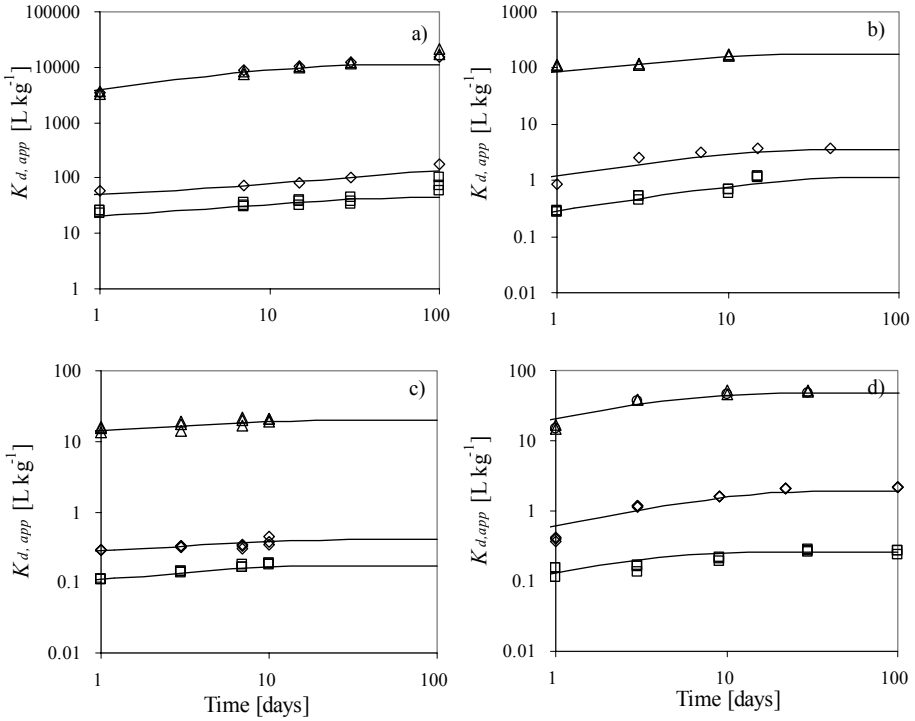

Fig. 4.15: Sorption kinetics of a) phenanthrene, b) 1,2-DCB, c) carbofuran and d) TCE with deltaic soil, aquifer sediment and peat. There are three replicates for each data point. $K_{d,app}$ was calculated from mass balance considerations during sorption kinetics experiments. Sorption kinetics experiments were conducted until $K_{d,app}$ approaches to $K_{d,eq}$ obtained in batch experiments with pulverised samples. Diamonds: deltaic soil; squares: aquifer sediment; triangles: peat. Lines represent the analytical solution of Crank (1975).

the "equilibrium distribution coefficient" ($K_{d,eq}$) obtained in batch experiments with pulverised samples.

The time required to reach equilibrium varies from solute to solute. Deltaic soil with phenanthrene, 1,2-DCB and TCE required ca. 30 - 100 days to reach equilibrium whereas carbofuran reached equilibrium within a time period of 7 - 10 days, respectively. The equilibration time of deltaic aquifer sediment and peat with the chemicals was also almost in

Tab. 4.18: Diffusion rate constant (D_a/a^2) and some related sorption parameters.

Nature of sorbents	Radius, a [geometric mean, cm]	Sorbates	D_a/a^2 [s^{-1}]	Equili. time [days]	Instan. sorption	[a]MWSE
Deltaic Soil	0.0005	Phenan.	7.15E-09	100	0.44	0.44
		1,2-DCB	1.38E-07	15-30	0.00	0.12
		Carbofuran	1.79E-07	7-10	0.55	0.06
		TCE	1.07E-07	30	0.09	0.12
Aquifer sediment	0.003	Phenan.	4.39E-08	30	0.44	0.20
		1,2-DCB	7.02E-08	15-30	0.00	0.19
		Carbofuran	2.19E-07	3-7	0.10	0.01
		TCE	3.29E-07	30	0.04	0.39
Peat	0.0008	Phenan.	5.34E-08	15-30	0.30	0.36
		1,2-DCB	1.36E-07	15	0.26	0.005
		Carbofuran	1.27E-07	10	0.70	0.008
		TCE	2.25E-07	3-7	0.00	0.10

[a] Mean weighted square error

the same order. An "apparent equilibrium" was reached in about 3 - 10 days for phenanthrene, 1,2-DCB and TCE and 1 - 3 days for carbofuran. This "apparent equilibrium" is defined at the time at which ca. 75 % of the compounds were sorbed. The rest of the compounds were sorbed when the kinetics experiments were carried out over an extended period of time. The sorptive uptake agreed very well with the analytical solution of the intraparticle diffusion model for a finite bath (Crank, 1975). Diffusion coefficients D_a were used as fitting parameters in the model. The diffusion rate constant (D_a/a^2) and some related parameters are listed in Tab. 4.18.

The diffusion rate constant increases with increasing water solubility for all the sorbates and sorbents except for TCE with deltaic soil. No correlation is observed between the diffusion rate coefficient and the grain size as all the solids have almost the same grain size (Fig. 4.16).

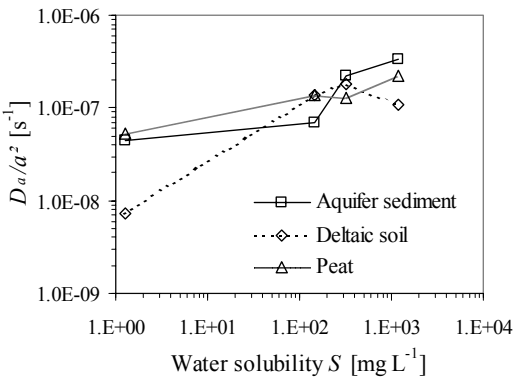

Fig. 4.16: Relationship between diffusion rate constants and water solubility.

4.3.2 Summary and discussion

The sorption kinetics of phenanthrene, 1,2-DCB, carbofuran and TCE with deltaic soil, aquifer sediment and peat were shown to be fairly fast; relatively slower for a strongly sorbing compound like phenanthrene and faster for a weekly sorbing compound like carbofuran. The slow sorption may be the result of the heterogeneous composition of soils and sediments. A rapid sorption (ca. 75 %) in this study could be sorption of up to 3 - 10 days for phenanthrene, 1,2-DCB and TCE and 1 - 3 days for carbofuran. There was not a clear correlation found between the diffusion rate constant and the grain size. The diffusion rate constant increases with increasing water solubilities of the compound investigated as can be expected from eq. (2.9). The slow sorption processes can be important for quantifying how much of the compounds appeared to be available for desorprtion.

4.4 Column experiments

4.4.1 Continuous input

Breakthrough curves obtained for fluorescein, a nonsorbing solute (tracer), were symmetrical in shape and the dispersion coefficient (D_H) determined by model fitting (Ogata and Banks, 1961) was independent of velocity. The velocity invariance is demonstrated in Fig. 4.17 where breakthrough curves for transport of fluorescein at two different velocities in deltaic aquifer sediment are presented.

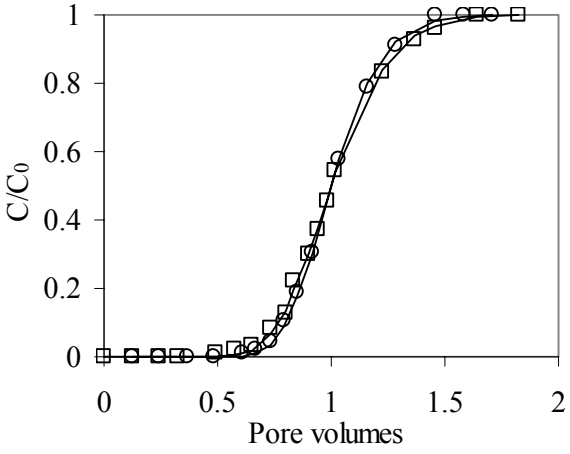

Fig. 4.17: Measured and modelled breakthrough curves of fluorescein for deltaic aquifer sediment obtained by using two pore-water velocities: the predicted breakthrough curves obtained with the advective – dispersive transport model of Ogata and Banks (1961) wherein the hydrodynamic dispersion coefficient (D_H) was used as a fitting parameter. Circles: data (v_a = 51 cm h^{-1}); squares: data (v_a = 21 cm h^{-1}); solid line: model. Mechanical longitudinal dispersivity α_l = 0.2 cm.

In Fig. 4.17 the simulated breakthrough curves were obtained by using the advective – dispersive solute transport model of Ogata and Banks (1961). The simulated breakthrough curves provide an excellent representation of the measured data. Such data are a good indication that transport is occurring under ideal hydrodynamic conditions, i.e., that hydrodynamic dispersion is the sole significant source of dispersion and the dispersion coefficent determined by use of the tracer may therefore be used to represent the dispersion coefficent of other dissimilar-sized solutes like phenanthrene.

Transport of reactive solutes is primarily governed by sorption processes, which for nonpolar organic compounds are controlled by the hydrophobicity of the compound and the sorbent characteristics. Therefore, retarded breakthrough will be observed for such solutes. The breakthrough curves for the reactive solutes were also analyzed with the one-site Ogata and Banks (1961) equilibrium model and the two-site Rosen (1954) nonequilibrium solute transport model. Examples of experimental results and the simulation data produced by the models are presented in Fig. 4.18 a-b and Tab. 4.19. In the equilibrium model, the dispersion coefficient (D_H) obtained from the tracer data was then used to analyse the reactive solute breakthrough curves. The value of K_d (or R_f) was used as a fitting parameter ($K_{d,app,fitted}$) in both models. In addition to the single fitting parameter ($K_{d,app,fitted}$) used in the equilibrium model, the tortuosity factor used to calculate the apparent diffusion coefficient (D_a) was introduced as fitting parameter in the

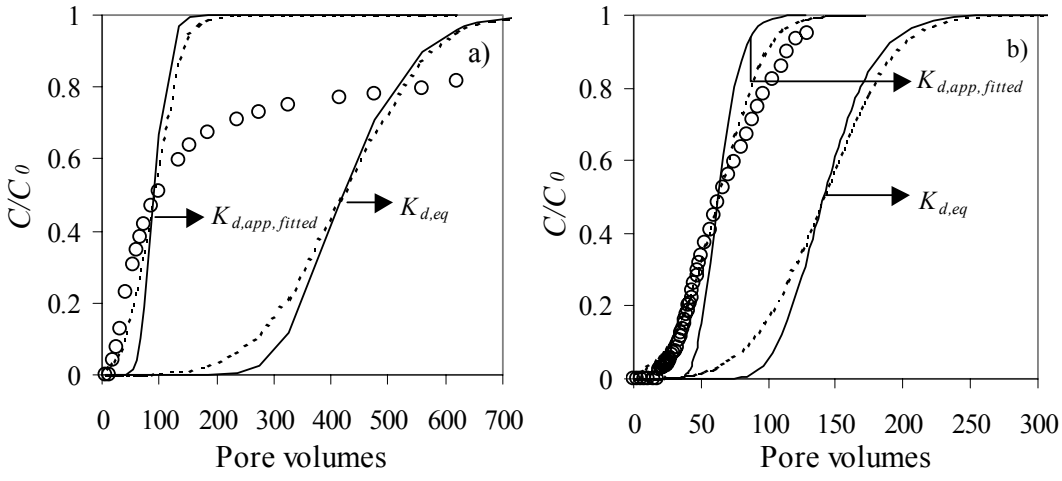

Fig. 4.18: Measured and simulated breakthrough curves of phenanthrene for a) deltaic soil (silty loam) and b) deltaic aquifer sediment (sandy silt). In each of the diagrams, the simulation consists of two sets of curves. K_d was used as fitting parameter ($K_{d,app,fitted}$) for the curves on the left side and for the other two curves equilibrium K_d ($K_{d,eq}$) was taken from batch experiments. Circles: measured data; solid lines: Ogata and Banks (1961); dotted lines: Rosen (1954).

Tab. 4.19: Values of distribution coefficients ($K_{d,app,fitted}$) for deltaic soil and deltaic aquifer sediment with phenanthrene, 1,2-DCB, carbofuran and TCE obtained by curve fitting of the breakthrough curves to the Ogata and Banks (1961) equilibrium model and the Rosen (1954) nonequilibrium model.

Sorbents	Sorbates	v_a (cm h^{-1})	[a]$K_{d,app,fitted}$ (L kg^{-1})	[b]$K_{d,eq}$ (L kg^{-1})	% K_d obtained in col. expe.	[c]R_f [-]	[d]$R_{0.5}$ [-]	$R_{0.5}/R_f$ [-]
Deltaic soil	Phenan.	78.82	29	161	19	-	-	-
Aqui. Sedi.	Phenan.	38.20	12.3	26	47	97	54	0.55
Aqui. Sedi.	1,2-DCB	16.56	0.81	1.35	60	3.56	3.05	0.85
Aqui. Sedi.	TCE	15.53	0.21	0.28	75	1.56	1.42	0.91
Aqui. Sedi.	Carbo.	18.55	0.11	0.15	73	1.36	1.29	0.94

[a] apparent K_d from column experiment obtained as fitting the model curves (Ogata and Banks, 1961; Rosen, 1954) (at C/C_0 = 0.5) to the observed data, [b] equilibrium K_d ($K_{d,eq}$) from batch experiment, [c] calculated using eq. (3.16), [d] calculated using eq. (3.19).

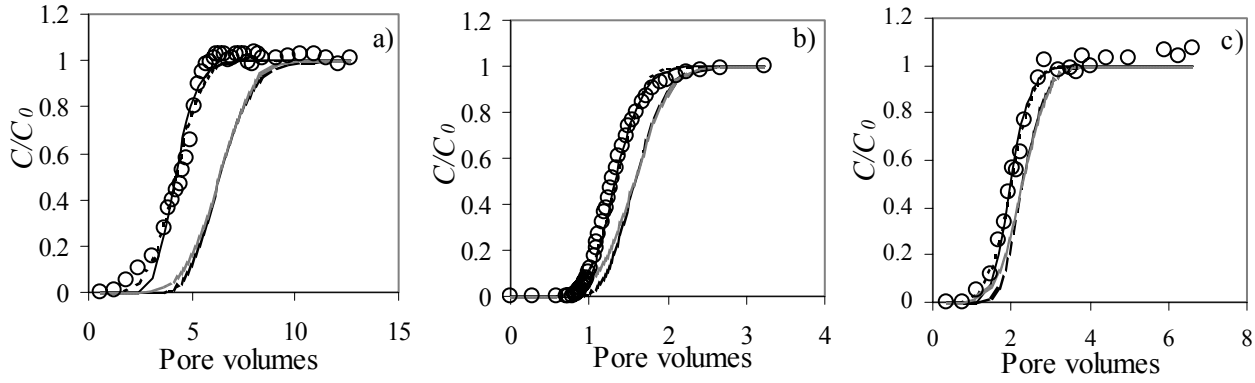

Fig. 4.19: Measured and simulated breakthrough curves of a) 1,2-DCB b) carbofuran and c) TCE with deltaic aquifer sediment (sandy silt). Circles: measured data; solid lines: Ogata and Banks, 1961 ($K_{d,app,fitted}$): dotted lines: Rosen, 1954 ($K_{d,app,fitted}$): dashed lines: Ogata and Banks, 1961 ($K_{d,eq}$): hatched lines: Rosen, 1954 ($K_{d,eq}$).

nonequilibrium model. Fig. 4.18a-b also shows the predicted BTCs based on equilibrium K_d values ($K_{d,eq}$) derived from batch experiments.
For highly hydrophobic organic chemicals like phenanthrene, which exhibit larger sorption capacity with deltaic soil (silty loam soil) (Fig. 4.18a), the column experiment shows extensive nonequilibrium effects on breakthrough. The column experiment for phenanthrene with deltaic aquifer sediment (Fig. 4.18b), which exhibits lower sorption capacity, also shows nonequilibrium effects on breakthrough. In all cases, predictions based on an equilibrium model (Ogata and Banks, 1961) with a single fitting parameter yields steeper breakthrough curves than the Rosen (1954) nonequilibrium model with two fitting parameters. The latter yields a better agreement with observation. The nonsymmetrical experimental breakthrough curves and the predicted breakthrough curves based on batch derived equilibrium K_d ($K_{d,eq}$) which remain far distant from the experimental data points, are indicative of a sorption related nonequilibrium process in the system with highly hydrophobic organic chemicals.

Column experiments were also carried out using aquifer sediment with phenanthrene, 1,2-DCB, TCE and carbofuran as solutes. The results are summarized in Figs. 4.19a-c and Tab. 4.19.

For the less sorbing organic chemicals such as 1,2-DCB, carbofuran and TCE, the breakthrough curves are almost symmetrical. Both the equilibrium and the nonequilibrium model give comparable results while the nonequilibrium model (Rosen, 1954) was superior to the equilibrium model (Ogata and Banks, 1961) for the case of 1,2-DCB. As it is shown in Fig. 4.19 equilibrium was almost achieved for the carbofuran and TCE.

4.4.2 Finite pulse input (macropore experiment)

4.4.2.1 Evaluation of conservative tracer breakthrough curve (BTC)

Fig. 4.20 shows the modelled BTC and experimental data for fluorescein. All the parameter values were determined independently (eqs. 2.50, 2.52 and 2.54) except for the tortuosity factor which was used as a fitting parameter in the simulation of tracer breakthrough for the estimation of the pore diffusion coefficient. Retardation factors were equal to 1 for both regions (matrix and macropore region, see Fig. 3.6).

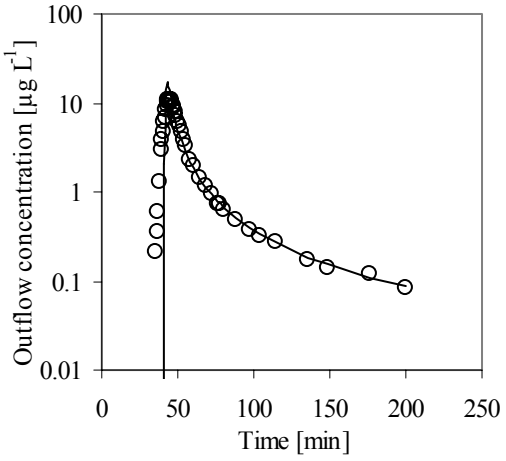

Fig. 4.20: Measured (symbols) and modelled (line) breakthrough curves for the conservative tracer (fluorescein). The pore diffusion coefficient (D_p) was obtained from the single parameter fit (tortuosity factor, τ_f) diffusion model (eqs 2.50, 2.52 and 2.54) with $\tau_f = 2$. $D_p = 3.07\times10^{-6}$ cm² s^{-1}.

The representation of the cylindrical shape of the region surrounding the macropore by a Cartesian co-ordinate according to eqs. (2.42) and (2.47) is justified by geometrical considerations using the mean displacement $\sqrt{D_p t_0}$ as a measure for the distance travelled by the tracer in the matrix region during a contact period of duration t_0. In this case, the area covered by the tracer in a cross section of the annulus (Fig. 3.6) equals $\pi\left(a+\sqrt{D_p t_0}\right)^2 - \pi a^2 = \pi D_p t_0 + 2\pi a\sqrt{D_p t_0}$. In the analytical model the corresponding area is $2\pi a\sqrt{D_p t_0}$ as the annulus is actually replaced by a rectangle with a length equal to the circumference of the cylindrical macropore. The relative error in area can be computed as:

$$\frac{\pi D_p t_0}{\pi D_p t_0 + 2\pi a\sqrt{D_p t_0}} = \frac{1}{1+2a/\sqrt{D_p t_0}} \quad (4.1)$$

For the above mentioned experiment this error is less than 9 %. This value quantifies the error introduced in model predictions due to the neglect of the cylindrical shape of the experimental set-up. From this and from the measured breakthrough curve it may also be concluded that the assumption of no dispersion in the macropore is a reasonable approximation in the model. For the tracer experiment, the pore diffusion coefficient was found to be 3.07×10^{-6} cm² s^{-1} which requires a reasonable tortuosity factor of 2.0. Mass recovery determined for both the experimental data as well as for the model were 90 % for an observation period of 200 min after solute injection.

4.4.2.2 Evaluation of retarded solutes breakthrough curves (BTCs)

Figs. 4.21a-d show the modelled BTCs and experimental data for carbofuran, TCE, 1,2-DCB and phenanthrene, respectively. The estimated apparent diffusion coefficient (D_a) and the fitted distribution coefficient (K_d) obtained from the proposed model are summarized in Tab. 4.20. A good agreement is observed between model and experimental data for all chemicals. For the less retarded solutes like carbofuran and TCE, only upto 35 % of the equilibrium K_d was obtained in the column experiment. On the other hand, the highly sorbing solutes like 1,2-DCB and phenanthrene, showed only 20 % of the equilibrium K_d.

During the sorption kinetics experiment, it was observed that kinetics of phenanthrene, 1,2-DCB and TCE with the soil was slower as compared to the carbofuran. This means that phenanthrene, 1,2-DCB and TCE need longer time (ca. 30-100 days) to reach equilibrium than carbofuran (equilibration time ca. 3-10 days).

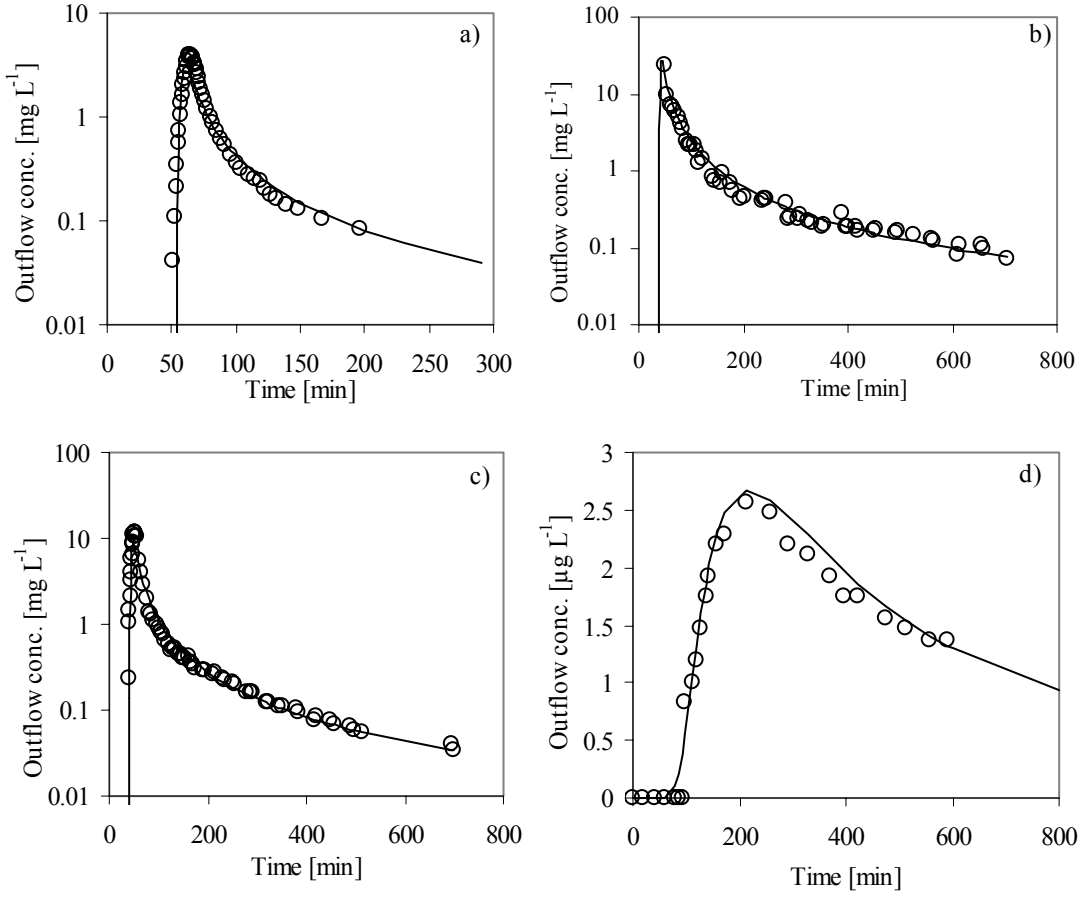

Fig. 4.21: Measured (symbols) and modeled (lines, eqs. 2.50, 2.52 and 2.54) breakthrough curves for a) carbofuran, b) TCE, c) 1,2-DCB and d) phenanthrene. For fitting and model parameters see Tab. 4.20. Note that the scale of the vertical axis is logarithamic for diagrams a) -c) but linear for diagram d).

Tab. 4.20: Summary of estimated pore (D_p) and apparent diffusion coefficients (D_a) and fitted distribution coefficient (K_d) of selected chemicals.

Chemical	Input conc. (mg L^{-1})	Equi. K_d, at input conc. (L kg^{-1})	K_d, model fit (L kg^{-1})	% K_d, obtained in column	R_{im} (from column)	D_p (cm^2 s^{-1})	D_a (cm^2 s^{-1})	% Mass balance (by moments)	
								Exp.	Model
Carbofu.	20	0.37	0.13	35	1.4	3.4×10^{-06}	2.37×10^{-06}	84	79
TCE	260	2.23	0.45	20	2.5	4.5×10^{-06}	1.82×10^{-06}	92	89
1,2-DCB	70	3.37	0.57	17	2.9	4.2×10^{-06}	1.47×10^{-06}	90	86
Phenan.	0.50	149	30	20	99	3.3×10^{-06}	3.36×10^{-08}	30	29

Using similar arguments as above, the model error due to the approximation of the cylindrical geometry by a rectangular one can also be determined for reactive tracers. For that, $\sqrt{D_p t_0}$ in eq. (4.1) has to be replaced by $\sqrt{D_a R_m t_0}$, thus accounting for the apparently reduced diffusion coefficient and the increased contact time. Errors of ca. 2 % for phenanthrene, 6 % for 1,2-DCB and ca. 9 % for TCE and carbofuran are obtained. Therefore, the geometrical approximation inherent to the model also appears to be justified for reactive transport simulations. The mass recoveries for experimental data and model simulations are also observed for the reactive solutes. Values obtained from experiments and model simulations are 30 % and 29 %, 90 % and 86 %, 92 % and 89 % and 84 % and 79 % for phenanthrene, 1,2-DCB, TCE and carbofuran, respectively for the corresponding observation time.

4.4.3 Summary and discussion

Column experiments were carried out with deltaic soil (silty loam) and deltaic aquifer sediment (sandy silt) using fluorescein as a conservative tracer, phenanthrene as highly sorbing solute and 1,2-DCB, TCE and carbofuran as rather weekly sorbing solutes for continuous input as well as finite pulse injection (macropore column experiment) with specified initial and boundary conditions.

In the case of continuous input injection, the experimental breakthrough curves were simulated using the one-site advective–dispersive equilibrium transport model of Ogata and Banks (1961) and the two-site Rosen (1954) nonequilibrium transport model. For deltaic soil which showed much higher sorption (K_d of the order of 161 L kg^{-1}) with phenanthrene and extensive nonequilibrium effects on breakthrough, neither of the models could represent the experimental breakthrough curves based on the batch derived sorption parameters. Similarly, for deltaic aquifer sediment which also showed fairly high sorption (K_d of the order of 26 L kg^{-1}) with phenanthrene, neither model could represent the experimental breakthrough curves based on the batch derived parameters. The nonequilibrium model, however, could capture the experimental data points better while considering K_d as fitting parameter instead of batch derived K_d values. For the deltaic aquifer sediment which showed very modest sorption (K_d of the order of in between 0.15 to 1.35 L kg^{-1}) with 1,2-DCB, TCE and carbofuran, both equilibrium and nonequilibrium based solute transport models yielded predictions in accordance with the batch derived column breakthrough observations.

In the finite pulse experiment, the effect of matrix diffusion on macropore flow is quantified by comparing breakthrough data from column experiments with the results of an analytical model. The analytical solution involves advection in the macropore, diffusion in the matrix region and linear sorption in both regions. These idealizations can be shown appropriate for simulating breakthrough of an inert tracer and several organic contaminants in the macropore/matrix region system. The excellent agreement of model results with measured breakthrough curves implies that the model covers all relevant transport processes. Fitted K_d for all the chemicals investigated were within the similar range of 20 – 35 % of the equilibrium K_d. The reason for this may be due to the fact that less soluble and slowly sorbing compounds, e.g. phenanthrene, have higher mean residence times in the column compared to shorter residence times of highly soluble, faster sorbing compounds, e.g. TCE. In particular, matrix diffusion is found to have a major impact on solute breakthrough. Sorption equilibrium in the matrix was not obtained during the time scale of the experiment and this presumably also affects contaminant transport in the field, i.e., faster migration than expected from batch equilibrium sorption isotherms.

5. APPLICATION OF RESULTS (Groundwater Risk Assessment)

5.1 Estimation of transport of organic compounds through soil to groundwater

Contamination of soils, sediments and water resources by anthropogenic organic chemicals has become a matter of increasing public and regulatory concern because of their toxicity and long-term sources of contamination. Since many of the environmental organic chemicals are suspected to have mutagenic, teratogenic and carcinogenic impact, the processes that affect the transport and fate of these contaminants must be understood in order to assess exposure risks to humans and the environment. According to German soil protection regulations, the sites where a risk for groundwater is suspected must be evaluated with respect to the contaminant concentrations to be expected in the seepage water and shallow groundwater and not on the contaminant level in soils or sediments.

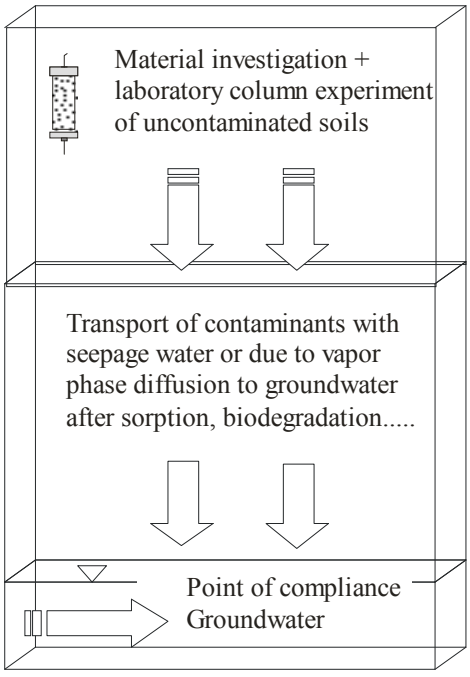

Fig. 5.1: Procedure of groundwater risk assessment from an uncontaminated soil using material investigations, column percolation tests and contaminant transport modelling.

Groundwater risk assessment can be based on the laboratory investigation of soil / sediment samples (percolation tests/leaching tests for uncontaminated/contaminated soils) and contaminant transport modelling and/or field investigations (Gracos, 1998). Here the groundwater risk assessment is evaluated based on the investigations of materials (using uncontaminated soils and sediments of Bangladesh) and column percolation tests. Different analytical solutions with specific initial and boundary conditions are used for the simulation of transport from the surface (source point of contamination) to the place of compliance. The place of compliance is considered to be the transition zone between the unsaturated and the saturated flow regimes (Fig. 5.1).

5.1.1 Simulations for the case of continuous input

Figs. 5.2a-c show the simulation results of phenanthrene transport through the soil (surface) to the groundwater table. The simulation was done for the case of deltaic aquifer sediment (sandy silt) having a porosity of ca. 35 % and a K_d of 45 L kg^{-1} (calculated using K_{fl} = 67 L kg^{-1} , $1/n$ = 0.83 and C_w = 10 µg L^{-1}) with a strongly sorbing compound like phenanthrene. The point of compliance is considered 2 m below ground surface (typical depth to groundwater table in many parts of Bangladesh). The other model input parameters are given in appendix A1. Fig. 5.2a predicts solute transport according to equilibrium retardation. As a persistent organic contaminant, phenanthrene would occur at the point of compliance after 1500 years with a concentration equal to the input concentration. Fig. 5.2b predicts the solute transport with retardation and biodegradation. As shown in the diagram, the biodegradable compound may reach the groundwater in very low concentrations. After 1000 years of application, a contaminant with a half-life (HL) of 10 years will only travel a distance of 20 cm from the ground surface. Fig. 5.2c shows the same prediction as of Fig. 5.2b with 20 % preferential flow (PF), i.e. 20 % of the contaminant mass travels so quickly that sorption and biodegradation are not effective.

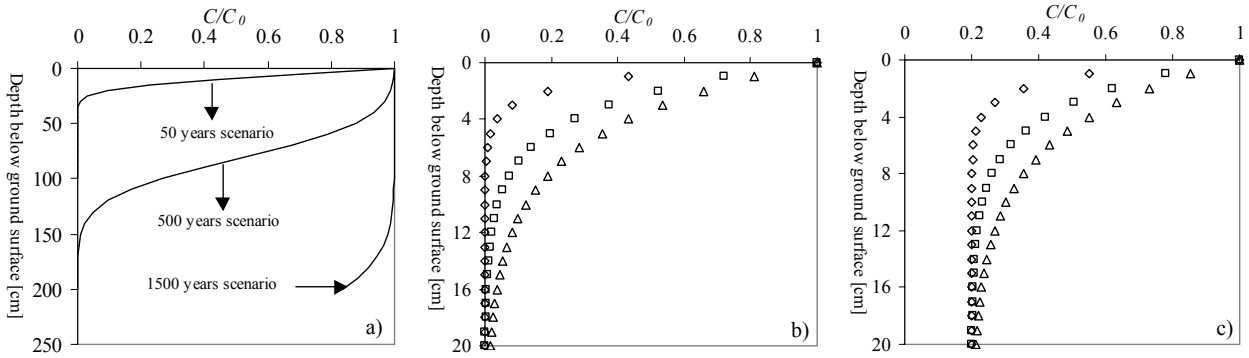

Fig. 5.2: Simulation of equilibrium transport of organic solute through surface soil (seepage water) to the groundwater table: a) solute transport with retardation, b) solute transport with retardation and biodegradation (time 1000 years) c) same as of b) with 20 % preferential flow (PF). Chemical: phenanthrene; Solid: sandy silt; Depth to groundwater table: 2.0 m; Pore water velocity: 35 cm year^{-1}; K_d: 45 (L kg^{-1}), Porosity: 0.35. Legend used: solid line: Ogata and Banks (1961); rectangles: half-life 1 year; squares: half-life 5 years; triangles: half-life 10 years.

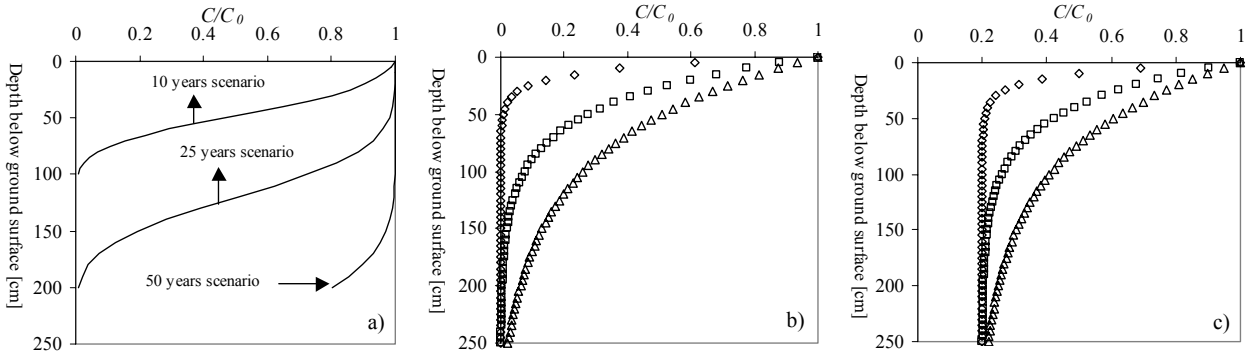

Fig. 5.3: Simulation of equilibrium transport of an organic solute through surface soil (seepage water) to the groundwater table: a) solute transport with retardation, b) solute transport with retardation and biodegradation (time 50 years) c) same as of b) with 20 % preferential flow (PF). Chemical: 1,2-DCB; Solids: sandy silt; Depth to groundwater table: 2.0 m; Seepage water velocity: 35 cm year^{-1}; K_d: 1.35 L kg^{-1}; Porosity: 0.35. Legend used: solid line: Ogata and Banks (1961); rectangle: half-life 1 year; square: half-life 5 years; triangle: half-life 10 years.

Fig. 5.3a-c shows the simulation with a rather weekly sorbing compound like 1,2-DCB. Here it is obvious that the contaminant will reach the groundwater table faster than a strongly sorbing compound.

5.1.2 Simulations for the case of Dirac pulse input

The simulation of pesticide transport was done using the PESTAN (pesticide analytical model) and compared with eqs. (2.31) and (2.32).

PESTAN was developed for initial screening assessments to evaluate the potential for groundwater contamination by aldicarb (trademark TEMIK) used for the control of nematodes, aphidas and mites in citrus grove. This model has also been tested under field and laboratory conditions (Enfield et al., 1982; Jones and Back, 1984; Melacon et al., 1986).

The present simulation was done for a carbamate pesticide, carbofuran, a widely used insecticide in irrigation in Bangladesh. The scenario deals with a hypothetical irrigation field where carbofuran is applied at a rate of 0.5 kg ha^{-1}. The recharge rate of groundwater was considered 1.14×10^{-6} cm s^{-1} which corresponds to the pore water velocity of 3.83×10^{-6} cm s^{-1}. The area of the irrigation field is assumed 1 hectare (10000 m²). The simulation was done for time periods of 50 days and 100 days. The other model input parameters are given in appendixA2.

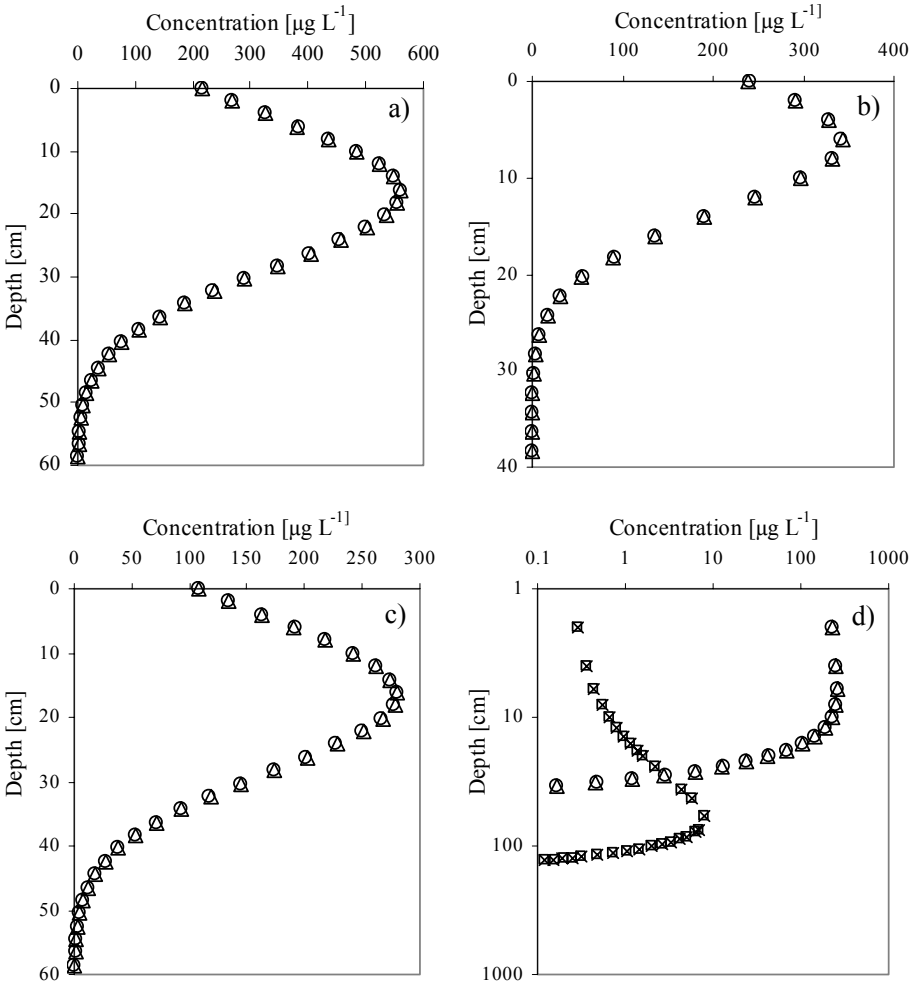

Fig. 5.4: Simulation of pesticide (carbofuran) transport and comparison of models between PESTAN and eqs (2.31) and (2.32): a) tracer, b) with retardation, c) with decay and d) retardation plus decay. Depth to groundwater table: 2 m; pore water velocity: 120 cm year^{-1}; K_d = 0.31 L kg^{-1}; porosity: 0.3; carbofuran application rate: 0.5 kg ha^{-1}; half-life: 50 days. Legend used: circle: PESTAN (50 days scenario); triangle: eqs. (2.31) and (2.32) (50 days scenario). In Fig. 5.4d, square and cross symbols correspond to the PESTAN and eqs. (2.31) and (2.32) respectively, for 100 days simulation.

The simulated results in Fig. 5.4a-d reveal that the eqs. (2.31) and (2.32) can give exactly the same result as PESTAN and may be useful in making preliminary assessments for estimating the transport of the pesticide through the soil to the groundwater table. A simulation period of 100 days (Fig. 5.4d, cross and square symbols) shows that a very low concentration of carbofuran can be observed at a depth of ca. 200 cm.

5.1.3 Simulations for the case of finite pulse input

In the soil unsaturated zone mechanisms like bypassing, fingering, or funnelling induce preferential flow (PF) by which contaminants are transported much faster than expected from average seepage water velocities and retardation. Moreover, the transport of dissolved and reactive organic chemicals through macropores is retarded by the interaction with the adjacent soil matrix (matrix diffusion). Consequently, the quantification of the effect of matrix diffusion of contaminants in fine grained soils (low permeability regions) coupled with

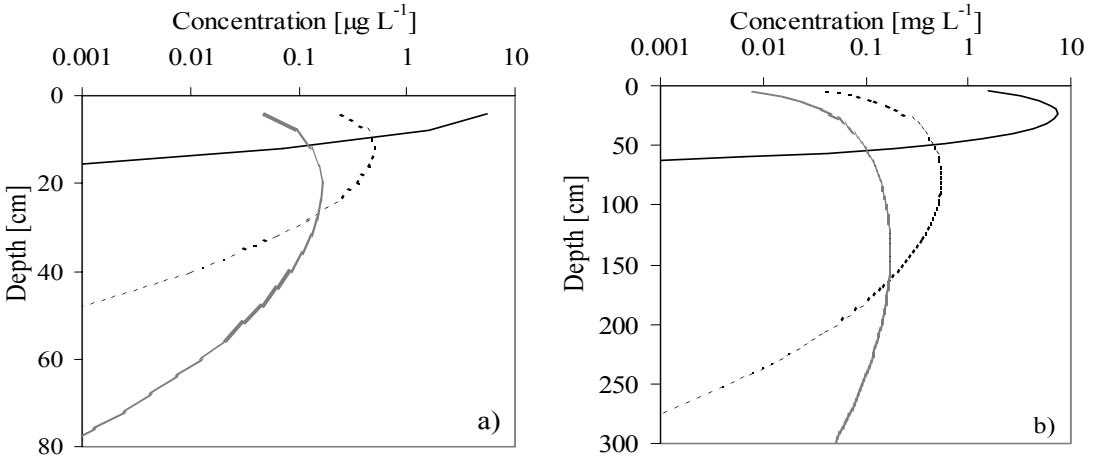

Fig. 5.5: Simulation of transport of a) phenanthrene and b) 1,2-DCB through deltaic soil (silty loam soil) by using the diffusion based preferential flow (PF) model (eqs. 2.50, 2.52 and 2.54). For input parameters see appendices A3 for phenanthrene and A4 for 1,2-DCB. Legend used: solid line: 5 days; dashed line: 50 days and hatched line: 200 days simulation period. Pulse duration (injection period) = 1 hour.

the effect of PF paths (macropores) is essential in order to properly predict solute transport. Groundwater risk assessment, therefore, is only feasible if the prediction tool allows for quantifying the coupled reactive processes together with the impact of PF on solute spreading in the unsaturated zone.

The above simulation was done using the proposed diffusion based PF model (eqs. 2.50, 2.52 and 2.54) for the case of phenanthrene as strongly sorbing compound and 1,2-DCB as weakly sorbing compound with deltaic soil (silty loam). The scenario deals with evaluating a site where a finite pulse (1 hour) of phenanthrene (for example) was assumed to come in contact with the surface soil and then move through the macropore coupled with the surrounding matrix region. The simulation was done for the time periods of 5 days, 50 days and 200 days. The initial concentrations were 0.1 mg L^{-1} and 100 mg L^{-1} for phenanthrene and 1,2-DCB, respectively. The other model input parameters are given in appendices A3 for phenanthrene and in A4 for 1,2-DCB. The simulated results reveal that contaminants will move rather quickly some distances with higher concentration due to the influence of a macropore (or PF) and then will be retarded due to the matrix diffusion mechanism (Fig. 5.5). For highly sorbing and less soluble chemicals, e.g. phenanthrene, a very low concentration of 0.001 µg L^{-1} may be found at a depth of about 80 cm after 200 days of simulation time. On the other hand, less sorbing but comparatively high soluble chemicals, e.g. 1,2-DCB, may reach the groundwater table (2 m) with a concentration of about 0.1 mg L^{-1} (for comparison with drinking water limit concentrations see Tab. 3.1)

5.1.4 Summary and discussion

Soil and groundwater pollution from historical urban and industrial activities exists in all countries of the world, and continues to occur. The major concern at many contaminated sites is the threat of groundwater quality through usage, leakages and disposal of petroleum fuels, chlorinated solvents, pesticides and nutrients. Since groundwater is the major source of drinking water and remediation of all contaminated sites is not feasible for most of the countries in the world, therefore integrated groundwater risk assessment procedures are needed for the ranking of sites, decision making on further use and remedial actions.

In the above, a groundwater risk assessment procedure using an uncontaminated soil/sediment sample is evaluated based on material investigations, column percolation tests and a contaminant transport modelling approach. Simple analytical solutions of solute transport with specific initial and boundary conditions can be used for the development of scenario-based models which in turn take the form of a scenario

approach as they may be applied to different situations in terms of classes/combinations of pollutants and site-specific conditions, such as climatic conditions, permeability and distance between the contamination and the groundwater level. Such a scenario approach allows to determine a priori whether, under given site conditions (subsurface permeability, distance to groundwater table, type of material) and contaminant properties (volatile/non-volatile/water soluble etc.), a minor, medium or high risk of groundwater pollution exists.

6. REFERENCES

Ahmed, K.M., Hoque, M., Hasan, M.K., Ravenscroft, P. and Chowdhury, L.R. (1998): Occurrence and origin of water well methane gas in Bangladesh. J. Geol. Soc. India, 51: 697-708.

Alam, M.K., Hassan, A.K.M.S., Khan, M.R. and Whitney, J.W. (1990): Geological map of Bangladesh, Geological survey of Bangladesh.

Alexander, M. (1999): Biodegradation and bioremediation. Academic press, San Diego.

Allen-King, R.M., Groenevelt, H., Warren, C.J. and Mackay, D.M. (1996): Non-linear chlorinated-solvent sorption in four aquitards. J. Contam. Hydrol., 22: 203-221.

Allen-King, R., Grathwohl, P. and Ball, W.P. (2002): New Modeling Paradigms for the Sorption of Hydrophobic Organic Chemicals to Heterogeneous Carbonaceous Matter in Soils, Sediments and Rocks. Advances in Water Research (Invited Paper, accepted)

Archie, G.E. (1942): The electrical resistivity log as an aid in determining some reservoir characteristics. Trans. A.I.M.E., 146: 54-61.

Baily, G.W. and White, J.L. (1970): Factors influencing the adsorption, desorption and movement of pesticides in soils. Residue Rev., 32: 29-32.

Baker, J.R., Mihelcic, J.R., Luehrs, D.C. and Hickey, J.P. (1997): Evaluation of estimation methods for organic carbon normalised sorption coefficients. Water Environ. Research, 69: 136-144.

Ball, W.P. and Roberts, P.V. (1991a): Long-term sorption of halogenated organic chemicals by aquifer material. 1. Equilibrium. Environ .Sci.Technol., 25: 1223-1236.

Ball, W.P. and Roberts, P.V. (1991b): Long-term sorption of halogenated organic chemicals by aquifer material. 2. Intraparticle diffusion. Environ. Sci. Technol., 25: 1237-1249.

Ball, W.P., Xia, G., Durfee, D.P., Wilson, R.D., Brown, M.J. and Mackay, D.M. (1997): Hot methanol extraction for the analysis of volatile organic chemicals on subsurface core samples from Dover Air Force Base, Delaware. Winter, GWMR, 104-121.

Bear, J. (1972): Dynamics of fluids in porous media. American Elsevier, New York, NY, 764p.

Borisover, M.D., Graber, E.R. (1997): Specific interactions of organic compounds with soil organic carbon. Chemosphere, 34, 1761-1776.

Brusseau, M.L. (1992): Nonequilibrium transport of organic chemicals: The impact of pore-water velocity. J. Contam. Hydrol., 9: 353-368.

Brusseau, M.L., Jessup, R.E. and Rao, P.S.C. (1991a): Nonequilibrium sorption of organic chemicals: Elucidation of rate-limiting processes. Environ. Sci. Technol., 25: 134-142.

Brusseau, M.L., Larsen, T. and Christensen, T.H. (1991b): Rate-limited sorption and nonequilibrium transport of organic chemicals in low organic carbon aquifer materials. Water Resour. Res., 27: 1137-1145.

Bucheli, T.D. and Gustafsson, Ö. (2001): Ubiquitous observations of enhanced solid affinities for aromatic organochlorines in field situations: are in situ dissolved exposures overestimated by existing partitioning models? Environ. Toxicol. Chem., 20: 1450-1456.

Burchill, S., Hayes, M.H.B.and Greenland, D.J. (1981): The chemistry of soil processes. John Wiley and Sons, Chichester, England, pp 221-400.

Carmo, A.M, Hundal, L.S. and Thompson, M.L. (2000): Sorption of hydrophobic organic compounds by soil materials: Application of unit equivalent Freundlich coefficients. Environ. Sci. Technol., 34: 4363-4369.

Carslaw, H.S. and Jaeger, J.C. (1959): Conduction of heat in solids. Oxford University Press, London, 2nd ed., 510 p.

Chiou C.T., Susan E. McGroddy, S.E. and Kile, D.E. (1998): Partition characteristics of polycyclic aromatic hydrocarbons on soils and sediments. Environ. Sci. Technol., 32: 264-269.

Chiou, C. T., Kile, D. E., Rutherford, D. W., Sheng, G. and Boyd, S. A. (2000): Sorption of selected organic compounds from water to a peat soil and its humic-acid and humin fractions: potential sources of the sorption nonlinearity. Environ. Sci. Technol., 34: 1254-1258.

Chiou, C. T., Mcgroddy, S. E. and Kile, D.E. (1998): Partition characteristics of polycyclic aromatic hydrocarbons on soils and sediments. Environ. Sci.Technol., 32: 264-269.

Chiou, C.T. and Kile, D. E. (1998): Deviations from sorption linearity on soils of polar and non-polar organic compounds at low relative concentrations. Environ. Sci. Technol., 32: 338-343.

Chiou, C.T. and Shoup, T.D. (1985): Soil sorption of organic vapours and effects of humidity on sorption mechanism and capacity. Environ. Sci. Technol., 19: 1196-1200.

Chiou, C.T., Peters, L.J. and Freed, V.H. (1979): A physical concept of soil-water equilibria for nonionic organic compounds. Science, 206: 831-832.

Chiou, C.T., Porter, P.E. and Schmedding, D.W. (1983): Partition equilibria of nonionic organic compounds between soil organic matter and water. Environ. Sci. Technol., 17: 227–231.

Chiou, C.T., Sawhney, B.L. and Brown, K. (1989): Theoretical Considerations of the Partition Uptake of Nonionic Organic Compounds by Soil Organic Matter. In: Baker JT, editor. Reactions and Movements of Organic Chemicals in Soils. Madison: Soil. Sci. Soc. Am., Inc. and Am. Soc. of Agronomy, Inc.

Choma, J., Burakiewicz-Mortka, W., Jaroniec, M. and Gilpin, R.K. (1993): Studies of the structural heterogeneity of microporous carbons using liquid/solid adsorption isotherms. Langmuir, 9: 2555-2561.

Coats, K.H. and Smith, B.D. (1964): Dead-end pore volume and dispersion in porous media. J. Soc. Pet. Eng., 4: 73-80.

Condon, J.B. (2000a/b): Equivalency of the Dubinin-Polanyi equations and the QM based sorption isotherm equation: Mathematical derivations (a), Simulations of heterogeneous surfaces (b). Microporous and mesoporous materials, 38: 359-383.

Crank, J. (1975): The mathematics of diffusion, 2nd ed. Oxford, U.K. (University Press), 414p.

Crittenden, J. C., Sanongraj, S., Bulloch, J. L., Hand, D. W., Rogers, T. N., Speth, T. F. and Ulmer, M. (1999): Correlation of Aqueous-Phase Adsorption Isotherms. Environ. Sci. Technol., 33: 2926-2933.

Deely, G.M., Reihard, M. and Stearns, S.M. (1991): Transformation and sorption of 1,2-dibromo-3-chloropropane in subsurface samples collected at Fresno, California. J. Environ. Qual., 20:547-556.

DIN 18123 (Deutsche Industrie Norm): Bestimmung der Korngrößenverteilung. Beuth Bauverlag GMBH, Berlin.

DIN 18124 (Deutsche Industrie Norm): Bestimmung der Korndichte mit dem Kapillarpyknometer. Beuth Bauverlag GMBH, Berlin.

Ditoro, D.M., Zarba, C.S., Hansen, D.J., Berry, W.J., Swartz, R.C., Cowan, C.E., Pavlou, S.P., Allen, H.E., Thomas, N.A. and Paquin, P.R. (1991): Technical basis for establishing sediment quality criteria for nonionic organic chemicals using equilibrium partitioning. Environ. Toxicol. Chem., 10: 1541-1583.

Dubinin, M.M. (1960): The potential theory of adsorption of gases and vapors for adsorbents with energetically nonuniform surfaces. Chem. Rev., 60: 235-241.

Dubinin, M.M. (1975): Physical adsorption of gases and vapors in microproes. D.A. Cadenhead, J.F. Danielli, M.D. Rosenberg (Eds.), progress in surface and membrane science, vol. 9, ISBN 0-12-571809-8, academic press, New York.

Enfield, C.G., Carsel, R.F., Cohen, S.E. and Walters, D.M. (1982): Approximating pollutant transport to groundwater. Groundwater, 20: 711-722.

Falatko, D.M. and Novak, J.T. (1992): Effects of biologically produced surfactants on the mobility and biodegradation of petroleum hydrocarbons. Water Environ. Res., 64: 163-169.

Freeze , P.A. and Cherry, J.A. (1979): Groundwater. Printice hall Inc., Englewood Cliffs, New York, 604p.

Freundlich, H. (1909): Kapillarchemie. Leipzig (Akademische Verlagsgesellschaft m.b.h.), 591p.

Gerstl, Z. (1990): Estimation of organic chemical sorption by soils. J. Contam. Hydrol., 6: 357-375.

Graber, E.R., Borisover, M.D. (1998): Hydration-Facilitated Sorption of Specifically Interacting Organic Compounds by Model Soil Organic Matter. Environ. Sci. Technol., 32: 258 – 263.

Gracos (Groundwater Risk Assessment at Contaminated Sites) (1998): The European Commision Community Research. Fifth (EC) framework program – energy, environment and sustainable development.

Grathwohl, P. (1990): Influence of organic matter from soils and sediments from various origins on the sorption of some chlorinated aliphatic hydrocarbons: Implication on Koc correlations. Environ. Sci. Technol., 27: 2360-2366.

Grathwohl, P. (1998): Diffusion in natural porous media. Kluwer Academic Publishers, Boston, USA, 207p.

Grathwohl, P. and Reinhard, M. (1993): Desorption of trichloroethylene in aquifer material: Rate limitation at the grain scale. Environ. Sci. Technol., 24: 1687-1693.

Grathwohl, P. and Rahman, M.M. (2002): Partitioning and pore-filling: Solubility-normalized sorption isotherms of nonionic organic contaminants in soils and sediments. Submitted to the Israel journal of chemistry, special issue: Environmental chemistry.

Gregg, S. J. and Sing, K. S. W. (1982): Adsorption, surface area and porosity. 2 ed., Academic Press, New York.

Grisak, G.E. and Pickens, J.F. (1981): An analytical solution for solute transport through fractured media with matrix diffusion. J. Hydrol., 52: 47-57.

Haderlein S. B., Weissmahr, K.W. and Schwarzenbach, R. P. (1996): Specific adsorption of nitroaromatic explosives and pesticides to clay minerals. Environ. Sci. Technol., 30: 612-622.

Halcrow, S.W and Partners Ltd. (1993): Southwest area water resources management project – FAP 4, Final Report , Vol. 5, Hydrology, Hydrogeology and RAOM, United Nations Development Programme (BGD/88/038).

Hamaker, J.W. and Thompson, J.M. (1972): Organic chemicals in the soil environment. Marcel Dekker, New York, pp. 49-143.

Hassett, J.J. and Banwart, W.L.(1989): The sorption of nonpolar organics by soils and sediments. Soil Sci. Soc. America, Inc., Madison, WI, SSSA special publication number 22.

Hoque, M., Ravenscroft, P. and Hassan, M.K. (1997): Investigation of groundwater salinity and gas problems in south east Bangladesh. Groundwater resources of Bangladesh, Bangladesh center for advanced studies.

Horvath, C and W. Melander. 1978. Reversed phase chromatography and the hydrophobic effect. Am. Lab. 10: 17-36.

Howard, P. H. (1991): Handbook of Environmental Fate and Exposure Data for Organic Chemicals: Pesticides . Lewis Publishers, Chelsea, MI, 3-15.

Jones, R.L. and Back, R.C. (1984): Monitoring aldicarb residues in Florida soil and water. Environ. Toxicol. Chem., 3: 9-20.

Jost, W. (1952): Diffusion in solids, liquids and gases, Academic Press, New York, 63p.

Jury, W.A., Elabd, H. and Resketo, M. (1986): Field study of napropamide movement through unsaturated soil. Water Resour. Res., 22: 749-755.

Kanazawa, J. (1989): Relationship between the soil sorption constants for pesticides and their physichemical properties. Environ. Toxicol. Chem., 8: 477-484.

Karapanagioti, H.K., Kleineidam, S., Sabatini, D.A., Grathwohl, P. and Ligouis, B. (2000): Impacts of Heterogeneous Organic Matter on Phenanthrene Sorption: Equilibrium and Kinetic Studies with Aquifer Material. Environ. Sci. Technol., 34: 406-414.

Karickhoff, S.W. (1981): Semi-empirical estimation of sorption of hydrophobic pollutants on natural sediments and soils. Chemosphere, 10: 833-846.

Karickhoff, S.W. (1984): Organic polutant sorption in aquatic systems. J. Hydraulic Eng., 110: 707-735.

Karickhoff, S.W., Brown, D.S. and Scott, T.A. (1979): Sorption of hydrophobic pollutants on natural sediments. Water Research, 13: 214-248.

Kenaga, E.E. and Goring, C.A.I. (1980): Relationship Between Water Solubility, Soil Sorption, Octanol-Water Partitioning, and Concentration of Chemicals in Biota. In: Eaton JG, Parrish PR, Hendricks AC, editors. Aquatic Toxicology, ASTM, pp 78-115.

Khan, F.H. (1991). Geology of Bangladesh. University Press Ltd., Dhaka, 207p.

Kleineidam, S., Rügner, H., Ligouis, B. and Grathwohl, P. (1999): Organic matter facies and equilibrium sorption of phenanthrene. Environ. Sci. Technol., 33: 1637-1644.

Kleineidam, S., Rada, H., Schüth, C. and Grathwohl, P. (2002): Solubility-Normalized Combined Pore-Filling-Partitioning Sorption Isotherms for Organic Pollutants. submitted to Environ. Sci. Technol.

Kookana, R.S., Schuller, R.D. and Aylmore, L.A.G. (1993): Simulation of simazine transport through soil columns using time-dependent sorption data measured under flow conditions. J. Contam. Hydrol., 14: 93-115.

Koskinen, W.L. and Harper, S.S. (1990): The retention processes: Mechanism. Pesticides in the soil environment. Soil science society of America, Madison, WI, pp. 51-77.

Lane, W.F and Loehr, R.C. (1992): Estimating the equilibrium aqueous concentration of polynuclear aromatic hydrocarbons in complex mixtures. Environ. Sci. Technol., 26: 983–990.

Leboeuf, E.J. and Weber, W.J.Jr. (1997): A distributed reactivity model for sorption by soils and sediments. 8. Sorbent organic domains: Discovery of a humic acid glass transition and an argument for a polymer-based model. Environ. Sci. Technol., 31: 1697–1702.

LeBoeuf, E.J. and Weber, W.J. Jr. (1999): Reevaluation of general partitioning model for sorption of hydrophobic organic contaminants by soil and sediment organic matter. Environ. Sci. Technol., 18: 1617-1626.

Lion, L.W., Stauffer, T.B. and McIntry, W.G.(1990): Sorption of hydrophobic compounds on aquifer materials: Analysis of methods and the effect of organic carbon. J. Contam. Hydrol., 5: 215-234.

Lyman, W.J. Reehl, W.F. and Sosenblatt, D.H. (1982): Handbook of chemical property estimation methods, Environmental behaviour of organic compounds. McGraw-Hill, Inc., New York.

Mackay, D.M. and Cherry, J.A. (1989): Groundwater contamination: Pump-and-treat remediation. Environ. Sci. Technol., 23: 630-636.

Manes, M. (1998): Activated Carbon Adsorption Fundamentals. In: Meyers RA, editor. Encyclopedia of Environmental Analysis and Remediation. John Wiley, New York.

McCall, P.J.and Agin, G.L. (1985): Desorption kinetics of picloram as affected by residence time in the soil. Envviron., Toxicol. Chem., 4: 37-44.

Melacon, S.M., Pollard, J.E. and Hern, S.C. (1986): Evaluation of SESOIL, PRZM and PESTAN in a laboratory column leaching experiment. Environ. Toxicol. Chem., 5: 865-878.

Mihelcic, J.R and Luthy, R.G. (1991): Sorption and microbial degradation of naphthalene in soil water suspensions under denitrification conditions. Environ. Sci. Technol., 25: 169-177.

Miller, G.C., Hevert, V.R. and Miller, W.W. (1989): Effect of sunlight on organic contaminants at the atmosphere-soil interface. Soil Sci. Soc. America, Inc., Madison, WI, SSSA special publication number 22.

Miller, G.C., Hevert, V.R. and Zepp, R.G. (1987): Chemistry and photochemistry of low-volatility organic chemicals on environmental surfaces. Environ. Sci. Technol., 21: 1164-1167.

Mills, A.C. and Biggar, J.W. (1969): Solubility-temperature effect on the adsorption of gamma and beta-BHC from aqueous and hexane solutions by soil materials. Soil. Sci. Soc. Am. Proc., 33: 210-216.

National Minor irrigation Development Project (1995): Topic report on Pesticide use in Bangladesh. Prepared by Sir William Halcrow &Partners Ltd. DHV consultants. Financed by Commission of the European Communities (Project no. ALA/90/13), The World Bank (IDA Credit no. 2246 BD).

Neumann, S.P. (1990): Universal scaling of hydraulic conductivities and dispersivities in geologic media. Water. Resour. Res., 26: 1749-1758.

Njoroge, B.N.K., Ball, P.W. and Cherry, R.S. (1998): Sorption of 1,2,4 – trichlorobenzene and tetrachloroethene within an authigenic soil profile: Changes in Koc with soil depth. J. Contam. Hydrol., 29: 347-377.

Nkedi-Kizza, P., Brusseau, M.L, Rao, P.S.C. and Hornsby, A.G. (1989): Nonequilibrium sorption during displacement of hydrophobic organic chemicals and ^{45}Ca through soil columns with aqueous and mixed solvents. Environ. Sci. Technol., 23: 814–820.

Nkedi-Kizza, P., Rao, P.S.C. and Hornsby, A.G. (1987): Influence of organic cosolvents on leaching of hydrophobic organic chemicals through soils. Environ. Sci. Technol., 21: 1107–1111.

Ogata, A. and Banks, R.G. (1961): A solution of the differential equation of longitudinal dispersion in porous media. U.S. Geological Survey Professional Paper, 411-A, Washington D.C.

Olsen, S.R. and Kemper, W.D. (1968): Movement of nutrients to plant roots. Adv. Agron., 20: 91-151.

Paulsen, P. D. and Cannon, F. S. (1999): Polytherm model for methylisobutylketone adsorption onto coconut-based granular activated carbon. Carbon, 37: 249-260.

Piatt, J.J, Backhus, D.A., Capel, P.D and Eisenreich, S.J. (1996): Temperature- dependent sorption of naphthalene, phenanthrene and pyrene to low organic carbon aquifer sediments. Environ. Sci. Technol., 30: 751-760.

Pignatello, J.J. (1989): Sorption dynamics of organic compounds in soils and sediments. Sawhnes, B.L. and Brown, K., eds., SSSA special publication number 22, Madison Wisconsin, USA, 45-80.

Pignatello, J.J. (1990): Slowly reversible sorption of aliphatic halocarbons in soils. I. Formation of residual fractions. Environ. Toxicol. Chem., 9: 1107-1115.

Pignatello, J.J. and Huang, L.Q. (1991): Sorptive reversibility of atrazine and metachlor residues in field soil samples. J. Environ. Qual., 20: 222-228.

Pignatello, J.J., Ferrandino, F.J. and Huang, L.Q. (1993): Elution of aged and freshly added herbicides from a soil. Environ. Sci. Technol., 27: 1563-1571.

Porter, L.K, Kemper, W.D., Jackson, R.D. and Steward, B.A. (1960): Chloride diffusion in soils as influenced by moisture content. Proc. Soil. Sci. Soc. Am., 24: 400-403.

Rahman, M.M., Liedl, R. and Grathwohl, P. (2002): Nonequilibrium sorption during macropore transport of organic contaminants in soils – Laboratory experiments and analytical modeling. Submitted to the journal of Water Resour. Res.

Rao, P.S.C. and Davidson, J.M. (1980): Estimation of pesticide retention and transformation parameters required in non-point source pollution models. Environmental impact of nonpoint source pollution, Ann Arbour Sci. Publi., Ann Arbour, MI, pp 23-67.

Rao, P.S.C., Green, R.E., Balasubramanian, V. and Kanehoro, Y. (1974): Field study of solute movement in a highly aggregated Oxisol with intermittent flooding. II. Picloram. J. Environ. Qual., 3: 197-202.

Rasmuson, A. and Neretnieks, I. (1981): Migration of radionuclides in fissured rock: The influence of micropore diffusion and longitudinal dispersion. J. Geophy. Res., 86: 3749–3758.

Reynolds, G.W., Hoff, J.T. and Gillham, R.W. (1990): Sampling bias caused by materials used to monitor halocarbons in groundwater. Environ. Sci. Technol., 24: 135-142.

Rosen, J.B. (1954): General numerical solution for solid diffusion in fixed beds. Ind. Eng. Chem., 46: 1590-1594.

Roth , K., Jury, W.A., Flühler, H. and Attinger, W. (1991): Field scale transport of chloride through an unsaturated field soil. Water. Resour. Res., 27: 2533-2541.

Rounds, S.A., Tiffany, B.A. and Pankow, J.F. (1993): Description of gas particle sorption kinetics with an intraparticle diffusion model: desorption experiments. Enviro. Sci. Technol., 27: 366-377.

Rügner, H., Kleineidam, S. and Grathwohl, P. (1999): Long term sorption kinetics of phenanthrene in aquifer materials. Enviro. Sci. Technol., 33: 1645-1651.

Sabljic, A., Gusten, H., Verhaar, H. and Hermans, J. (1995): UQSAR modelling of soil sorption, improvements and systematics of log Koc vs. log Kow correlations. Chemosphere, 31: 4489-4514.

Schnoor, J.L. (1996): Environmental modelling: Fate and transport of pollutants in water, air and soil. John Wiley and Sons, Inc. New York., 684p.

Schwarzenbach, R. P. Gschwend, P. M. and Imboden, D. M. (1993): Environmental Organic Geochemistry. John Wiley and sons, New York, 681p.

Schwarzenbach, R.P. and Westall, J. (1981): Transport of nonpolar organic compounds from surface water to groundwater: laboratory sorption studies. Environ.Sci.Technol., 15: 1361-1367.

Scow, K.M. and Alexander, M. (1992): Effect of diffusion on the kinetics of biodegradation: Experimental results with synthetic aggregates. Soil. Sci. Soc. Amer. J., 56: 128-134.

Scow, K.M. and Johnson, C. (1997): Effects of sorption on biodegradation of soil pollutants. Advance in agronomy, Academic, San Diego, pp. 1-56.

Selim, H.M., Davidson, J.M. and Manselll, R.S. (1976): Evaluation of a two-site adsorption-desorption model for describing solute transport in soils. Proc. summer conf. on comp. simu., Washington, D.C.

Shackelford, C.D. and Daniel, D.E. (1991a): Diffusion in saturated soil. I. Background. Am. Soc. Civ. Eng, Geo. Eng., 117(3).

Shackelford, C.D. and Daniel, D.E. (1991b): Diffusion in saturated soil. II. Results for compacted clay. Am. Soc. Civ. Eng, Geo. Eng., 117(3).

Shelton, D.R. and Parkin, R.B. (1991): Effect of moisture on sorption and biodegradation of carbofuran in soil. J. Agr. Food Chem., 39: 2063-2068.

Smith, E.H. (1991): Modified solution of homogeneous surface diffusion model for adsorption. J. Environ. Eng-ASCE, 117: 320-338.

Smith, A.H., Lingas, E.O. and Rahman, M. (2000): Contamination of drinking water by arsenic in Bangladesh : a public health emergency. Bull. World Health organization, 78: 1093-1102.

Sontheimer, H., Cornel, P. and Seym, M. (1983):Untersuchungen zur Sorption von aliphatischen Chlorkohlwasserstoffen durch Boden aus Grundwasserleitern. Veröffent. Des Ber. Und Lehrstuhls für wasserchemie und DVGW-Forschungstelle am Engler Bunte Institut, Karlsruhe, 21: 1-46.

Sposito, G. (1984): The surface chemistry of soils. Oxford University Press, New York.

Steinberg, S.M., Pignatello, J.J. and Sawhney, B.L. (1987): Persistence of 1,2-Dibromomethane in soils: entrapement in intraparticle micropores. Environ. Sci. Technol., 21: 1201-1208.

Stevenson, F.J. (1982): Role and function of humus in soil with emphasis on adsorption of herbicides and chelaton of microorganisms. Bioscience, 22: 643-650.

Szecsody, J.E. and Bales, R.C. (1991): Chemosphere, 22: 1141-1153.

Tao, S., Piao, H.S., Dawson, R., Lu, X.X and Hu, H.Y. (1999): Estimation of organic carbon normalized sorption coefficient for soils using the fragment constant method. Environ. Sci. Technol., 33: 2719-2725.

USDA (United state department of agriculture) (1992): Keys to soil taxonomy. 5th ed., Blacksburgh, Virginia, 541p.

Van Genuchten, M.T. and Wierenga, P.J. (1976): Mass transfer studies in sorbing porous media: Analytical solutions. Soil. Sci. Soc. Am, J, 40: 473-479.

Verschueren, K. (1996): Handbook of Environmental Data on Organic Chemicals.- 3rd ed.

Voice, T.C and Weber, W.J. (1983): Sorption of hydrophobic compounds by sediments, soils and suspended solids. I. Theory and background. Water Research, 17: 1433-1441.

von Oepen, B., Kordel, W. Klein, W. and Schuurmann, G. (1991): Predictive QSPR models for estimating soil sorption coefficients: Potential and limitation based on dominating processes. The science of the total environment, 109/110: 343-354.

Wauchope, R.D., Savage, K.E. and Koskinen, W.C. (1983): Weed Sci. 31: 744.

Webb, O.F., Phelps, T.J., Bienkowski, P.R., Digrazia, P.M., Reed, G.D., Appelgate, B., White, D.C. and Sayler, G.S. (1991): Development of a differential volume reactor system for soil biodegradation studies. Appl. Biochem.Biotechnol., 28-9 (SPR): 5-19.

Weber, W. J.Jr. (1972): Physicochemical process for water quality control. John Wiley & Sons Inc., New York.

Weber, W.J., McGinley, P.M. and Katz, L.E. (1992): A distributed reactivity model for sorption by soils and sediments. 1: conceptual basis and equilibrium assessments. Environ. Sci. Technol., 26: 1955-1962.

Weber, W.J.Jr., and Huang, W. (1996): A distributed reactivity model for sorption by soils and sediments. 4. Intraparticle heterogeneity and phase distribution relationships under nonequilibrium conditions. Environ. Sci. Technol., 30: 881-888.

Weber, W. J. Jr., LeBoeuf, E.J., Young, T. M. and Huang, W (2001): Contaminant interactions with geosorbent organic matter: insights drawn from polymer sciences. Water Res., 35: 853-868.

Wefer-Roehl, A., Graber, E.R., Adar, E., Nativ, R., Borisover, M.D. and Ronen, Z. (2001): Chemosphere, 44: 1121 – 1131.

Weissenfels W.D., Klewer, H.J. and Langhoff, J. (1992): Adsorption of polycyclic aromatic hydrocarbons (PAHs) by soil particles: Influence of biodegradability and biotoxicity. Appl. Microbiol. Biotechnol., 36: 689-696.

Wood, G. O (2001): Affinity coefficients of the Polanyi/Dubinin adsorption isotherm equations: A review with compilations and correlations. Carbon, 39: 343-356.

Woodburn, K.B., Lee, L.S., Rao, P.S.C. and Delfino, J.J. (1989): Comparison of sorption energetics for hydrophobic organic chemicals by synthetic and natural sorbents from methanol/water solvent mixtures. Environ. Sci. Technol., 23: 407-423.

Worch, E. (1993): Eine neue Gleichung zur Berechnung von Diffusionskoeffizienten geloester Stoffe. Vom Wasser, 81: 289-297.

Wu, S.-C. and Gschwend, P.M. (1986): Sorption kinetics of hydrophobic organic compounds to natuarl sediments and soils. Environ. Sci. Technol., 20: 717-725.

Wu, S.-C. and Gschwend, P.M. (1988): Numerical modelling of sorption kinetics of organic compounds to soil and sediment particles. Water Resour. Res., 24: 1373-1383.

Xia, G., Ball, W. P. (1999): Adsorption-partitioning uptake of nine low-polarity organic chemicals on a natural sorbent. Environ. Sci. Technol., 33: 262-269.

Xing, B. and Pignatello, J. J. (1997): Dual-mode sorption of low-polarity compounds in glassy poly(vinyl chloride) and soil organic matter. Environ. Sci. Technol., 31: 792-799.

Xing, B., Pignatello, J.J. and Gigliotti, B. (1996): Competitive sorption between atrazine and other organic compounds in soils and model sorbents. Environ. Sci. Technol., 30:2432-2440.

Young, D.F. and Ball, W.P. (1998): Estimating diffusion coefficients in low-permeability porous media using a macropore column. Environ. Sci. Technol., 32: 2578–2584.

Appendix A1

Model input parameters for the simulation for continuous input injection (Chapter 5, Section 5.1.1)

Chemical: phenanthrene

Solid: Deltaic aquifer sediment (sandy silt)

Field / Environmental parameters

Depth below ground surface [cm] = 200

Pore water velocity [cm s^{-1}] = 1.15×10^{-6}

Flow effective porosity [n, -] = 0.35

Solid density [ρ, g cm^{-3}] = 2.69

Bulk density [ρ_b, g cm^{-3}] = 1.71

Sorption / Dispersion / Diffusion parameters

Freundlich Coefficient [K_{fr}, L kg^{-1}] = 67

Freundlich Exponent [1/n, -] = 0.83

Concentration in water [mg L^{-1}] = 10

Distribution coefficient [K_d, L kg^{-1}] = 45

Retardation factor [R_f, -] = 220

Aqueous diffusions coefficient [D_{aq}, cm^2 s^{-1}] = 6.71×10^{-6}

Pore diffusion coefficient [D_p, cm^2 s^{-1}] = 1.89×10^{-9}

Dispersivity [α_l, cm] = 0.2

Hydro. dispersion coefficient [D_H, cm^2 s^{-1}] = 5.57×10^{-6}

Decay constant (s^{-1}) = 2.19×10^{-8} (half life e.g., 1 year)

Appendix A2

Model input parameters for the simulation of pulse input injection using PESTAN and eqs. (2.31) and (2.32) (Chapter 5, Section 5.1.2)

Chemical: carbofuran (carbamate pesticide)
Solid: Deltaic aquifer sediment (sandy silt)

Water solubility [S, mg L^{-1}] = 320
Pore water velocity [v_a, cm s^{-1}] = 3.83×10^{-6}
Distribution coefficient [K_d, L kg^{-1}] = 0.31
Decay constant (s^{-1}) = 1.6×10^{-07} (half life e.g., 50 days)
Flow effective porosity [n, -] = 0.30
Bulk density [ρ_b, g cm^{-3}] = 1.60
Saturated water content [-] = 0.4
Characteristic curve coefficient [-] = 7.75
Saturated hydraulic conductivity [cm hr^{-1}] = 1
Hydro. dispersion coefficient [D_H, cm^2 s^{-1}] = 1.66×10^{-5}
Number of application of waste [-] = 1
Waste application rate [kg ha^{-1}] = 0.5

Appendix A3

Model input parameters for the simulation of finite pulse input injection (Chapter 5, Section 5.1.3)

Chemical: phenanthrene

Solid: Deltaic soil (silty loam soil)

Pore water velocity [cm s^{-1}] = 5.02×10^{-3}

Macro pore porosity [n_m, -] = 0.37

Matrix region porosity [n_{im}, -] = 0.45

Solid density [ρ, g cm^{-3}] = 2.69

Bulk density [ρ_b, g cm^{-3}] = 1.48

Aqueous diffusions coefficient [D_{aq}, cm^2 s^{-1}] = 6.7×10^{-6}

Tortuosity factor [τ_f, -] = 2.0

Pore diffusion coefficient [D_p, cm^2 s^{-1}] = 3.33×10^{-6}

App. Diff. Coeff. [D_a, cm^2 s^{-1}] = 5.95×10^{-9}

Freundlich Coefficient [K_{fr}, L kg^{-1}] = 232

Freundlich Exponent [$1/n$, -] = 0.92

Distribution coefficient [K_d, L kg^{-1}] = 170

Retardation factor [R_m, -] = 559

Retardation factor [R_{im}, -] = 1

Initial concentration [C_0, mg L^{-1}] = 0.1

Pulse duration [t_0, s] = 3600

Appendix A4

Model input parameters for the simulation of finite pulse input injection (Chapter 5, Section 5.1.3)

Chemical: 1,2 DCB

Solid: Deltaic soil (silty loam soil)

Pore water velocity [cm s^{-1}] = 5.14×10^{-3}

Macro pore porosity [n_m, -] = 0.37

Matrix region porosity [n_{im}, -] = 0.45

Solid density [ρ, g cm^{-3}] = 2.69

Bulk density [ρ_b, g cm^{-3}] = 1.48

Aqueous diffusions coefficient [D_{aq}, cm^2 s^{-1}] = 8.45×10^{-6}

Tortuosity factor [τ_f, -] = 2.0

Pore diffusion coefficient [D_p, cm^2 s^{-1}] = 4.23×10^{-6}

App. Diff. Coeff. [D_a, cm^2 s^{-1}] = 3.68×10^{-7}

Freundlich Coefficient [K_{fr}, L kg^{-1}] = 8.16

Freundlich Exponent [$1/n$, -] = 0.76

Distribution coefficient [K_d, L kg^{-1}] = 3.19

Retardation factor [R_m, -] = 11.5

Retardation factor [R_{im}, -] = 1

Initial concentration [C_0, mg L^{-1}] = 100

Pulse duration [t_0, s] = 3600

In der Reihe C der Tübinger Geowissenschaftlichen Arbeiten (TGA) sind bisher erschienen:

Nr. 1: Grathwohl, Peter (1989): Verteilung unpolarer organischer Verbindungen in der wasserun-gesättigten Bodenzone am Beispiel der leichtflüchtigen aliphatischen Chlorkohlenwasser-stoffe. 102 S.

Nr. 2: Eisele, Gerhard (1989): Labor- und Felduntersuchungen zur Ausbreitung und Verteilung leichtflüchtiger chlorierter Kohlenwasserstoffe (LCKW) im Übergangsbereich wasserunge-sättigte/wassergesättigte Zone. 84 S.

Nr. 3: Ehmann, Michael (1989): Auswirkungen atmogener Stoffeinträge auf Boden- und Grund-wässer sowie Stoffbilanzierungen in drei bewaldeten Einzugsgebieten im Oberen Buntsand-stein (Nordschwarzwald). 134 S.

Nr. 4: Irouschek, Thomas (1990): Hydrogeologie und Stoffumsatz im Buntsandstein des Nord-schwarzwaldes. 144 S.

Nr. 5: Sanns, Matthias (1990): Experimentelle Untersuchungen zum Ausbreitungsverhalten von leichtflüchtigen Chlorkohlenwasserstoffen (LCKW) in der wassergesättigten Zone. 122 S. **(Vergriffen!)**

Nr. 6: Seeger, Thomas (1990): Abfluß- und Stofffrachtseparation im Buntsandstein des Nord-schwarzwaldes. 154 S.

Nr. 7: Einsele, Gerhard & Pfeffer, Karl-Heinz (Hrsg.) (1990): Untersuchungen über die Auswir-kungen des Reaktorunfalls von Tschernobyl auf Böden, Klärschlamm und Sickerwasser im Raum von Oberschwaben und Tübingen. 151 S.

Nr. 8: Douveas, Nikon G. (1990): Verwitterungstiefe und Untergrundabdichtung beim Talsper-renbau in dem verkarsteten Nord-Pindos-Flysch (Projekt Pigai-Aoos, NW-Griechenland). 165 S.

Nr. 9: Schlöser, Heike (1991): Quantifizierung der Silikatverwitterung in karbonatfreien Deck-schichten des Mittleren Buntsandsteins im Nordschwarzwald. 93 S.

Nr. 10: Köhler, Wulf-Rainer (1992): Beschaffenheit ausgewählter, nicht direkt anthropogen beein-flußter oberflächennaher und tiefer Grundwasservorkommen in Baden-Württemberg. 144 S.

Nr. 11: Bundschuh, Jochen (1991): Der Aquifer als thermodynamisch offenes System. – Untersu-chungen zum Wärmetransport in oberflächennahen Grundwasserleitern unter besonderer Berücksichtigung von Quellwassertemperaturen (Modellversuche und Geländebeispiele). 100 S. **(Vergriffen!)**

Nr. 12: Herbert, Mike (1992): Sorptions- und Desorptionsverhalten von ausgewählten polyzyklischen aromatischen Kohlenwasserstoffen (PAK) im Grundwasserbereich. 111 S.

Nr. 13: Sauter, Martin (1993): Quantification and forecasting of regional groundwater flow and transport in a karst aquifer (Gallusquelle, Malm, SW-Germany. 150 S.

Nr. 14: Bauer, Michael (1993): Wasserhaushalt, aktueller und holozäner Lösungsabtrag im Wutachgebiet (Südschwarzwald). 130 S.

Nr. 15: Einsele, Gerhard & Ricken, Werner (Hrsg.) (1993): Eintiefungsgeschichte und Stoffaustrag im Wutachgebiet (SW-Deutschland). 215 S.

Nr. 16: Jordan, Ulrich (1993): Die holozänen Massenverlagerungen des Wutachgebietes (Süd-schwarzwald). 132 S.

Nr. 17: Krejci, Dieter (1994): Grundwasserchemismus im Umfeld der Sonderabfalldeponie Billigheim und Strategie zur Erkennung eines Deponiesickerwassereinflusses. 121 S.

Nr. 18: Hekel, Uwe (1994): Hydrogeologische Erkundung toniger Festgesteine am Beispiel des Opalinustons (Unteres Aalenium). 170 S. **(Vergriffen!)**

Nr. 19: Schüth, Christoph (1994): Sorptionskinetik und Transportverhalten von polyzyklischen aromatischen Kohlenwasserstoffen (PAK) im Grundwasser - Laborversuche. 80 S.

Nr. 20: Schlöser, Helmut (1994): Lösungsgleichgewichte im Mineralwasser des überdeckten Muschelkalks in Mittel-Württemberg. 76 S.

Nr. 21: Pyka, Wilhelm (1994): Freisetzung von Teerinhaltsstoffen aus residualer Teerphase in das Grundwasser: Laboruntersuchungen zur Lösungsrate und Lösungsvermittlung. 76 S.

Nr. 22: Biehler, Daniel (1995): Kluftgrundwässer im kristallinen Grundgebirge des Schwarzwaldes – Ergebnisse von Untersuchungen in Stollen. 103 S.

Nr. 23: Schmid, Thomas (1995): Wasserhaushalt und Stoffumsatz in Grünlandgebieten im württem-bergischen Allgäu. 145+ 92 S.

Nr. 24: Kretzschmar, Thomas (1995): Hydrochemische, petrographische und thermodynamische Untersuchungen zur Genese tiefer Buntsandsteinwässer in Baden-Württemberg. 142 S. **(Vergriffen!)**

Nr... 25: Hebestreit, Christoph (1995): Zur jungpleistozänen und holozänen Entwicklung der Wutach (SW-Deutschland). 88 S.

Nr... 26: Hinderer, Matthias (1995): Simulation langfristiger Trends der Boden- und Grundwasser-versauerung im Buntsandstein-Schwarzwald auf der Grundlage langjähriger Stoffbilanzen. 175 S.

Nr... 27: Körner, Johannes (1996): Abflußbildung, Interflow und Stoffbilanz im Schönbuch Waldgebiet. 206 S.

Nr... 28: Gewald, Thomas (1996): Der Einfluß der Desorptionskinetik bei der Freisetzung von Tri-chlorethen (TCE) aus verschiedenen Aquifersanden. 67 S.

Nr... 29: Schanz, Ulrich (1996): Geophysikalische Untersuchungen im Nahbereich eines Karst-systems (westliche Schwäbische Alb). 114 S.

Nr... 30: Renner, Sven (1996): Wärmetransport in Einzelklüften und Kluftaquiferen – Untersuchungen und Modellrechnungen am Beispiel eines Karstaquifers. 89 S.

Nr... 31: Mohrlok, Ulf (1996): Parameter-Identifikation in Doppel-Kontinuum-Modellen am Beispiel von Karstaquiferen. 125 S.

Nr... 32: Merkel, Peter (1996): Desorption and Release of Polycyclic Aromatic Hydrocarbons (PAHs) from Contaminated Aquifer Materials. 76 S.

Nr. 33: Schiedek, Thomas (1996): Auftreten und Verhalten von ausgewählten Phthalaten in Wasser und Boden. 112 S.

Nr. 34: Herbert, Mike & Teutsch, Georg (Hrsg.) (1997): Aquifersysteme Südwestdeutschlands - Eine Vorlesungsreihe an der Eberhard-Karls-Universität Tübingen. 162 S.

Nr. 35: Schad, Hermann (1997): Variability of Hydraulic Parameters in Non-Uniform Porous Media: Experiments and Stochastic Modelling at Different Scales. 233 S.

Nr. 36: Herbert, Mike & Kovar, Karel (Eds.) (1998): GROUNDWATER QUALITY 1998: Remediation and Protection - Posters -.- Proceedings of the GQ'98 conference, Tübingen, Sept. 21-25, 1998, Poster Papers. 146 S.

Nr. 37: Klein, Rainer (1998): Mechanische Bodenbearbeitungsverfahren zur Verbesserung der Sanierungseffizienz bei In-situ-Maßnahmen. 106 S.

Nr. 38: Schollenberger, Uli (1998): Beschaffenheit und Dynamik des Kiesgrundwassers im Neckartal bei Tübingen. 74 S.

Nr. 39: Rügner, Hermann (1998): Einfluß der Aquiferlithologie des Neckartals auf die Sorption und Sorptionskinetik organischer Schadstoffe. 78 S.

Nr. 40: Fechner, Thomas (1998): Seismische Tomographie zur Beschreibung heterogener Grund-wasserleiter. 113 S.

Nr. 41: Kleineidam, Sybille (1998): Der Einfluß von Sedimentologie und Sedimentpetrographie auf den Transport gelöster organischer Schadstoffe im Grundwasser. 82 S.

Nr. 42: Hückinghaus, Dirk (1998): Simulation der Aquifergenese und des Wärmetransports in Karstaquiferen. 124 S.

Nr. 43: Klingbeil, Ralf (1998): Outcrop Analogue Studies – Implications for Groundwater Flow and Contaminant Transport in Heterogeneous Glaciofluvial Quaternary Deposits. 111 S.

Nr. 44: Loyek, Diana (1998): Die Löslichkeit und Lösungskinetik von polyzyklischen aromatischen Kohlenwasserstoffen (PAK) aus der Teerphase. 81 S.

Nr. 45: Weiß, Hansjörg (1998): Säulenversuche zur Gefahrenbeurteilung für das Grundwasser an PAK-kontaminierten Standorten. 111 S.

Nr. 46: Jianping Yan (1998): Numerical Modeling of Topographically-closed Lakes: Impact of Climate on Lake Level, Hydrochemistry and Chemical Sedimentation. 144 S.

Nr. 47: Finkel, Michael (1999): Quantitative Beschreibung des Transports von polyzyklischen aro-matischen Kohlenwasserstoffen (PAK) und Tensiden in porösen Medien. 98 S.

Nr. 48: Jaritz, Renate (1999): Quantifizierung der Heterogenität einer Sandsteinmatrix (Mittlerer Keuper, Württemberg). 106 S.

Nr. 49: Danzer, Jörg (1999): Surfactant Transport and Coupled Transport of Polycyclic Aromatic Hydrocarbons (PAHs) and Surfactants in Natural Aquifer Material - Laboratory Experi-ments. 75 S.

Nr. 50: Dietrich, Peter (1999): Konzeption und Auswertung gleichstromgeoelektrischer Tracer-versuche unter Verwendung von Sensitivitätskoeffizienten. 130 S.

Nr. 51: Baraka-Lokmane, Salima (1999): Determination of Hydraulic Conductivities from Discrete Geometrical Characterisation of Fractured Sandstone Cores. 119 S.

Nr. 52: M^{c}Dermott, Christopher I. (1999): New Experimental and Modelling Techniques to Investigate the Fractured System. 170 S.

Nr. 53: Zamfirescu, Daniela (2000): Release and Fate of Specific Organic Contaminants at a Former Gasworks Site. 96 S.

Nr. 54: Herfort, Martin (2000): Reactive Transport of Organic Compounds Within a Heterogeneous Porous Aquifer. 76 S.

Nr. 55: Klenk, Ingo (2000): Transport of Volatile Organic Compounds (VOC's) From Soilgas to Groundwater. 70 S.

Nr. 56: Martin, Holger (2000): Entwicklung von Passivsammlern zum zeitlich integrierenden Depositions- und Grundwassermonitoring: Adsorberkartuschen und Keramikdosimeter. 84 S.

Nr. 57: Diallo, Mamadou Sanou (2000): Acoustic Waves Attenuation and Velocity Dispersion in Fluid-Filled Porous Media: Theoretical and Experimental Investigations. 101 S.

Nr. 58: Lörcher, Gerhard (2000): Verarbeitung und Auswertung hyperspektraler Fernerkundungsdaten für die Charakterisierung hydrothermaler Systeme (Goldfield/Cuprite, Yellowstone National Park). 158 S.

Nr. 59: Heinz, Jürgen (2001): Sedimentary Geology of Glacial and Periglacial Gravel Bodies (SW-Germany): Dynamic Stratigraphy and Aquifer Sedimentology. 102 S.

Nr. 60: Birk, Steffen (2002): Characterisation of Karst Systems by Simulating Aquifer Genesis and Spring Responses: Model Development and Application to Gypsum Karst. 122 S**.**

Nr. 61: Halm, Dietrich & Grathwohl, Peter (Eds.) (2002): Proceedings of the 1st International Workshop on Groundwater Risk Assessment at Contaminated Sites (GRACOS). 280 S.

Nr. 62: Bauer, Sebastian (2002): Simulation of the genesis of karst aquifers in carbonate rocks. 143 S.

Nr. 63: Rahman, Md. Mokhlesur (2002): Sorption and Transport Behaviour of Hydrophobic Organic Compounds in Soils and Sediments of Bangladesh and their Impact on Groundwater Pollution – Laboratory Investigations and Model Simulations. 73 S.